University College London

University of London

Department of Civil and Environmental Engineering

Physical Characteristics of Flocs in Water Treatment Processes

by

Sze Chun Gary Lau

A thesis submitted to the University of London for the degree of Doctor of Philosophy

ProQuest LLC
789 East Eisenhower Parkway
P.O. Box 1346
Ann Arbor, MI 48106-1346

Abstract

Aluminium sulphate, calcium nitrate, and two cationic polymers have been used to coagulate and flocculate dilute kaolin and latex suspensions (< 100 mg/l) in a stirred vessel. The effects of the different destabilising agents on the resulting flocs have been monitored using a simple continuous optical technique based on turbidity fluctuations and the behaviour of these flocs under shear conditions and the possibility of subsequent floc re-formation have been investigated.

The results showed vast differences in behaviour regarding to floc breakage and re-formation between the systems. For a low molecular weight, high charge polymer (A) and calcium nitrate, floc breakage was almost completely reversible. However, for aluminium sulphate, limited floc re-formation was observed on restoring previous shear conditions after breakage. For a high molecular weight polymer (B), limited floc breakage was observed.

Moreover, a new automated monitoring technique based on cake and vacuum filtration has been developed to assess the filterability of flocs. The technique is reliable and provides reproducible results. The results showed that polymer A was more effective in enhancing filterability than polymer B for both kaolin and latex suspensions. However, polymers do not have a significant influence on the filterability of flocs if the primary particles involved have high sphericity.

Acknowledgements

First of all, I would like to thank Prof. J. Gregory for his supervision, patience and introducing me to critical thinking and writing.

I would also like to thank Dr. C. S. B. Fitzpatrick for encouraging me and giving me the opportunity to join the Public Health group as a research student and the technical staff in the Public Health laboratory, Mr. M. Saleem in particular, for their assistance.

Finally, I would like to thank my closest friends for their endurance, understanding, forgiveness and love.

Contents

List of Figures

List of Tables

List of Symbols

a	: radius of spherical particles.....	m
a_1	: radius of original particles.....	m
A_1	: effective cross-sectional area of the light beam.....	m^2
A_2	: Hamaker constant.....	J
b	: slope of straight line.....	
c	: solids concentration of the suspension.....	$g\ m^{-3}$
c_i	: molar concentration.....	$mol\ l^{-1}$
C_1	: constant.....	
C_2	: scattering cross-section of a particle.....	m^2
d	: distance between spherical particles.....	m
d_{max}	: maximum floc diameter.....	m
D_1	: diffusion coefficient of original particles.....	$m^2\ s^{-1}$
D_F	: fractal dimension.....	
D_i	: diffusion coefficient of particle i.....	$m^2\ s^{-1}$
D_j	: diffusion coefficient of particle j.....	$m^2\ s^{-1}$
E	: electrical potential applied between two electrodes.....	V
F	: filter area.....	m^2

g : gravity acceleration..... $m\ s^{-2}$

G : velocity gradient (shear rate)..... s^{-1}

$\overline{G}$: effective shear rate..... s^{-1}

Gt : Camp number.....

H : depth of filter cake..... m

J_{ij} : total number of collisions between particles i and j..... $m^{-3}\ s^{-1}$

k : Boltzmann's constant..... $J\ K^{-1}$

k_F : flocculation rate coefficient..... $m^3\ s^{-1}$

K_1 : constant.....

K_2 : permeability..... m^2

L_1 : distance between electrodes..... m

L_2 : floc size..... m

l : optical path length..... m

M : floc mass..... kg

n : constant.....

N : particle number concentration..... m^{-3}

N_0 : initial particle number concentration..... m^{-3}

N_i : particle number concentration of particle i..... m^{-3}

N_j	: particle number concentration of particle j.....	m^{-3}
P	: power input per unit mass.....	$J\ s^{-1}\ kg^{-1}$
ΔP	: pressure difference between filter cake and membrane filter.....	Pa
Q	: scattering coefficient.....	
R	: ratio (rms/dc).....	
R_T	: total resistance to filtration.....	m^{-1}
R_c	: filter cake resistance.....	m^{-1}
R_{ij}	: collision radius of particles i and j.....	m
R_m	: membrane filter resistance.....	m^{-1}
S	: specific surface.....	m^{-1}
t	: flocculation or filtration time.....	s
T	: absolute temperature.....	K
U	: particle mobility.....	$m^2\ s^{-1}\ V^{-1}$
v	: particle velocity or velocity of approaching fluid.....	$m\ s^{-1}$
V	: volume of filtrate or fluid.....	m^3
V_A	: total energy of attraction (van der Waals interaction energy).....	J
V_R	: total energy of repulsion.....	J

V_T	: total energy of interaction.....	J
x	: distance from the Stern plane.....	m
z_i	: valence (charge) of ion i.....	
α_1	: collision efficiency factor.....	
α_2	: specific resistance to filtration.....	$m\ g^{-1}$
ε	: filter cake porosity.....	
ε'	: rate of energy dissipation.....	$m^2\ s^{-3}$
ε_W	: permittivity of water.....	$m^{-3}\ kg^{-1}\ s^4\ A^2$
ϕ	: volume fraction of suspended particles (solids concentration).....	$g\ m^{-3}$
η	: dynamic (absolute) viscosity.....	$m^{-1}\ kg\ s^{-1}$
κ	: Debye-Hückel parameter.....	m^{-1}
λ	: Kolmogorov microscale.....	m
ν	: kinematic viscosity.....	$m^2\ s^{-1}$
ρ	: density of water.....	$kg\ m^{-3}$
ρ_s	: density of particles.....	$kg\ m^{-3}$
τ	: half-time.....	s
ψ	: potential at a distance x from the Stern plane.....	V

ψ_δ : Stern potential..... V

ζ : zeta potential at the plane of shear..... V

Chapter 1

Introduction

1.1 Prologue

Many impurities in water are present as colloidal species which will not settle readily or which cannot be removed by direct filtration. Conventional separation techniques are not particularly efficient for particles of colloidal dimensions; it is necessary to increase their sizes and settling characteristics for better removal.

In many instances, the most effective way is to promote particle flocculation whereby larger units of agglomerate or flocs are formed, which may be removed by subsequent solid-liquid separation processes such as sedimentation or filtration.

The structure and the physical properties (size and density in particular) of flocs play a very important role in water treatment as they can strongly influence the performance of the separation processes employed. Extensive research has been conducted in this area and experimental studies concerned with the physical and structural properties of flocs are well documented.

However, it is often difficult to compare findings from these studies because of the vast differences in the materials and experimental conditions employed by individual researchers. Consequently, new concepts and theories may become difficult to justify. Therefore, it is of considerable practical and fundamental interest to investigate and compare different systems under controlled conditions.

All conventional wastewater treatment processes produce large quantities of waste material in the form of a dilute solid mixture known as sludge (Lu et al., 2003). The removal of water from sludge in dewatering units depends on the structural and physical characteristics of flocs (Knocke et al., 1987; Wu et al., 2003b; Zhao, 2003). Transportation is usually the largest component of sludge disposal cost and since

transportation of dewatered sludge is less expensive than transportation of liquid sludge, it is important to understand the mechanism of and to optimise the process of sludge dewatering.

1.2 Objectives

There have been numerous previous research studies concerning floc properties under the influences of different destabilising agents and shear conditions (Clark and Flora, 1991; Ditter et al., 1982; Spicer et al., 1998; Yukselen and Gregory 2002 and 2004) but not many of which were able to provide information that was directly comparable with one another or experimental techniques that could allow other researchers to easily build-up on due to the vast differences in the materials and experimental conditions employed. Thus it is important to provide experimental information that is concise, comparable and extractable and that allows potential follow-up experiments to be easily conducted without elaborate procedures.

Although research studies concerning the development of a laboratory scale dewaterability and filterability monitoring device or technique have been carried out in the past by researchers such as de Moor and Gregory (1982), Gregory and de Moor (1984), the monitoring devices developed or techniques employed were time consuming (see also Section 2.10.3.1) and often required extraction and transfer of flocs beforehand, which could cause damage and unwanted flocculation to flocs before they were being monitored. It is necessary to develop an automated technique that allows continuous monitoring without any physical interference to the flocs.

The purpose of the present study is to:

- Investigate the influences naturally occurring kaolin particles (plate-like and irregular in both size and shape) (see Section 2.11.1) and synthetic latex particles (spherical and uniform in all aspects) (see Section 2.11.2) have on floc formation (see Sections 2.3 and 2.5), breakage (see Section 2.7) and re-formation (see Section 2.7.2) respectively. Similar research studies have been carried out in the past (Besra et al., 2000; Mota et al., 2003; Ozan et al., 2000) but most of these were comparing particles that were similar in nature or with near sphericity or in a different context.

- Systematically compare the physical characteristics (size in particular) of flocs formed under different mechanisms of particle destabilisation (see Sections 2.3.1 and 2.4.3) using a variety of destabilising agents during formation, breakage and re-formation. Recent research studies conducted by Yukselen and Gregory (2002 and 2004) did not select a comprehensive range of destabilising agents to allow comparisons to be made between different particle destabilising mechanisms and with a limited range of experimental variables. They used dilute kaolin stock suspensions in London tap water with added humic acid for their experiments and carried out high speed rapid mixing (see Section 2.6.1) and floc breakage at 400 rpm. The present study uses a wider range of destabilising agents and lower speed stirring for rapid mixing and floc breakage.

- Develop a laboratory scale, automated monitoring technique based on cake filtration (see Section 2.10.3); cake filtration is the major mechanism of moisture removal in most mechanical dewatering devices (Wu et al., 2003a), to assess the effects different destabilising agents and primary particles have on the dewaterability and filterability of flocs under controlled conditions.

Chapter 2

Literature Review

2.1 Nature of Colloids and Inter-Particle Forces

Colloidal particles may be inorganic or organic, hydrophilic or hydrophobic and they are generally defined as less than 1 μm in size, although this is not a rigid boundary. The diagram in Figure 2.1 shows the appropriate separation techniques for particles of different nature and sizes. For colloidal suspensions involved in natural waters, the majority of the particles are negatively charged due to the dissociation of surface ionic groups or the preferential adsorption of ions.

A colloidal suspension is described as stable when the dispersion shows little or no tendency to aggregate. The most important interactions influencing the stability of colloidal suspension are electrical repulsion (double layer repulsion) and van der Waals attraction.

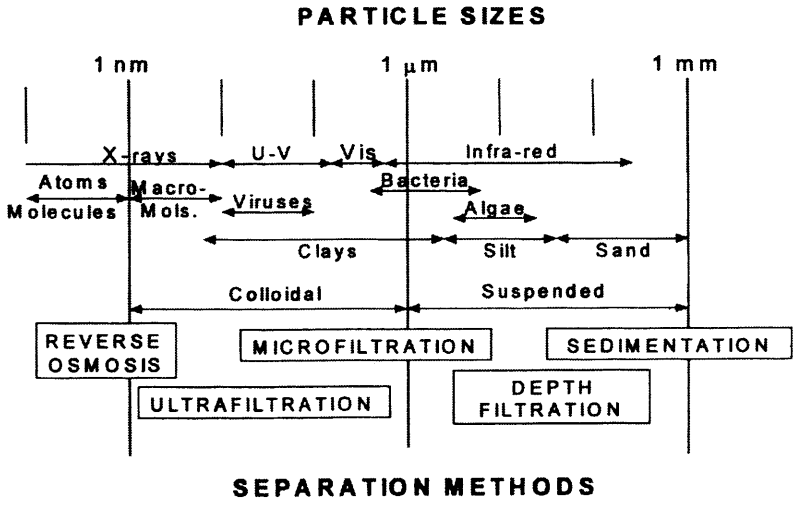

Figure 2.1 Particles of different nature and sizes together with appropriate separation methods (Gregory, 2000).

2.1.1 Hydrophilic and Hydrophobic Colloids

Hydrophilic colloids are water-soluble and disperse readily in water. They can be dehydrated and redispersed repeatedly to form a suspension. Hydrophilic colloids include gelatine, starch, gum, proteins and most bio-colloids. Hydrophobic colloids, on the other hand, are water-insoluble and do not redisperse spontaneously in water once dehydrated. Metal oxide and metal halide are examples of hydrophobic colloids (Bratby, 1980).

Hydrophilic colloids are stabilised by the formation of adherent thick layers of oriented water molecules around individual colloids (Faust and Aly, 1983), the amount of water bound by hydrophilic colloids, in some cases, may be three to ten times their own dry mass (Bratby, 1980). Hydrophobic colloids are stabilised by the repulsive forces of the charged double layer and sometimes by an adsorbed hydrophilic layer. Colloids with a high surface potential (zeta potential) tend to produce stable suspension. Most natural waters contain species of both hydrophilic and hydrophobic colloids.

2.1.2 Origin of Particle Surface Charge

The origin of the electrical charge carried by a particle can vary. Charge imbalance resulting from lattice imperfections at the solid surface can contribute to surface charge as demonstrated by some clay particles; surface charges of this type are independent of the pH of the liquid. Chemical reactions either be ionisation reactions with functional groups or co-ordinate bonding of solutes to the solid surface can also contribute to surface charge (Hutchison and Healy, 1990). In the case of aqueous dispersions, the most frequent origin is the adsorption of negative ions (OH^- in particular).

2.1.3 Van der Waals Interaction

Van der Waals forces are the molecular cohesive forces of attraction that increase in intensity as particles approach each other. These forces are negligible when the particles are far apart but become dominant when particles contact (Viessman and Hammer, 1985).

The van der Waals interaction energy V_A, between equal spherical particles of radius a separated by a distance d is given by:

$$V_A \approx -\frac{A_2 a}{12d} \tag{2.1}$$

where A_2 is the Hamaker constant; typically in the range of 0.3 to 10 × 10^{-20} J, which depends on the physical properties of the particles and water. The above equation only applies when $d \ll a$.

2.1.4 Electrical Double Layer

The first of the electrical double layer is made up of the charged particle surface and the stationary layer of adsorbed ions (Stern layer) and the second is a diffuse layer of counter ions distributed under the influence of electrostatic forces and random Brownian motion as shown in Figure 2.2.

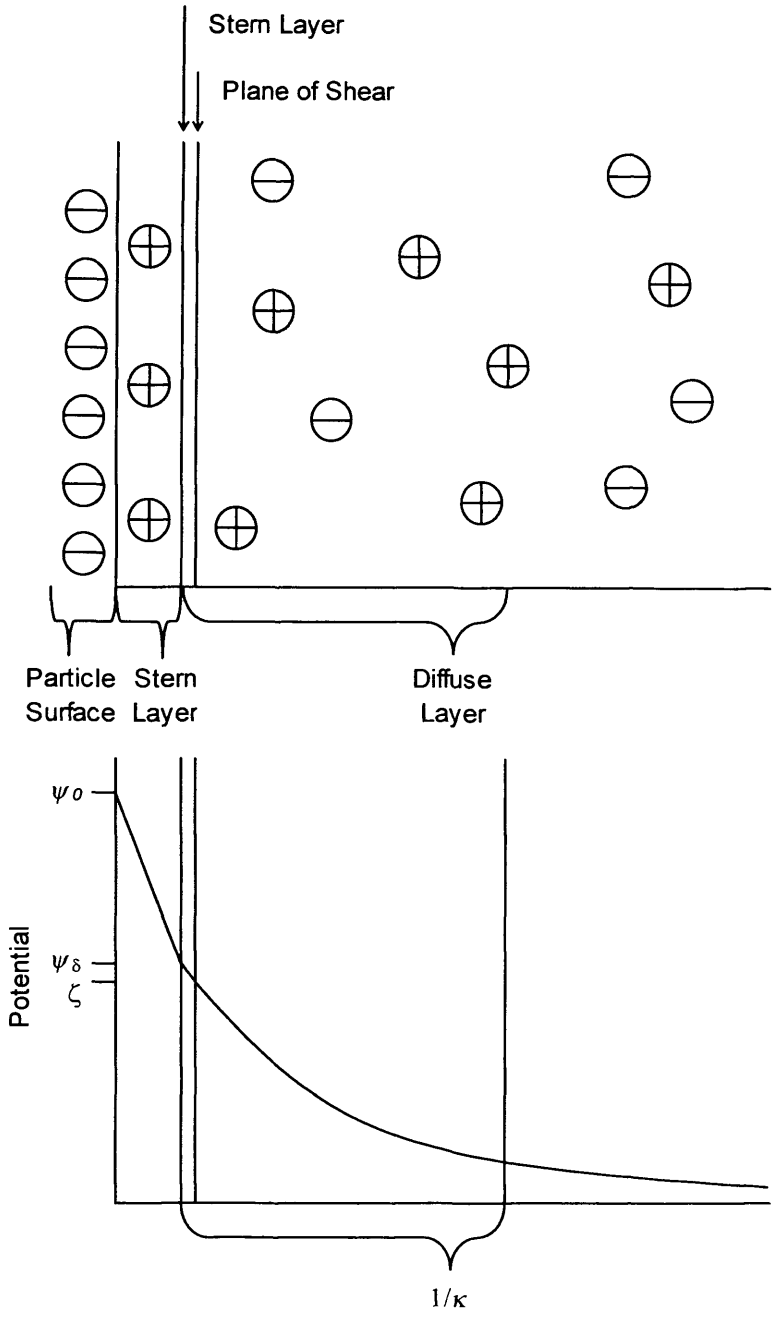

Figure 2.2 Electrical double layer surrounding a colloidal particle (Kohler, 1991).

In the diffuse layer, the electric potential falls exponentially from the particle surface, according to:

$$\psi = \zeta \exp(-\kappa x) \tag{2.2}$$

where ψ is the potential at a distance x from the Stern plane; ζ is the zeta potential at the plane of shear, which is usually assumed to coincide with the Stern potential ψ_δ (which

is not directly measurable) (Gregory, 2000). The plane of shear separates the immobile rigid layer of adsorbed ions (Stern layer) that moves together with the particle from the mobile diffuse layer of counter ions (Birdi, 2003; Masschelein, 1992; Schramm, 2001).

ζ can be derived experimentally using electrokinetic techniques, such as particle micro-electrophoresis (see Section 2.12.3), in which the velocity of a particle within an electric field is determined (Gregory, 2000). κ is the Debye-Hückel parameter which has the dimensions of reciprocal length (m^{-1}). The parameter κ depends on the ionic strength of the solution and for aqueous solutions at 25°C:

$$\kappa = 2.32 \times 10^9 \sqrt{\sum c_i z_i^2} \tag{2.3}$$

where c_i is the molar concentration and z_i the valence (charge) of ion i and the sum is taken over all ions present in the water (Gregory, 2000).

$1/\kappa$ is a characteristic length (thickness of the diffuse layer). Examples of $1/\kappa$ given by solutions of different ionic strength: deionised water ~ 1 μm, sodium solution of 1 mM ~ 9.6 nm (corresponds with the sodium nitrate concentration used for experiments described in Sections 3.1, 3.2 and 3.3) and River Thames water ~ 4 nm (Gregory, 2000). In general, the higher the level of dissolved salts, the lower the distance.

When two charged particles (identical spheres) approach each other, their diffuse layers overlap and there is repulsion between the particles. The electrical repulsion energy between two charged particles of radius a separated by a distance d is given approximately by:

$$V_R \approx 2\pi a \varepsilon \zeta^2 \exp(-\kappa d) \tag{2.4}$$

where ε is the permittivity of water (Gregory, 2000).

The magnitude of the repulsion at a given separation distance depends on the zeta potential and on κ. In concentrated salt solutions the repulsion will be of very short range.

2.1.5 DLVO Theory

A quantitative theory based on van der Waals attraction and diffuse double layer repulsion being the sole operative factors for colloidal stability was developed independently by Deryagin and Laudau (1941) and Verwey and Overbeek (1948). This is now generally known as the DLVO theory.

Van der Waals attraction and electrical repulsion are assumed to be additive and combine to give the total energy of interaction between particles as a function of separation distance:

$$V_T = V_A + V_R \tag{2.5}$$

where V_T is the total energy of interaction, V_A the total energy of attraction and V_R the total energy of repulsion.

The DLVO theory predicts a strong repulsion of particles in solutions of low ionic strength, where the electrical double layer thickness is greater, and a weak attraction minimum (the secondary minimum) in solutions of higher ionic strength, where the cloud of cations is compressed and the electrical double layer thickness is minimal (Marshall, 1990).

The total interaction between particles may be positive (repulsion) or negative (attraction) depending on the relative magnitudes of the electrical repulsion and van der Waals attraction. In many cases there is a potential energy barrier, which tends to prevent contact of particles as shown in the potential energy diagram in Figure 2.3. The particles are then said to be stable and would be difficult to flocculate.

At small separation distance, two colliding particles need to have sufficient energy to overcome the energy barrier to come close enough into the primary minimum in order to form a stable aggregate. Once the energy barrier is removed or overcome, for example, in practical flocculation process, by the energy imparted by fluid motion, particles should be able to come into close contact and be held in the deep primary energy minimum.

Aggregation of particles larger than about 1 μm can also occur at large separation distance in the secondary minimum, at which the particles do not come into close contact. The secondary minimum can give rather weak aggregates, which are easily redispersed.

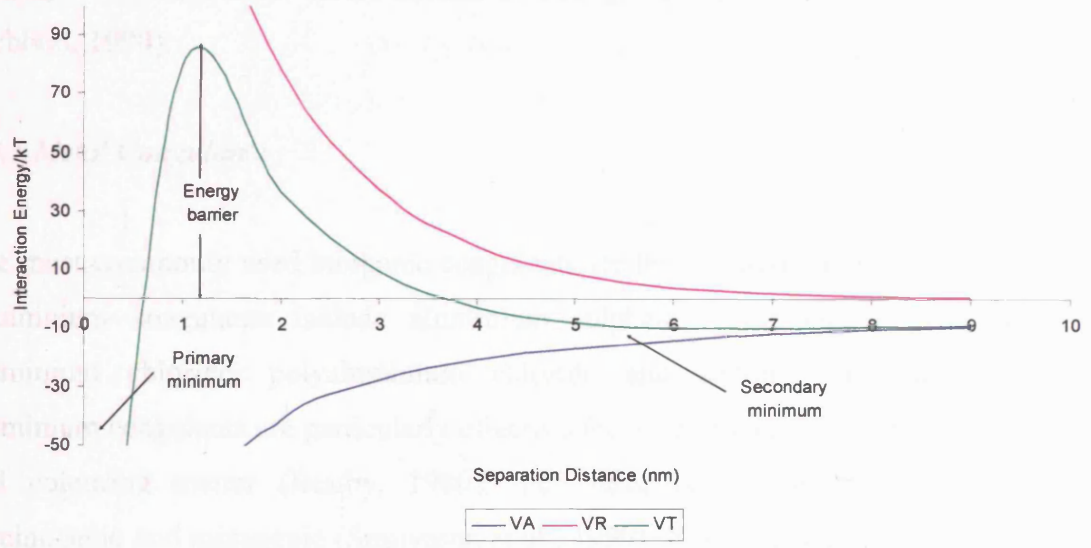

Figure 2.3 Potential energy diagram for the interaction of spherical colloidal particles, assuming that $A = 2$ kT, $a = 500$ nm, $\zeta = 0.025$ V, $\varepsilon = 7.08 \times 10^{-19}$ $CV^{-1}nm^{-1}$ and $\kappa = 0.734$ nm^{-1}. The energies are plotted in units of kT, where k is the the Boltzmann's constant and T is the absolute temperature.

Moreover, accompanying problems occur when adsorbed polymers are present in a system due to the fact that not only a third factor has to be taken into account but that V_R and (usually to a lesser extent) V_A require also modification as compared with the situation in the absence of polymer (Ives, 1978)

2.2 Coagulants

Coagulants are either inorganic or organic chemical substances being used to clarify contaminated waters via a variety of mechanisms. Inorganic coagulants are the most widely used for water and wastewater treatment and they are usually salts of iron or aluminium. Organic coagulants, also known as flocculants, are often synthetic polyelectrolytes in anionic, cationic or non-ionic forms.

In general, the choice of coagulant for the treatment of a particular kind of water depends on coagulation control tests, past experience in treatment of water of similar quality and the overall economics involved. The amount of coagulant employed to achieve the required water quality for a particular system, on the other hand, must be determined experimentally using a jar test apparatus which simulates the stages of mixing, flocculation and sedimentation at a range of coagulant doses and pH values (Tebbutt, 1990).

2.2.1 Metal Coagulants

The most commonly used inorganic coagulants are those based on aluminium and iron. Aluminium coagulants include aluminium sulphate; commonly known as alum, aluminium chloride, polyaluminium chloride and sodium aluminate. Although aluminium coagulants are particularly effective for water containing appreciable organic and colouring matter (Bratby, 1980), they have been suspected of being both carcinogenic and mutagenic (Srinivasan et al., 1999). It is necessary to take appropriate measures to keep aluminium residue in treated water at a low level (Shi et al., 2004).

Iron coagulants which include ferric sulphate, ferrous sulphate and ferric chloride, on the other hand, can operate over a wider pH and temperature range (Bratby, 1980). Although iron coagulants pose less health risks than aluminium coagulants, there have been complaints of their high corrosivity causing corrosion problems that shorten the life expectancy of equipment and pipelines in water treatment plants (Shi et al., 2004).

2.3 Coagulation

In the colloid literature, the term coagulation is used to describe the mechanism of particle destabilisation, which involves the usage of salts. In water and wastewater treatment practices, however, the term coagulation implies the step where particles are destabilised, which may be triggered by a coagulant or Brownian motion (Gregory, 2000).

Coagulation is generally carried out as a unit process in surface water purification to destabilise turbidity-producing substances (colloidal solids, clay particles, organics, bacteria and algae), colour and taste and odour producing compounds (resulting from

decaying vegetation or industrial wastes) in surface water to the point at which clarification can be achieved by flocculation followed by sedimentation and filtration (Viessman and Hammer, 1985).

Although fundamentally a separate process from flocculation (see Section 2.5), coagulation is in practice followed immediately by flocculation. By itself, coagulation does not produce a specific improvement in water quality, but it is essential for the success of follow-up purification processes such as flocculation, sedimentation and filtration (Masschelein, 1992).

2.3.1 Types of Destabilisation

The main mechanisms involved in the destabilisation of suspended particles include double layer compression, charge neutralisation (adsorption destabilisation) and precipitate entrapment (sweep coagulation).

- Double layer compression occurs when an indifferent electrolyte is added to a suspension in order to increase the concentration of ions. An indifferent electrolyte contains ions which are neither charge-determining nor specifically adsorbing (Bratby, 1980). Most 1:1 electrolytes can be considered as indifferent when the electrolyte concentration is not too high (Koopal, 1993).

  An increase in ion concentration has the effect of decreasing the thickness of the electrical double layer surrounding individual particles. Subsequently, the distance between adjacent particles caused by repulsive electrical forces is reduced, which leads to the promotion of attractive forces between them. Double layer compression is caused by an increase in ionic concentration but it is independent of the concentration of particles involved within a particular system.

- Charge neutralisation occurs when the repulsive charges of particles are neutralised by adsorption of oppositely charged ions. This has the effect of promoting particle-particle aggregation through adsorption. Typically, particle destabilisation through charge neutralisation occurs when the zeta potential of particles lies in the range of ± 10 mV (Hogg, 2000).

For some particles, an overdose is possible with this type of destabilisation, which leads to particle charge reversal. The required amount of ions should be proportional to the quantity of particles present in order to effect destabilisation (Binnie et al., 2002). Adsorbable ionic species are observed to destabilise hydrophobic colloids at much lower concentrations than is the case with ionic species of low adsorbability (Bratby, 1980).

- Precipitate entrapment occurs when salts of aluminium or iron are precipitated at intermediate pH values with particles incorporated within their structure, which is essentially a sweep action. The success of precipitate entrapment depends on the amount of salt added and the alkalinity and pH of a system but it is independent of the chemical nature of primary particles involved (Packham, 1963).

The hydrolysis of Al^{3+} can provide different products depending on the pH of the flocculation system involved. A simplified hydrolysis scheme is shown below:

$$Al^{3+} \rightarrow Al(OH)^{2+} \rightarrow Al(OH)_2^+ \rightarrow Al(OH)_3 \rightarrow Al(OH)_4^-$$

As the pH increases, soluble cationic species of different charge densities are formed which are then followed by the formation of an uncharged hydroxide precipitate. In the case of Al^{3+}, an amorphous precipitate can be formed at intermediate pH values. With further increase in pH, a soluble anionic aluminate ion may result (Duan and Gregory, 2003). In addition, aluminium hydroxide precipitate shows an isoelectric point (i.e.p.) where the net surface charge is zero. At pH values below approximately 8 (Van Benschoten and Edzwald, 1990), the precipitate is positively charged and at higher pH values it has a negative charge.

At very low concentrations of aluminium sulphate, typically a few μM at around neutral pH, only soluble species are present (Duan and Gregory, 2003). Dentel (1991) proposed a *Precipitation Charge Neutralisation* (PCN) model, which combines the effects of surface precipitation (James and Healy, 1972) and the deposition of colloidal hydroxide particles (a few nm in size) (see Figure 2.4) to explain particle destabilisation through charge neutralisation at moderate aluminium sulphate concentrations ($\approx$ 7.5 μM $Al_2(SO_4)_3$); particles may also become

destabilised under electrostatic patch mechanism depending on how the colloidal hydroxide particles are distributed on particle surfaces.

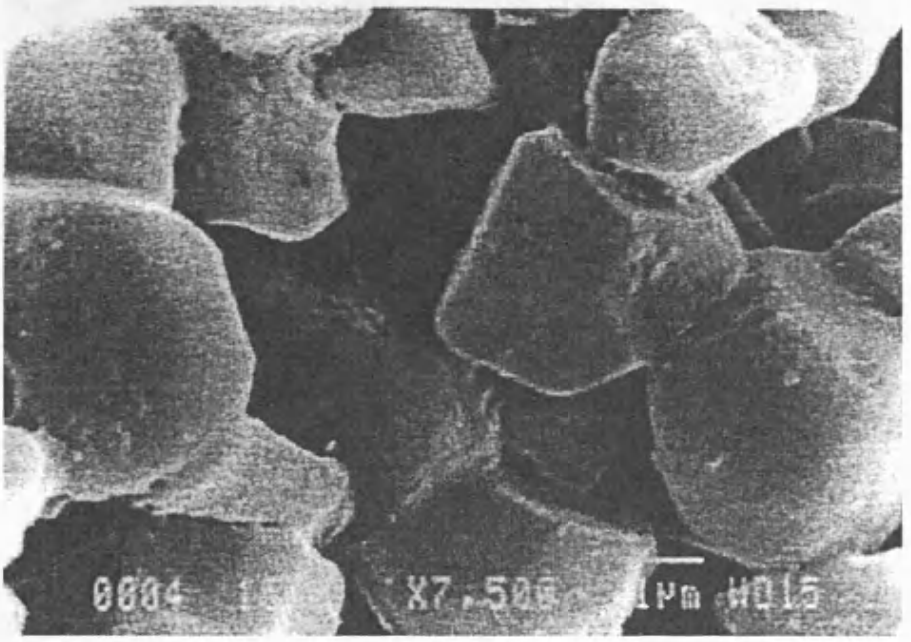

Figure 2.4 Scanning electron micrograph showing rice starch granules covered with colloidal aluminium hydroxide particles in an underdosed state prior to optimal (sweep) coagulation (Bache et al., 1999).

At high aluminium sulphate concentrations ($\geq$ 30 μM $Al_2(SO_4)_3$), colloidal hydroxide particles form a coating on primary particles, reversing their charge. Aggregation of the colloidal hydroxide particles then occurs, either on the particle surfaces or in bulk solution and effecting sweep coagulation, which the primary particles are embedded in an amorphous precipitate (see Figure 2.5) although details of this process still remains unclear (Duan and Gregory, 2003).

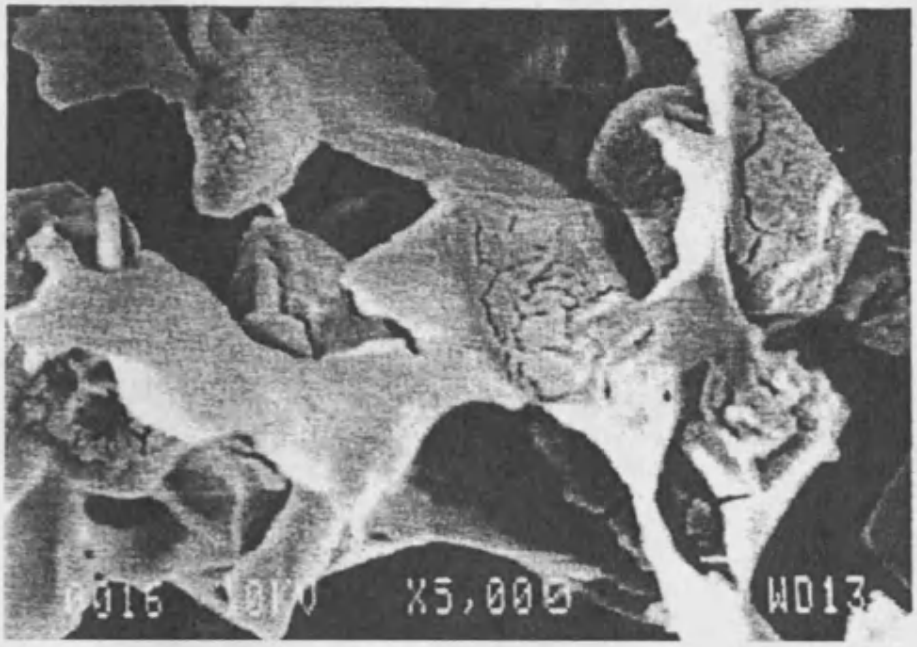

Figure 2.5 Scanning electron micrograph showing rice starch granules covered with colloidal aluminium hydroxide particles in an overdosed state beyond optimal (sweep) coagulation, together with artefact of the bulk precipitate caused by the dyeing process during sample preparation (Bache et al., 1999).

Duan (1997) demonstrated the differences between particle destabilisation through charge neutralisation and sweep coagulation by coagulating kaolin particles with 5 μM and 40 μM $Al_2(SO_4)_3$ respectively at pH 7 under the same conditions. Figure 2.6 shows that for 5 μM alum where charge neutralisation is the operative mechanism, flocculation takes place almost immediately after coagulant dosing but the floc growth is gradual and slow and a plateau (limiting floc size) is reached soon after depending on the stirring rate. For 40 μM alum (sweep coagulation), the onset of floc formation is considerably delayed after coagulant dosing but followed by a very rapid floc growth resulting in flocs several times the size of those formed under charge neutralisation.

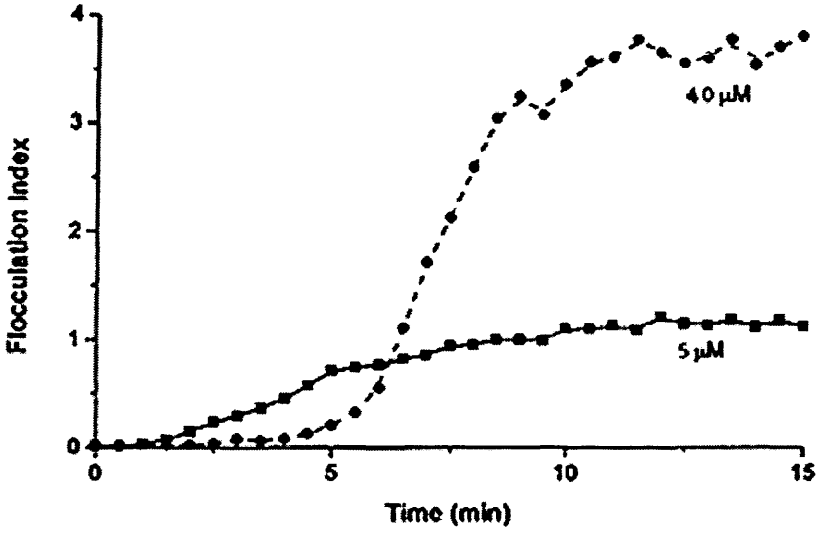

Figure 2.6 Flocculation curves showing the differences between particle destabilisation through sweep coagulation and charge neutralisation (Duan, 1997).

Precipitate entrapment generally gives better particle removal than charge neutralisation due to the open structure of the resulting hydroxide flocs, which allows surrounding particles to be further captured (Duan and Gregory, 2003). In addition, particle destabilisation under conditions of precipitate entrapment tends to be more tolerant towards coagulant overdose than particle destabilisation through charge neutralisation, which is clearly an advantage in process control. However, the method of precipitate entrapment usually demands a larger amount of coagulant, which leads to a higher cost of chemicals and produces voluminous sludge which is more difficult to dewater (Bache et al., 1999).

Moreover, particle destabilisation can be achieved by adjusting the pH of a suspension to the i.e.p., which the particles have no net charge. However, it may be impractical if the i.e.p. occurs in an inconvenient pH range (Hogg, 2000).

2.3.2 Effect of Temperature

Camp et al. (1940) found that changes in temperature have no significant effect on floc development as long as the coagulation takes place at the optimum pH. Morris and Knocke (1984), on the other hand, reported that hydroxide flocs are weaker in

conditions of low temperature and flocculants aids are often added to strengthen the flocs in these circumstances.

However, other authors such as Bache et al. (1996) and Hanson and Cleasby (1990) observed that lower temperatures could affect the solubility of aluminium, which subsequently causes the operating pH to shift from the optimum pH. This phenomenon can seriously inhibit floc development, if the pH is left unadjusted (Bache et al., 1999).

2.4 Polymeric Flocculants

Manufacturing control can deliver a wide variety of synthetic polymers of different molecular weights and different charge densities containing chemical groups that undergo electrolytic dissociation in solution resulting in a long chain of highly charged ions. Commercially available polymers are manufactured by a number of companies under a variety of trade names. The most frequently used flocculants are polymers derived from the acrylamide monomer (Mortimer, 1991). The classification of polymers is based primarily on their ionic character, charge density and molecular weight. The selection of a polymer remains a process of trial and error for different types of water.

2.4.1 Structure of Polymers

Synthetic polymers are obtained through homopolymerisation or copolymerisation of acrylamide monomers. Acrylamide is homopolymerised to form polyacrylamide, a non-ionic polymer (Akers, 1975). Anionic polymers may be obtained by hydrolysing acrylamide (Masschelein, 1992) or by copolymerising acrylamide with acrylic acid or sodium acrylate (Yen, 1976). Cationic polymers may be obtained by copolymerising acrylamide with a suitable cationic monomer, such as dimethylaminoethyl acrylate or methacrylate (Gregory, 1986). Figure 2.7 shows how the neutral amide group may be replaced by other charged groups.

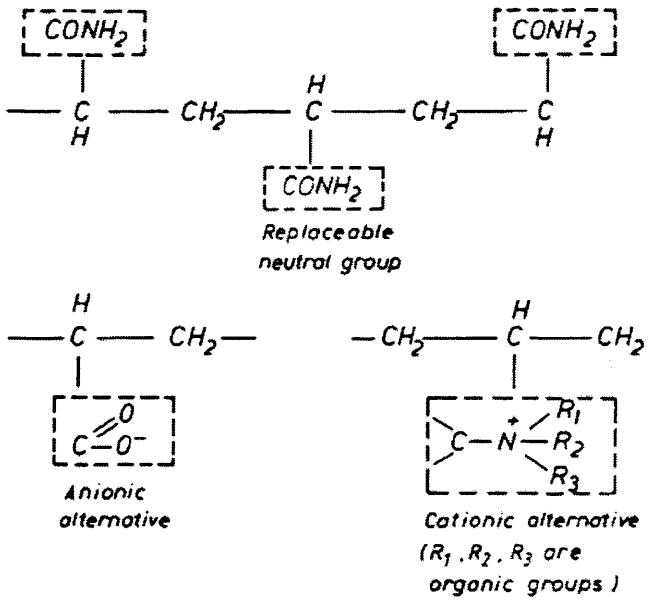

Figure 2.7 Polymer types (Barnes and Wilson, 1983).

2.4.2 Characteristics of Polymers

The charge density and molecular weight of a particular polymer both influence the destabilisation mechanism and resulting floc formation, the degree depending on the type of polymer and the system to which it is applied.

A polymer with low charge density assumes a coiled, almost spherical configuration due to the random diffusion of the polymer segments. At high charge density, stretching of the polymer is significantly increased through intra-molecular electrostatic repulsion between charged units. An increased solution viscosity results. The configuration of polymer is also influenced by the ionic strength of a solution. The polymer becomes increasingly stretched when the ionic strength of a solution is low.

High molecular weight polymers tend to adsorb strongly and essentially irreversibly onto solid surfaces unless opposed by strong repulsive forces (Fleer et al., 1993). In order to take full advantage of the binding action of these polymers, it is necessary to ensure that the polymer is uniformly distributed within the floc structure (Hogg, 1999).

Lower molecular weight polymers ($< 10^5$) function very well as dispersants. Polymers with molecular weight in excess of 10^6 are capable of enhancing floc growth and

strength and reducing floc breakage, especially in previously destabilised suspensions (Hogg, 2000). Adding small amounts of these polymers to a previously destabilised system can increase the limiting floc size (see Section 2.7) to as much as 200 to 300 μm even in a highly turbulent environment (Rattanakawin, 1998).

Polymers with even higher molecular weight (> 10^7) are difficult to dissolve because considerable time is required to untangle the long chains. However, high shear stirring cannot be employed to speed up the untangling of the polymers because of the breakdown of the polymer chains (Bratby, 1980).

2.4.3 Destabilisation with Polymers

Polymers are commonly used to strengthen weak flocs. The two principal mechanisms, which bring about particle destabilisation using polymers, are referred to as the bridging mechanism and the electrostatic patch mechanism. Although they are fundamentally separate mechanisms, the overall mechanism of destabilisation in some instances may be contributed by both phenomena.

2.4.3.1 Bridging Mechanism

Bridging mechanism is mainly associated with the destabilisation of suspended particles using long chain polymers. Before any bridging can occur, polymer segments need to be adsorbed to the suspended particles. The mechanism of the adsorption of polymer segments to a solid surface depends on both the chemical characteristics of the polymer and the adsorbent surface. It is important that the polymer is dispersed evenly throughout the solution for adsorption to occur evenly on all particles because the adsorption of polymers to particle surfaces is essentially irreversible with respect to dilution.

2.4.3.1.1 Adsorption

In the case of non-ionic polymers and polymers bearing the same charge as the suspended particles, several adsorption mechanisms exist such as hydrogen bonding and ionic bonding. Hydrogen bonding occurs when there are suitable hydrogen bonding sites available on the surfaces of suspended particles and non-ionic polymer segments.

Ionic bonding usually occurs when, for example, positive ions in a suspension bind themselves to the anionic polymer and the negatively charged particles, acting as a link between the two. The level of attraction between the polymer and suspended particles is strongly dependent upon the ionic strength of a suspension. Increased ionic strength may also enhance adsorption by reducing repulsion between particles and polymer segments.

Polymer molecules may be transported to suspended particles by diffusion or by applied shear for adsorption to occur. Transport by applied shear is usually more important for high molecular weight polymers and is often employed in practice (Gregory, 1996).

Polymer adsorption to particles by diffusion transport is usually rapid compared to the rate of particle collision. Polymer adsorption to particles by applied shear, on the other hand, can be relatively slow compared to the particle collision rate. This means that particles could collide before they were fully destabilised, which explains the lag time often observed in practice before the onset of observable particle flocculation (Gregory, 1996).

2.4.3.1.2 Bridging

After adsorption has taken place at one segment of a polymer chain, the rest of the polymer chain extends into the suspension and gradually becomes adsorbed at more points along its length to adjacent particles, until eventually there are no dangling ends extending into the suspension thus forming a number of bridges as shown in Figure 2.8.

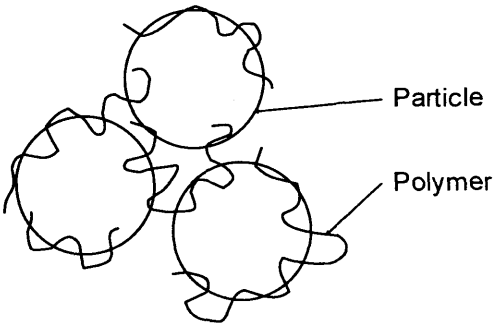

Figure 2.8 Formation of polymer bridges between particles.

The strength of a floc depends on the number of bridges formed between particles as well as the number of available adsorption sites on individual particles to accommodate polymer segments from neighbouring particles. If an excess of polymer is added, too many adsorption sites per particle will be occupied which in turn preventing bridge formation and subsequently causing particles to restabilise.

Healy and La Mer (1964) argued that optimum flocculation occurs when colliding particles are 50% covered with polymer. Bridging may not occur at a lower particle surface coverage when bare particle surface areas are predominant over the few areas with adsorbed polymer due to a lack of contact between the different areas.

Intense mixing may disrupt the formation of polymer bridges and give rise to desorption and rearrangement of polymer segments on the surface of suspended particles. Although efficient mixing is required on polymer addition to a suspension, the mixing should not be too violent and for a long period of time.

2.4.3.2 Electrostatic Patch Mechanism

Kasper (1971) and Gregory (1973) proposed that for a system where the surface charge density of the particles is quite low and the oppositely charged polymer has a high charge density, the bridging model is often inadequate. Rather than adsorption of parts of a polymer chain at only a few sites on the surface of a particle, with the remainder of the unattached polymer segments extending into the suspension to promote bridging, virtually complete adsorption of polymer segments (flat configuration) onto the surface of a particle takes place.

The adsorbed polymer segments thus form a charge mosaic with alternating regions of positive and negative charge (Bratby, 1980) (see Figure 2.9). Destabilisation occurs when the charge mosaics of adjacent particles align to provide strong electrostatic attraction. This phenomenon is described as the electrostatic patch mechanism. Stronger flocs are formed under this mechanism than would be expected of simple charge neutralisation but not as strong as those formed by bridging with long chain polymers (Gregory, 2000).

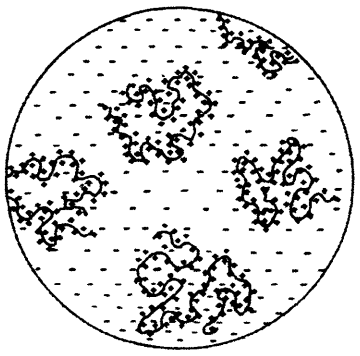

Figure 2.9 Colloidal particle with alternating regions of positive and negative charge (Gregory, 1973).

2.4.4 Ageing of Polymeric Flocculants

Narkis and Rebhun (1966) first reported the ageing of polyacrylamide solutions as a change in solution viscosity over a period of weeks or months. They attributed this to the disentanglement of polyacrylamide molecules and stated that the ageing effect was nothing to do with molecular weight degradation but a change in polymer configuration.

Owen et al. (2002) studied the impact of polymeric flocculant ageing on flocculation performance. They used a commercial high molecular weight non-ionic polyacrylamide to flocculate kaolin particles. The polymer has an average molecular weight of 20×10^6 and it was aged at different periods of time ranging from an hour to 6 days.

They found that the required amount of polymer to achieve measurable flocculation decreased as the age of the polymer increased, with optimal flocculation performance attained at 72 hours of ageing. Flocculation caused by using an an hour old polymer solution consumed 75% more polymer than the optimum. Results from settling tests and focused beam reflectance measurement (FBRM) showed that the ageing of polymer has no effect on the aggregate structure (density); shifts in aggregate density were only observed with variations in mixing intensity.

They attributed the ageing effect to a delay in the release of discrete polymer chains from highly entangled species; polymers of high molecular weight have extensively long chains which tend to tangle, appropriate ageing allows enough time for the long

chain polymers to untangle for flocculation. Further ageing may cause the discrete long chain polymers to re-conform leading to a slightly lower level of flocculation. This is due to the possibility that hydrogen bonds within the structure of the polymer chains are being attacked by water molecules causing the more active extended long chain polymers to become more compact and coiled and less reactive over time (Klein and Westerkamp, 1981; Kulicke and Kniewske,1981; Kulicke, 1986).

2.5 Flocculation

In the colloid literature, the term flocculation is used to describe the mechanism of particle destabilisation, which involves some kind of bridging effect. In water and wastewater treatment practices, however, the term flocculation implies the post coagulation process where large aggregates (flocs) are formed as a result of fluid motion (Gregory, 2000). During the flocculation process, chemically treated water is mixed gently using mechanical stirrers or in-line static mixers, or other more sophisticated techniques such as baffled chambers or gas dispersion which will give equivalent effects to cause particles to collide and agglomerate into larger heavier flocs.

Since there is a net loss of one particle when two particles collide to form an aggregate, the rate of flocculation can be written as the rate of reduction of particle (number) concentration:

$$-\frac{dN}{dt} = \alpha_1 k_F N^2 \qquad (2.6)$$

where N is the particle number concentration, t is the flocculation time, α_1 is the collision efficiency factor (fraction of collisions leading to aggregation) and k_F is the flocculation rate coefficient (depends on collision mechanism).

Three different collision mechanisms involved during flocculation are:

- Brownian motion, which is responsible for perikinetic flocculation.

- Induced velocity gradients (or fluid shear), giving orthokinetic flocculation.

- Differential settling, in which particles of different size (or density) settle at different rates.

Brownian motion is important for particles with diameter smaller than about 1 μm. Shear stress and differential settling, on the other hand, are important for larger particles (Logan and Wilkinson, 1991).

2.5.1 Perikinetic Flocculation

Perikinetic flocculation arises from the natural process of thermal agitation (Brownian movement) which promotes the aggregation of particles. Flocculation during this stage commences immediately after destabilisation. Perikinetic flocculation is only significant for colloidal particles.

As particles collide under the effect of Brownian motion, small flocs are formed, hence the reduction in total particle concentration. Consequently, Brownian motion has progressively less effect on particle movement due to the increase in size and the magnitude of the energy barrier increases progressively in relation to the cross section of the small flocs (Masschelein, 1992).

In water treatment, perikinetic flocculation is not sufficient to give the required floc size and density and the reduction in total particle concentration.

Smoluchowski in 1916 calculated collision frequency between i and j particles assuming that particles diffuse towards a stationary particle in a radial direction:

$$J_{ij} = 4\pi R_{ij}(D_i + D_j)N_i N_j \qquad (2.7)$$

where R_{ij} is the collision radius assuming $R_{ij} = a_i + a_j$. D_i and D_j are the diffusion coefficients. N_i and N_j are the particle number concentrations.

For spherical particles, the diffusion coefficient is given by the Stokes-Einstein equation:

$$D_i = \frac{kT}{6\pi a_i \mu} \tag{2.8}$$

where k is the Boltzmann's constant, T the absolute temperature and μ the dynamic viscosity of a liquid.

If particles are of roughly equal size and every collision leads to aggregation ($\alpha = 1$), the total particle concentration N, falls according to:

$$-\frac{dN}{dt} = 8\pi D_1 a_1 N^2 = k_F N^2 \tag{2.9}$$

(a_1 and D_1 refer to original, primary particles)

The rate constant k_F, is then independent of particle size:

$$k_F = 8\pi D_1 a_1 = \frac{4kT}{3\mu} \tag{2.10}$$

which has a value of 6.13×10^{-18} $m^3 s^{-1}$ for particles in water at 25 °C.

Integration of the rate equation (with $N = N_0$ at $t = 0$) gives:

$$N = \frac{N_0}{1 + k_F N_0 t} \tag{2.11}$$

There is a characteristics halving-time τ, in which the particle concentration is reduced to half of its original value ($N = N_0/2$):

$$N = \frac{N_0}{1 + t/\tau} \tag{2.12}$$

where $\tau = 1/k_F N_0$.

For a suspension of $N_0 = 2 \times 10^{13}$ m^{-3} (corresponds with the amount of latex used for experiments described in Sections 3.1 and 3.2) at 25 °C, it would require 2.3 hours for the particle concentration to fall to half of its original value.

2.5.2 Orthokinetic Flocculation

Orthokinetic flocculation arises from induced velocity gradients of liquid. Such velocity gradients occur in flocculation systems through mechanical mixing, disturbing flow pathways through sludge blanket or filter layers. The effect of velocity gradients within a body of liquid is to promote relative velocities between particles thereby providing opportunity for contact.

The Smoluchowski treatment (1917) for uniform shear field gives the collision rate as:

$$J_{ij} = \frac{4}{3} N_i N_j (a_i + a_j)^3 G \tag{2.13}$$

where G (dv/dz) is the local velocity gradient or shear rate.

For identical spheres, radius, the initial flocculation rate, assuming $\alpha = 1$, is given by:

$$-\frac{dN}{dt} = \frac{16}{3} N_0^2 G a_1^3 ; k_F = \frac{16}{3} G a_1^3 \tag{2.14}$$

The rate depends on the cube of the particle size, unlike perikinetic flocculation, where the rate is almost independent of particle size.

Comparing the two rate constants:

$$\frac{k_F(ortho)}{k_F(peri)} = \frac{4G\mu a_1^3}{kT} \tag{2.15}$$

For $G = 10\ s^{-1}$ and 20 °C in water, the rates are equal when $a_1 \approx 0.5$ μm. The perikinetic rate becomes much slower than orthokinetic rate when there are larger particles and higher shear rates.

Alternatively, orthokinetic rate can be formulated in terms of the volume fraction of suspended particles (solids concentration) ϕ. For spherical particles, with number concentration N_0, this is:

$$\phi = \frac{4}{3} N_0 \pi a_1^3 \tag{2.16}$$

The degree of flocculation is greatly influenced by ϕ. Flocculation tends to be more rapid if there is a high level of solids. If ϕ remains constant during a flocculation process:

$$-\frac{dN}{dt} = \frac{4G\phi N}{\pi} = k_1 N \tag{2.17}$$

Integral form:

$$\ln\left(\frac{N_0}{N_t}\right) = k_1 t = \frac{4Gt\phi}{\pi} \tag{2.18}$$

However, the assumption of a constant volume fraction of solids during a flocculation process is not realistic in most cases, since flocs usually adopt a rather open, fractal structure, as they grow larger. This means that the occupied volume can be much larger than the actual volume of the primary particles.

The *Camp number Gt* is a dimensionless number often used to characterise flocculation units (degree of flocculation) in water treatment plants. A certain value of *Gt* could be

achieved either with a high shear rate for a short time or a low shear rate for a longer time, provided that Gt is kept constant. This ignores the breakage of flocs, which occurs at high shear rates.

All practical flocculation processes take place under turbulent conditions, therefore the Smoluchowski treatment of uniform laminar shear is no longer applicable. In this case, Camp and Stein (1943) derived an effective shear rate $\overline{G}$, in terms of the average power input P, to a volume of fluid V:

$$\overline{G} = \sqrt{\frac{P}{\mu V}} \tag{2.19}$$

2.5.3 Differential Settling

Differential settling refers to the process in which collisions of particles arise from particles of different size or density settling at different rates. If particles in suspension are settling at different velocities, then the faster settling particles may collide with slower settling particles, leading to aggregation. The flocs will then settle faster due to their increased mass, and possibly experience further collisions and aggregations (Ives, 1978). This becomes an important flocculation mechanism when flocs have grown quite large.

In this case, the collision frequency between i and j particles is given by:

$$J_{ij} = \frac{2\pi g}{9\mu} N_i N_j (\rho_s - \rho)(a_i + a_j)^3 (a_i - a_j) \tag{2.20}$$

where g is the acceleration due to gravity, ρ_s and ρ are the densities of particle and water respectively.

2.5.4 Hydrodynamic Effects

The previous treatment of flocculation rates has assumed that all particle collisions lead to permanent attachment (see Sections 2.5.1 and 2.5.2). However, the effect of hydrodynamic forces can prevent particles from coming into close contact, even when

there is no repulsion between particles. Hydrodynamic effects arise because displacement of fluid within the narrowing gap between colliding particles becomes increasingly difficult (Thomas et al., 1999).

Hydrodynamic effects in perikinetic flocculation reduce the particle diffusion coefficients at close approach. In the absence of any other interactions such as van der Waals forces and long-rage attractive forces, this effect would prevent particle aggregation altogether. In practice, hydrodynamic resistance reduces the rate of perikinetic flocculation by a factor of about two.

In orthokinetic flocculation, hydrodynamic effects are more important and can significantly reduce the flocculation rate. They cause particles in shear flow to deviate from rectilinear paths, which can greatly reduce the collision rate of hard spheres (Lee, 1991). This effect is probably less important for flocs, because they usually have a rather open structure, with some permeability (Wolynes and McCammon, 1977).

2.6 Importance of Mixing

The most important functions of mixing in water and wastewater treatment practices are:

- to disperse destabilising agents evenly within a system for effective particle destabilisation (rapid mixing); and

- to promote the growth of flocs until they are large enough be removed by follow-up purification processes (slow mixing).

Rapid mixing tends to be brief and is usually employed after the addition of destabilising agents and followed by a long period of constant slow mixing. Depending on the rate of shear employed during slow mixing, flocs of different structures may result. Stronger and more compact but smaller flocs are usually formed under high velocity gradients due to a continuous breakdown of the larger parent flocs. Large porous flocs tend to form under low velocity gradients but a longer time is required to reach the optimum floc size. For a given velocity gradient there will be a limiting flocculation time beyond which floc particles will not grow further. The break-up of

large flocs under high shear rates can offer a simple method of increasing floc compactness and suggests that some degree of floc fragmentation by fluid shear may not always be undesirable (Spicer et al., 1998).

2.6.1 Rapid Mixing

There are different views concerning the importance of rapid mixing on coagulation and flocculation. Han and Lawler (1992) claimed that the main reason behind mixing is to keep growing aggregates suspended without breakage; they believed that mixing should be kept minimal. Dharmappa et al. (1993), on the other hand, found that the most important parameter for optimal coagulation and flocculation is rapid mixing. Studies focused on the nature of coagulants and the different mechanisms involved in relation to rapid mixing have been subjected to a lack of consideration towards the break-up of aggregates during rapid mixing (Bache et al., 1999; Rossini et al., 1999).

It is often difficult to justify the importance of rapid mixing when recommendations proposed by different researchers tend to contradict one another. For example, in studying the effect of rapid mixing on alum-induced coagulation, Amirtharajah and Mills (1982) found that rapid mixing is significant if adsorption and charge neutralisation are the principal mechanisms instead of precipitate entrapment, while researchers such as Rossini et al. (1999) found that rapid mixing has significant effects on residual turbidity based on their jar test study using alum.

Although evidence suggests that rapid mixing has no apparent effect on the settled water turbidity as a function of time (Amirtharajah and Mills, 1982; Rossini et al., 1999), effective rapid mixing can lead to the formation of stronger flocs by exploiting the electrostatic bonding between primary particles. In another study on flocculation by synthetic polymers, rapid mixing was found to be critical in colloid bridging (Amirtharajah and Jones, 1996).

2.6.2 Mixing of Polymers

The adsorption of polymer molecules on particles and the formation and breakage of particle-particle bonds are all affected by the nature of the applied velocity gradients.

Polymers are often made into rather viscous stock solutions before being added to suspensions. Small lumps of polymer can often be seen mixing with a suspension which may either take a long time to dissolve or act as primary particles for floc formation. Poor mixing of polymers can lead to local overdosing and restabilisation of some particles which leads to the formation of cloudy residue in some flocculated suspensions (Gregory and Li, 1991).

Although theoretically, intense mixing would be a good way to disperse polymers, polymer chains can be broken under high shear rates. As a consequence, degradation products become less effective as flocculants. Irreversible flocculation can also occur under such condition that flocs do not re-form from the fragments. In addition, prolonged mixing without further addition of polymer is found to cause irreversible floc breakage. Extremely short mixing time, on the other hand, can lead to reduced floc size and increased floc fragility due to poor polymer adsorption (Hogg, 1999).

2.7 Floc Breakage

Essentially, a floc is made up of primary particles, which are bound together to form an irregular structure incorporating a substantial amount of fluid within its framework. Most flocs are formed under fluid motions and as they grow larger, they are also broken by the shear stresses created by the fluid forces.

A limiting floc size is reached after a characteristic time of shear-induced flocculation, when equilibrium is established between the growth and the fragmentation of flocs. This phenomenon is dependent upon the power input P, which is related to the effective shear rate (mean velocity gradient) $\overline{G}$ (see Equation 2.19).

The maximum floc size d_{max}, is given by the following empirical expression:

$$d_{\max} = C_1 P^{-n} \tag{2.21}$$

where C_1 and n are constants (Gregory, 2000). Depending on the mode of break-up, the value of n is usually around 0.2 to 0.4 (Thomas, 1964; Argaman and Kaufman, 1970; Parker et al., 1972; Tomi and Bagster, 1978; Tambo and Hozumi, 1979; Sakurai and

Harano, 1982; Francois, 1987; Ivanauskas, 1984; Ivanauskas et al., 1985; Mühle et al., 1989; Leentvaar and Rebhun, 1983).

The ability of a floc to withstand breakage caused by fluid forces is dependent upon the compactness, shape and the size of the floc as well as the strength of the particle-particle bonds. It is evident that primary particle bonding is influenced by electrostatic forces and the strength of a floc deteriorates when such bonding is poor within the floc structure. Unsatisfactory dewatering and inefficient adsorption of non-ionic polymer for strengthening and sludge conditioning are often related to bulk precipitates formed with impaired primary particle bonding within the structure (Bache et al., 1999).

Under shear stresses, larger flocs tend to break at the weakest points in the floc structure, which produce smaller but stronger and more compact flocs (Ives, 1978). Small flocs may also be subject to surface erosion under fluid motions (Gregory, 2000).

Moreover, flocs consisting primarily of hydroxide precipitates tend to erode and break more easily than those consisting mainly of primary particles due to the weak bonding exists between precipitates within the floc structure. Such structure is subject to breakdown, which leads to filter breakthrough (Bache et al., 1999).

2.7.1 Turbulence Modelling in Flocculation

An isotropic model has been adopted to describe turbulence in flocculation as a series of eddies of decreasing size. Although large eddies formed under fluid motions possess most of the fluid's kinetic energy, the energy is transferred via a series of energy dissipating eddies of decreasing size where it is eventually dissipated by viscous forces.

The length scale of the smaller energy-dissipating eddies, is called the Kolmogorov microscale:

$$\lambda = \left(\frac{\nu^3}{\varepsilon'}\right)^{\frac{1}{4}} \tag{2.22}$$

where λ is the Kolmogorov microscale, ν the kinematic viscosity and ε' the rate of energy dissipation (Thomas et al., 1999).

It is generally accepted that fragmentation occurs when flocs are larger than the Kolmogoroff microscale, while erosion of floc surfaces occurs when flocs are smaller than the Kolmogoroff microscale (Mühle, 1993). However, experimental work by Yeung and Pelton (1996) suggested that more compact flocs were more likely to undergo surface erosion whereas less compact flocs were more likely to undergo fracture.

2.7.2 Reversible and Irreversible Floc Breakage

Two types of floc dynamics have been observed: reversible and irreversible floc dynamics. Reversible floc dynamics applies to flocs, which are capable of returning to their original average floc size after breakage when the original shear rate is re-applied. Irreversible floc dynamics, on the other hand, applies to flocs which are unable to attain their original average floc size after breakage when the original shear rate is re-applied.

Reversible floc breakage occurs when primary particles are destabilised with an ionic salt, for example, NaCl. Reversible floc breakage is possible because the van der Waals binding forces between primary particles are not affected by floc fragmentation and re-growth. Irreversible floc growth occurs when the destabilising agent is either a polymer or a precipitated solid, for example, $Al(OH)_3$ (Spicer et al, 1998). Yukselen and Gregory (2004) studied the reversibility of alum flocs under high shear. They found that only limited re-growth of flocs occurred when the original shear rate was restored, indicating a significant irreversibility of the floc break-up process.

It has been suggested that flocs formed using hydrolysing metal salts tend not to have the same structure as the original flocs when the original mixing speed is re-applied after breakage, instead smaller but denser flocs are formed (Clark and Flora, 1991; Francois, 1987).

2.8 Fractal Nature of Flocs

Flocs formed from random aggregation processes are generally mass fractals, meaning that the floc structure is scale-invariant. A schematic structure consisting of fractal units is shown in Figure 2.10. The growth of flocs, under many conditions, leads to rather

open fractal structures, for which the effective density decreases as the size increases (Gregory, 1997).

The relationship between the mass M and size L_2 of a floc is given by:

$$M \propto L_2^{D_F} \tag{2.23}$$

where D_F is the fractal dimension which describes the way in which the floc solids are distributed throughout the floc volume (Gregory, 1997); the lower the D_F, the more open is the floc structure.

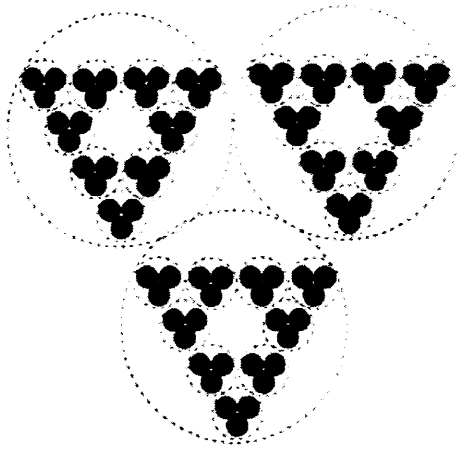

Figure 2.10 Two dimensional model of self-similar structure (Gregory, 1997).

2.9 Simulation of Flocs

When solid particles aggregate, the resulting flocs may adopt many different structures. Simulation models have been developed to enable floc structure to be characterised and two of the most commonly used simulation models are:

- Diffusion limited aggregation (DLA)
- Reaction limited aggregation (RLA)

The RLA model suggests that not all particles adhere at the first contact due to a certain level of repulsion exists between them. Therefore, particles are more able to inter-penetrate into the floc structure. A variety of floc structures tend to form under RLA conditions.

The DLA model, on the other hand, suggests that there is no repulsion between colliding particles and that each particle collision leads to attachment. Flocs formed under DLA conditions tend to be less compact and less dense than those formed under RLA conditions.

In addition, floc structures can be described in terms of particle-cluster aggregation and cluster-cluster aggregation. With the particle-cluster aggregation model, a particle is able to penetrate some way into a cluster before encountering another particle and sticking as shown in Figure 2.11. For the cluster-cluster aggregation model, attachment between two clusters occurs at the first contact without inter-penetrating into one another to a significant extent as shown in Figure 2.12, which leads to a much more open structure (Strenge, 1993).

Figure 2.11 Particle-cluster aggregation model (Gregory, 1997).

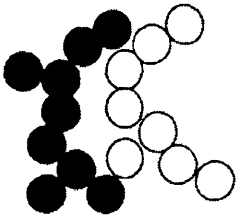

Figure 2.12 Cluster-cluster aggregation model (Gregory, 1997).

However, in many cases, single-particle addition to growing clusters is not a realistic model, since, throughout most of an aggregation process, growth occurs as a result of cluster-cluster encounters which leads to rather open structures, for which the effective density decreases as the size increases (Gregory, 1997).

The two limiting regimes of cluster-cluster aggregation have been well researched and it is now generally recognised that diffusion limited cluster-cluster aggregation and reaction limited cluster-cluster aggregation yield aggregate mass fractal dimensions of 1.75 and 2.1 respectively (Glover et al., 2000).

2.10 Filtration

In general, filtration is the separation of solid particles from a suspension. Different basic filtration techniques exist which are distinguished by the way separation is accomplished. Figure 2.13 shows the basic mechanisms of cake filtration, cross-flow membrane filtration and deep-bed filtration.

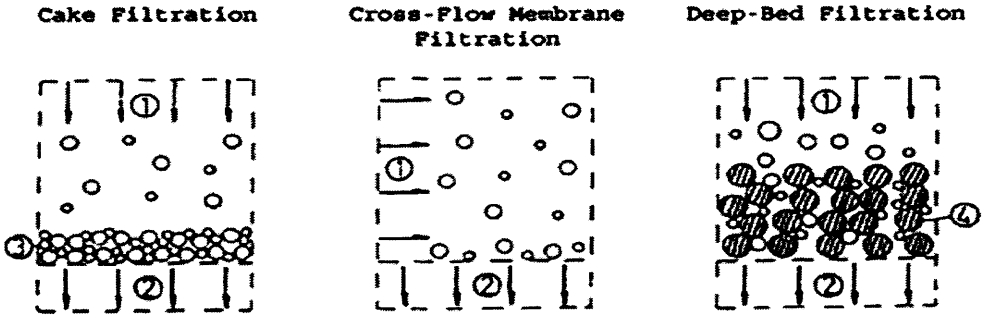

Figure 2.13 Principal filtration methods. 1, suspension flow; 2, filtrate flow; 3, filter cake; 4, filter grains layer (Stroh, 1993).

2.10.1 Deep-Bed Filtration

Deep-bed filtration is usually applied to the clarification of extremely fine to colloidal size particle suspensions with low solids contents (< 1% by volume) (Stroh, 1993). Filtration of this kind involves the deposition of particles within the coarse pores of a granular medium, for example, a bed of sand, gravel or activated carbon.

Filter cleaning is necessary and a backwash procedure is carried out when the filtration rate or required filtrate quality can no longer be maintained (Tebbutt, 1990). Deep-bed filtration is commonly used for water purification and beverage production processes (Stroh, 1993).

2.10.2 Cross-Flow Membrane Filtration

Cross-flow filtration is advantageous for the clarification of colloidal particle suspensions of low solids contents, which are difficult to filter. Cross-flow filtration is commonly employed in food or beverage processing and environmental control (Stroh, 1993).

Cross-flow filtration involves the retention of particles on the surface of a filter medium, which is usually a membrane in a specific configuration. Filtration of this kind is so effective that the filtrate is almost free of particles. During the filtration, it is important to avoid fouling of the filter media, by a customised backwash procedure depending on the nature of the fouling (Lau, 2000) or the filtration rate will be decreased drastically due to a high permeation resistance (Stroh, 1993).

2.10.3 Cake Filtration

Cake filtration; sometimes referred as dead-end filtration, is the major mechanism of moisture removal in most low-pressure mechanical filtration systems due to the low cost and easy operation (Wu et al., 2003a). Filtration of this kind is usually applied to suspensions with a high solids content (> 10% by volume) (Stroh, 1993).

Cake filtration involves a porous filter medium, which acts as a cake formation initiator and a cake support. Under the influence of a driving pressure difference, the solids contained in a suspension are retained on the surface of the filter medium forming a superficial filter cake which itself becomes the principal filter medium, while the filtrate is extracted on the downstream side of the medium (Stroh, 1993). The pressure difference can be achieved simply by raising pressure on one side of the filter medium or by utilising gravitational force on the filter medium. In vacuum filtration, a negative pressure is applied to the filter medium (Way, 1983).

It has always been observed that high concentrations of dispersed particles have a negative effect on filtration rates (Mikkelsen and Keiding, 2002). During the filtration cycle, suspensions with a high content of both fine and deformable particles can lead to the blinding of filter medium and the formation of dense cakes with extremely high permeation resistances (Sorensen et al., 1995).

In order to establish an acceptable filtration rate, coagulation and flocculation are often employed prior to filtration to provide aggregates of high porosity to allow an adequate permeability, for without them the filtration of such suspensions is not economically viable (Stroh, 1993).

2.10.3.1 Filterability of Coagulated and Flocculated Suspensions

The filterability of a suspension can be improved through coagulation and flocculation. Higgins and Novak (1997a and 1997b) have shown that the dewatering and settling of activated sludge can be improved by adding Ca^{2+} and Mg^{2+} as soluble salts to the sludge. Yukselen and Gregory (2002) studied the dewatering properties of kaolin flocs formed using alum, polyaluminium chloride and a cationic polymer, they found that cationic polymer flocculated kaolin flocs gave the best dewaterability, while alum coagulated kaolin suspension gave the least.

The filterability of coagulated and flocculated suspensions depends on the structure of the aggregates and their modification due to liquid flow and applied pressure (Hogg, 2000). Filterability is strongly influenced by the aggregation of particles due to the comparatively small effective surface area of aggregates relative to individual particles. Also the aggregates may pack less effectively, leading to a higher porosity and subsequently an increased permeability. The filterability of coagulated or flocculated suspensions can be a useful means of assessing the performance of coagulants and polymeric flocculants, and used as an indication of the degree of coagulation and flocculation (La Mer, 1966; Gregory and de Moor, 1984; Yukselen and Gregory, 2002). For this reason, various tests have been developed based on the filterability of suspensions to measure the specific resistance to filtration.

Conventional filterability tests are time consuming and subject to some uncertainties. The Buchner funnel test is rather inconvenient and time consuming for routine

measurements, although the specific resistance to filtration may be easily calculated if the curve obtained by plotting the volume of filtrate against time is parabolic due to the increasing thickness of deposited particles (see Section 2.10.3.3) (de Moor and Gregory, 1982).

Tests based on the measurement of re-filtration rates developed by La Mer (1966) to assess the performance of polymeric flocculants has not been widely applied due to some uncertainties (Uriarte, 1971).

The measurement of capillary suction time (CST) developed by Gale and Baskerville (1960 and 1967) is a very rapid technique for the determination of suspensions filterability, but it does not give absolute values of specific resistance (Gregory and de Moor, 1984) and it is only useful for suspensions with quite high suspended solids concentration (> 1%) such as sludge (de Moor and Gregory, 1982).

2.10.3.2 Filter Cake Compressibility

The compressibility of aggregates plays a major role in characterising the structure and filterability of a filter cake (Wu et al., 2003a). Filter cakes consisting primarily of metal hydroxides are subject to deformation under pressure (Barnes and Wilson, 1983). Flocculated suspensions tend to produce highly compressible filter cakes (Grace, 1953; Hogg, 2000), which exhibit reducing porosity and hence increasing specific resistance with increasing pressure (Barnes and Wilson, 1983).

The compressibility of a filter cake can be controlled to some extent according to the amount of polymer added to a suspension. High compressibility can be obtained by rapid addition of a relatively small amount of polymer to a suspension, while a high polymer dosage can be used to reduce compressibility (Hogg, 2000).

In addition, the compressibility of a filter cake can be reduced by slowly adding polymer to a suspension. This also helps to ensure uniform distribution of polymer within the filter cake and to strengthen the integrity of flocs which is important in reducing cake cracking in vacuum filtration (Hogg, 2000). However, strong flocs do not guarantee optimal dewatering efficiency and floc strength has very little influence on the dewatering by vacuum filtration (Wu et al., 2003a)

2.10.3.3 Specific Resistance to Filtration

When a suspension is filtered through a membrane with pore sizes smaller than the particles of the suspension, the pores become blocked, followed by the formation of a filter cake, which increases in thickness with further deposition of particles (de Moor and Gregory, 1982). The thicker the filter cake becomes the higher the resistance to filtration is likely to be. The total resistance to filtration R_T is inversely related to permeability and is defined in terms of the volume flow rate (Gregory and de Moor, 1984). The rate of filtration defined by Carman (1938) is:

$$\frac{dV}{dt} = \frac{F\Delta P}{\mu R_T} \tag{2.24}$$

where F is the area of the filter and V is the volume of filtrate produced in a time t. ΔP is the pressure difference between the filter cake and the membrane filter and μ is the dynamic viscosity of the fluid.

R is a combination of the filter cake resistance R_c and the membrane resistance R_m. If R_m remains constant and all particles are removed to give a uniform filter cake, then:

$$R = R_m + \frac{\alpha_2 cV}{F} \tag{2.25}$$

where c is the concentration of the suspension and α_2 is the specific resistance to filtration.

Darcy's law gives the relationship between permeability and laminar flow rate through a homogenous filter cake:

$$\mathrm{v} = \frac{K\Delta P}{\mu H} \tag{2.26}$$

where v is the velocity of the approaching fluid, K is the permeability of the filter cake and H is the depth of the filter cake.

The permeability K is characteristic of the filter cake and is related to the cake structure by the Carman-Kozeny equation:

$$K = \frac{\varepsilon^3}{5S^2(1-\varepsilon)^2} \tag{2.27}$$

where ε is the porosity of the filter cake and S is the specific surface. The value 5 in the Carman-Kozeny equation is an empirical constant. However, for many systems of interest, the value is very close to 5 (Gregory and de Moor, 1984).

Specific resistance to filtration should depend only on the physical characteristics (size, shape and density) of the suspended particles and their state of aggregation. The specific resistance to filtration is related to the permeability K_2 by:

$$\alpha = \frac{1}{K_2\rho(1-\varepsilon)} \tag{2.28}$$

where ρ is the density of the particles (Gregory and de Moor, 1984).

Substituting R from Equation 2.25 into Equation 2.24 followed by integration at constant ΔP constant gives the well-known parabolic filtration equation:

$$t = \frac{\mu}{F\Delta P}\left(R_m V + \frac{\alpha c V^2}{2F}\right) \tag{2.29}$$

Linearisation gives:

$$\frac{t}{V} = \frac{\mu R_m}{F\Delta P} + \left(\frac{\mu\alpha c}{2F^2\Delta P}\right)V \tag{2.30}$$

If the volume of filtrate is measured as a function of time under constant pressure, then a plot of t/V against V should give a straight line (see Figure 2.14), the slope of which can be used to calculate the specific resistance to filtration. Equation 2.30 is based on a number of assumptions and may not apply in all cases, especially if the filter cake is compressible (Gregory and de Moor, 1984).

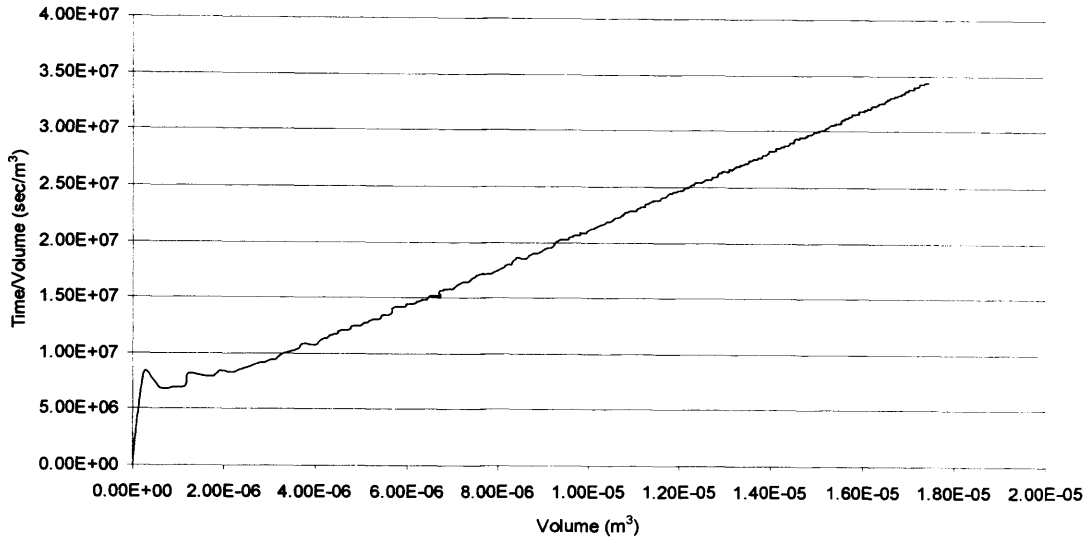

Figure 2.14 Time/Volume against Volume plot for a kaolin suspension.

Equation 2.30 can be presented as:

$$\frac{t}{V} = \text{constant} + bV \tag{2.31}$$

in which the slope of the straight line b is given by:

$$b = \frac{\mu c \alpha}{2F^2 \Delta P} \tag{2.32}$$

2.10.4 Hydrodynamic Permeability of Flocs

A floc is composed of individual clusters of self-similar fractals (Rogak and Flagan, 1990) and the overall permeability of a floc is dependent on the distribution of pore sizes within its structure relative to the number and sizes of these clusters (Jullien and Botet, 1987). Pores formed between the largest clusters are capable of controlling the overall permeability of a floc (Li and Logan, 2001).

Several research studies have suggested the possibility of fluid flowing through flocs as well as around them depending on their porosities. Tsou et al. (2003) studied the fluid-flow through free-settling sludge flocs using a bubble tracking technique. They found

that approximately 55 to 76% of the approaching fluid flowed through rather than around the flocs under test. Li and Logan (2001) carried out a similar study based on the Brinkman (1947) equation and found that more than 40% of the fluid flow approaching a free-settling floc with fractal dimension $D_F = 1.7$ could flow through its interior.

Using the same equation, Vanni (2000) found that for highly porous flocs, fluid is able to flow efficiently through the floc structure. Fluid-flow through more compact flocs ($D_F \geq 2$), on the other hand, was found to be more distorted due to the increasingly impermeable floc structure towards the centre and therefore takes an alternative route along the edge of the floc instead where permeability is higher. For highly compact flocs ($D_F \geq 2.5$), the permeability of the floc is so low that it can be regarded as impermeable.

However, aggregates occurring naturally may have multi-level structure (Clark and Flora, 1991; Jorand et al., 1995; Sanin and Vesilind, 1996, Lee, 1999, Biggs et al. 2000) and a single fractal dimension is often insufficient to characterise the interior structure of a floc (Wu et al., 2002). Gorczyca and Ganczarczyk (1999) and Wu et al. (2000) proposed that a floc is composed of micro-flocs, which are themselves formed from flocculi consisting of primary particles as shown in Figure 2.15. Since floculi, micro-flocs, and flocs exhibit different structures, two or more fractal dimensions may be required to confirm the overall permeability of a floc.

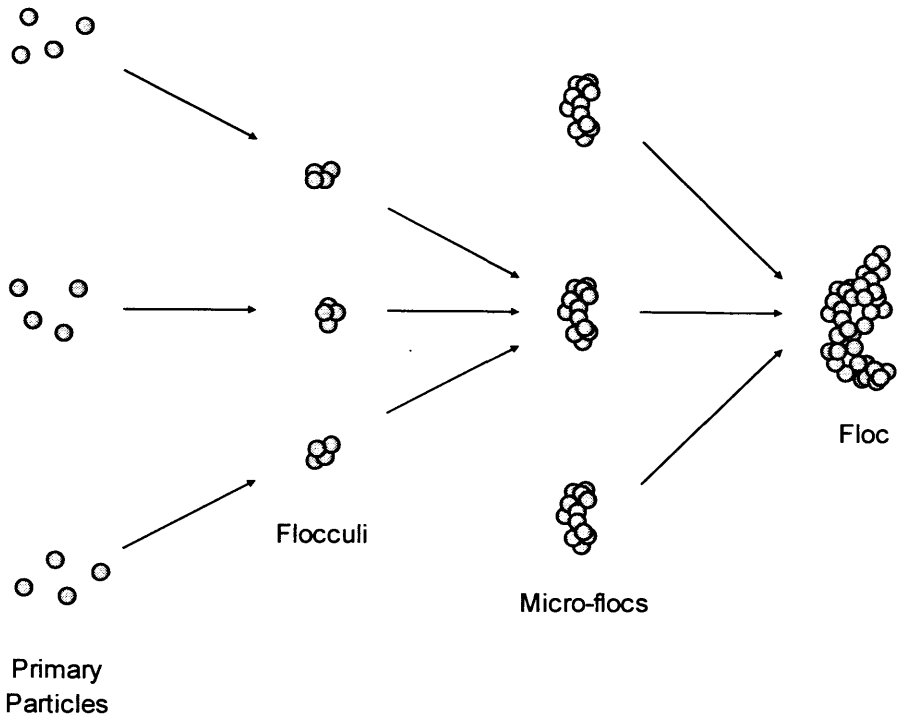

Figure 2.15 Successive development of a floc with multi-fractal dimensions.

2.11 Particles Commonly Used for Flocculation Studies

Kaolinite and synthetic latex particles are widely used as model particles for colloid and flocculation studies. The popularity of these particles arises not only from their fine size but also from their ready availability.

2.11.1 Kaolin

Kaolin is a soft white clay composed chiefly of the mineral kaolinite. Kaolin is very important in the ceramics industry and it is used extensively as a filler in the manufacture of rubber, paper, paint and textiles and as a constituent of medicines (Isaacs et al., 1991).

Pure kaolinite ($Al_2Si_2O_5OH_4$) has a simple structure and it is resistant to weathering (Coles and Yong, 2002). Kaolinite is considered to be crystalline when many layers of the kaolinite are hydrogen bonded together (Bohn et al., 1985; Sposito, 1989; Yong et

al., 1992). Images of some well-crystallised Kiralyhegy kaolinite obtained by scanning electron microscopy (SEM) are shown in Figures 2.16 and 2.17.

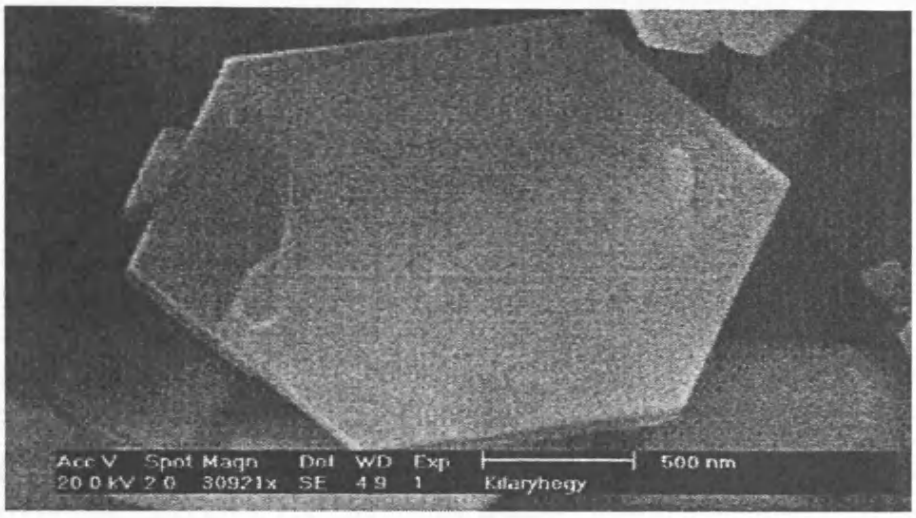

Figure 2.16 Scanning electron micrograph showing the top surface of a well crystallised hexagonal Kiralyhegy kaolinite (Zbik and Smart, 2002).

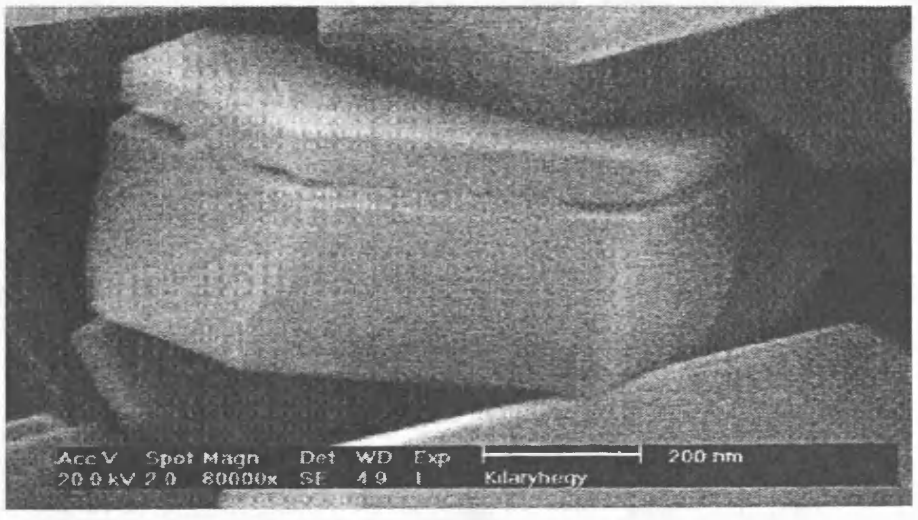

Figure 2.17 Scanning electron micrograph showing the sides of a crystalline Kiralyhegy kaolinite (Zbik and Smart, 2002).

Kaolinite is composed of a single sheet of octahedrons and a single sheet of tetrahedrons with oxygen atoms linking the two in between as shown in Figure 2.18. A single octahedral unit consisted of two sheets of closely packed oxygen atoms or hydroxyls in which an aluminium ion is embedded in an octahedral coordination as shown in Figure 2.19. A single tetrahedral unit, on the other hand, consisted of oxygen atoms or

hydroxyls with a silicon atom located right in the middle of the tetrahedron as shown in Figure 2.20.

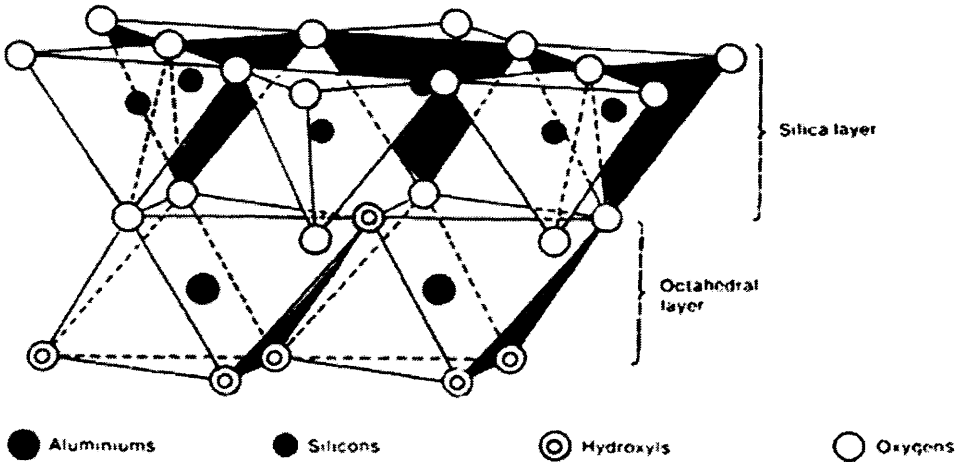

Figure 2.18 Schematic sketch of the structure of kaolin (IDF, 1988).

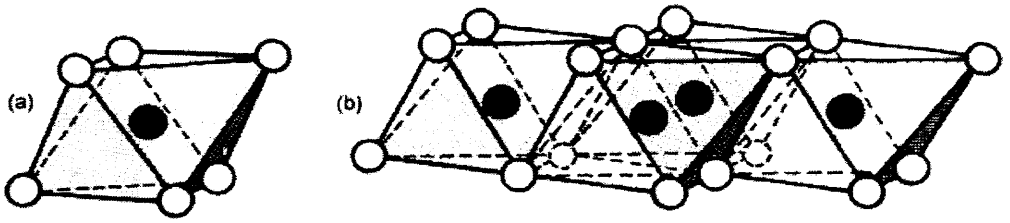

Figure 2.19 Schematic sketch of (a) a single octahedral unit, and (b) a sheet of octahedral units (IDF, 1988).

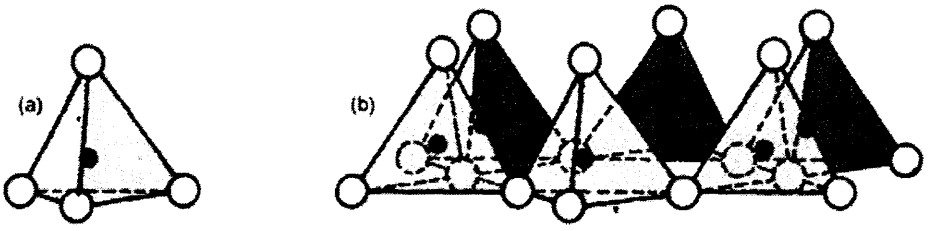

Figure 2.20 Schematic sketch of (a) a single silica tetrahedron, and (b) a sheet of silica tetrahedrons arranged in a hexagonal network (IDF, 1988).

The layered structure has a unit cell thickness of 0.713 nm according to Grim (1968). The charge of the surface built up of silica tetrahedrons is not influenced by pH. The

surface charge of the sheet of octahedrons and the edges, on the other hand, are pH dependent similar to gibbsite, $Al(OH)_3$. The total charge of the kaolinite basal and edge surfaces is greater when fewer kaolinite layers are bonded together (Coles and Yong, 2002). In addition, it is believed that the sheet of silica tetrahedrons is hydrophobic due to the basal oxygen atoms whereas the edges and the surface built up of octahedrons are hydrophilic (Braggs, 1993; Jepson, 1984).

Values quoted for the specific surface area of kaolinite are from 10 to 20 m^2/g (Yong et al., 1992) or 10 to 50 m^2/g (Uehara and Gillman, 1972). Ferris and Jepson (1975) found that the edges of a Cornwall kaolinite comprise 12% of its total surface area. Much larger edge contribution of 27-34% to the total kaolinite surface area was found via SEM and atomic force microscopy (AFM) studies by Brady et al. (1996) and Zhou and Maurice (1995). Bickmore et al. (2002) estimated an edge contribution to be as large as 33.1% while Zbik and Smart (1999) observed an edge contribution of 26% via AFM measurements for a Georgia KGa-1 kaolinite sample and a North Queensland kaolinite sample.

When a concentrated suspension of plate-like clay particles flocculates under the influence of Brownian motion, three distinctive modes of particle association may occur: face to face (FF), edge to face (EF) and edge to edge (EE) (Van Olphen, 1964). Flocs that are formed under the FF mode tend to be more compact, especially when the primary clay particles are large and thin. Flocs that are formed under the EF and EE modes, on the other hand, tend to be voluminous three-dimensional card house structures (Luckham and Rossi, 1999).

At low pH values (< 5.5), kaolinite forms a card house structure due to the electrostatic attraction between the negatively charged basal surface and the positively charged edge surface as shown in Figure 2.21 (Schofield and Samson, 1953; Braggs et al., 1994).

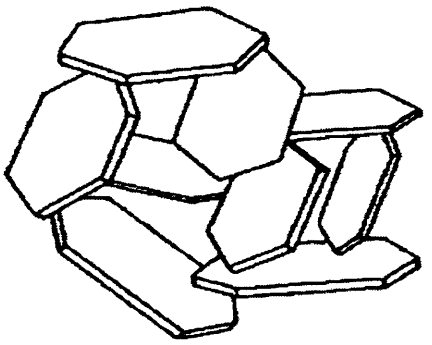

Figure 2.21 Card house structure (Taylor et al., 2002).

At high pH values (> 5.5) both the kaolinite basal and edge surfaces are negatively charged and therefore the particles contact one another in a Bänder model arrangement as shown in Figure 2.22 (Taylor et al., 2002).

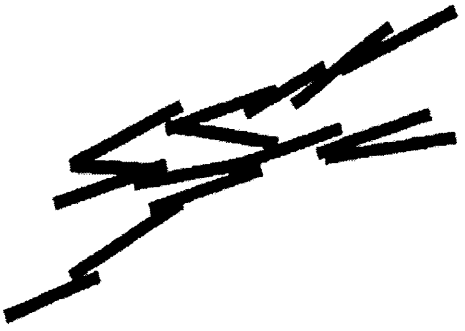

Figure 2.22 The Bänder model (Taylor et al., 2002).

The Bänder model arrangement first proposed by Weiss and Frank (1961) which describes a band like structure is preferred upon the card house theory (Norrish, 1954; Callaghan and Ottewill, 1974).

2.11.2 Latex

Latex particles are spherical polymers produced commercially for a wide variety of applications. Manufacturing control can deliver latex particles with different chemical and physical properties (Ferrick et al., 1989).

Latex particles can be made into different sizes via different methods of polymerisation. Sub-micron latex particles are commonly produced under emulsion polymerisation. Much larger latex particles with diameters of > 100 μm are produced under suspension polymerisation, while latex particles with diameters range from 2 to 20 μm are produced under swollen emulsion polymerisation; also known as the Norwegian process (Bangs, 1984). Latex particles obtained by polymerisation under emulsifier-free conditions using potassium persulphate as a free radical initiator bear mainly sulphate surface groups with a small proportion of carboxylic acid and hydroxyl groups as a result of oxidation during polymerisation (Pefferkorn and Widmaier, 1998).

Uniform latex particles are commonly used as test particles for filter media evaluation; latex particles in the colloidal size range are of special interest for light scattering studies. Figure 2.23 shows a photomicrograph of uniform latex particles.

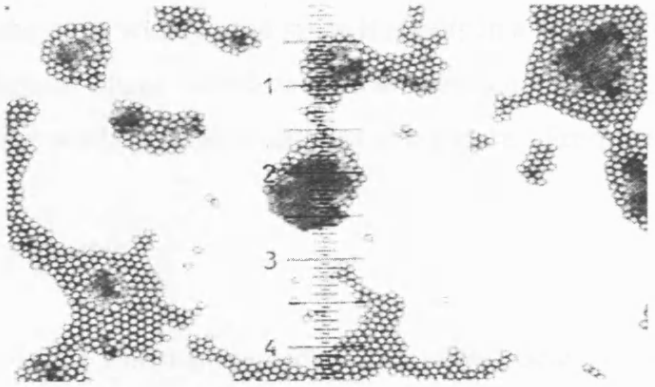

Figure 2.23 Uniform latex particles with mean diameter of 2.020 μm under a magnification of ×548 (Bangs, 1984).

2.12 Determination of the Physical Characteristics of Particles and Flocs

The physical characteristics of particles and flocs, such as size, density and porosity have great influence on the effectiveness of solid-liquid separation processes. Different methods of measurement and monitoring techniques of different nature have been developed to provide quantitative information on the physical characteristics of particles and flocs. In the following sections some methods of measurement and particle monitoring techniques will be reviewed.

2.12.1 Basic Determination of the Size of Particles and Flocs

Particles or flocs occurring in real systems are almost always irregular in shape and of different sizes. It is possible to define the size of these objects in two fundamentally different ways:

- Equivalent sphere
- Statistical diameter

2.12.1.1 Equivalent Sphere

Equivalent sphere is a method of measurement which a particle or a floc is represented by a sphere equivalent to its length or more commonly its projected area. The equivalent sphere approach is the most widely used since it results in a single parameter description of an object of irregular shape which serves to describe diameter, area, volume and surface area due to the mathematical properties of a sphere (Freshwater, 1975).

2.12.1.2 Statistical Diameter

Statistical diameter is the linear dimension of an object being measured in a specific way. The two most well known statistical diameters are the Feret diameter and the Martin diameter.

The Feret diameter is the distance between two parallels in the direction which an object is being projected. The Martin diameter, on the other hand, is the distance between two points where the area of the projected object is divided in two equal parts, as shown in Figure 2.24. These measurements are not meaningful when applied to a single object and only gain significance when applied to describe large collections of particles or flocs (Freshwater, 1975).

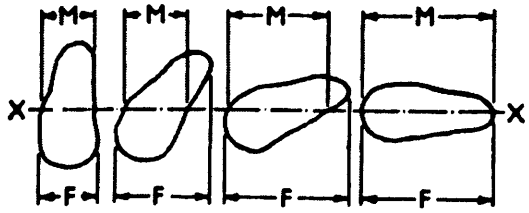

Figure 2.24 M: Martin Diameter; F: Feret diameter (Freshwater, 1975).

2.12.2 Turbidity Fluctuations

The concept of turbidity fluctuations was first introduced by Gregory and Nelson (1984) to monitor the state of flocculation. The technique is based on the fact that light transmitted through a flowing suspension of particles shows random fluctuations about an average value, which are due to random variations in the number and size of particles in the light beam (Gregory, 1998). Useful information can be derived on the state of particle aggregation and the size and structure of growing flocs by measuring the fluctuations in light transmission through a flowing suspension.

The technique usually involves simple optoelectronic devices, such as light-emitting diodes and photodiode detectors and a sample flowing by gravity or a pump in a transparent plastic tube which can be directly monitored as shown in Figure 2.25. When a flow of particles or flocs passes the light beam through the plastic tube, the amount of light reaching the detector is reduced. The fluctuations in light transmission are measured as fluctuations in the output voltage of a photodiode detector.

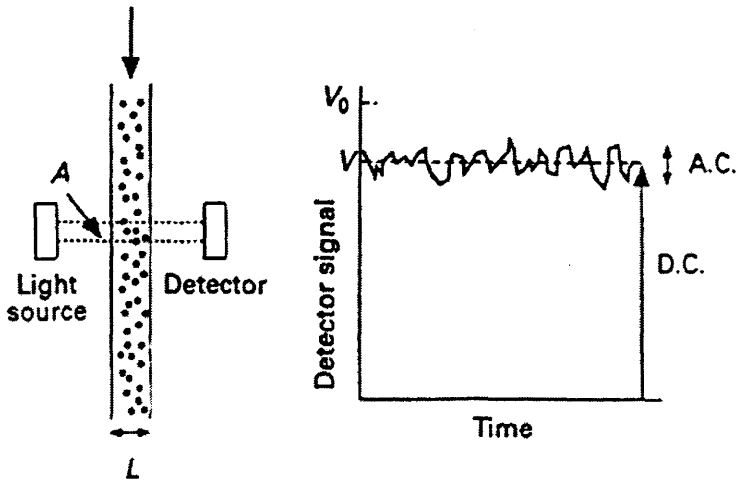

Figure 2.25 Turbidity fluctuations (Gregory and Chung, 1995).

The root mean square (rms) value of the fluctuating ac signal (random variations in the number of particles in the sample) can be derived, which is related to the average number concentration and size of the suspended particles. rms is usually divided by the mean (dc) value of transmitted light intensity, which depends on the turbidity of the suspension, to give a ratio value R commonly referred as the flocculation index. For low concentration of uniform particles, the ratio is given by:

$$R = \frac{rms}{dc} = \sqrt{\frac{Nl}{A_1}} C_2 \tag{2.34}$$

where A_1 is the effective cross-sectional area of the light beam and l is the optical path length. The ratio R, depends on the square root of the particle concentration due to the Poisson distribution (Gregory, 1985).

Larger particles can be monitored more sensitively. Using the definitions of the scattering cross-section of a particle C_2, and the volume fraction ϕ (total volume of particles per unit volume of suspension), the above expression can be converted to:

$$\frac{R}{\sqrt{\phi}} = \sqrt{\frac{3\pi la}{4A}} Q \tag{2.35}$$

For a constant volume concentration, the fluctuating signal, as measured by the ratio R, depends on the square root of the particle size and the scattering coefficient Q (Gregory, 1998).

Particle monitoring based on turbidity fluctuations is comparably more sensitive than conventional turbidity measurements for particles larger than around 1 μm. It has been proven that the ratio output of the commonly used photometric dispersion analyser (PDA), an all-in-one electrical device based on turbidity fluctuations, can accurately reflect the state of aggregation, which offers a useful aggregation index for determining the optimal coagulant dosage (Huang and Chen, 1996; Kan and Huang, 1998). A typical experimental set-up with a PDA is shown schematically in Figure 2.26.

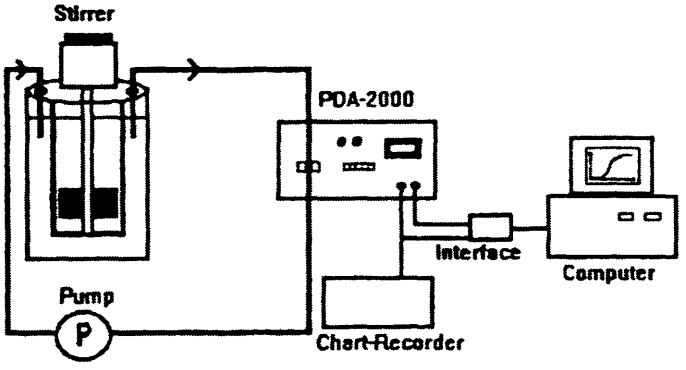

Figure 2.26 Typical experimental set-up with a PDA (Gregory and Duan, 1998).

The real limitations to turbidity fluctuations comes from random noise in the measuring system, which can be minimised with high quality optoelectronic devices (Gregory, 1998) and at high solids concentrations where transmitted light intensity is too low.

2.12.3 Particle Micro-Electrophoresis

Particle micro-electrophoresis is commonly used to monitor particle mobility. The determination of particle mobility usually involves a microscopic viewing of particle movement within a cell under the influence of an electric field. The direction which the particles migrate depends on the ionic character of the particles. Since particle mobility is related to the surface charge density of particles suspended within the cell, particle

micro-electrophoresis can provide useful information on the stability of a suspension and the adsorption behaviour of coagulants and flocculants.

Particle mobility is given by:

$$U = \frac{V}{E / L_1} \tag{2.36}$$

where V is the particle velocity and E is the electrical potential applied between two electrodes separated by a distance L_1.

The zeta potential ζ, defined as the potential at the plane of shear (see Section 2.1.4) is given by:

$$\zeta = \frac{K_1 \mu \eta}{\varepsilon_W} \tag{2.37}$$

where η and ε_W are the dynamic viscosity and the permittivity of the medium respectively and K_1 is a constant depending on the thickness of the double layer $1/\kappa$ and the particle radius a.

Chapter 3

Experimental Specifications

3.1 Determination of Optimal Coagulant and Flocculant Concentration Using a Combination of Turbidity Fluctuations and Turbidity Analysis

3.1.1 Equipment

- *Curve Fitting Programme*

TableCurve supplied by Jandel Scientific Software, USA was used. TableCurve is a powerful curve fitting programme, which fits a wide range of equations, to a given data set, so that the most suitable can be chosen.

- *Data Logger and Data Logging Software*

PICO ADC-16 and PicoLog (Pico Technology Ltd.) were used. PICO ADC-16 is a self contained high accuracy data logger for use with PCs and compatibles and connects to the RS232 serial port. The ADC-16 is supplied with PicoLog, a ready-to-use DOS and Windows data logging software.

- *Flocculation Monitoring Instrument*

Flocculation was monitored using either a Photometric Dispersion Analyser (PDA 2000) or a Flocculation Analyser Type A1 (Rank Brothers Ltd., UK). The Flocculation Analyser Type A1 is a prototype of the more commonly used PDA 2000 and both monitoring instruments are technically similar.

The light source is a high intensity light-emitting diode at a wavelength of 850 nm and the transmitted light is continuously monitored by a photodiode with peak sensitivity at

about the same wavelength. The effective beam width is about 1 mm, so A (cross-sectional area of the beam) ≈ 0.8 mm^2.

The flow cell supplied with the monitoring instruments can accommodate standard plastic tubing with an internal diameter of 1 to 3 mm (see Figure 3.1). A sampling tube with an internal diameter of 3 mm would be slightly compressed when fitted within the flow cell giving an effective optical path length of about 2 mm. This compression means that the light is passing through a parallel-sided section of the tube (Gregory and Chung, 1995).

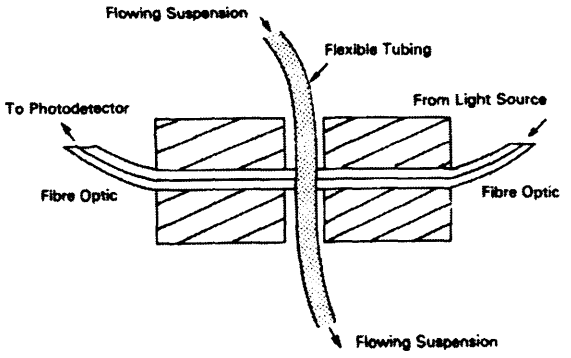

Figure 3.1 Schematic flow cell.

- *Flocculation Vessel*

A 500 ml square plastic bottle was used.

- *Mechanical Glass Stirrer*

A glass stirrer consisting of two identical paddles and a 10 mm diameter spindle was used. The paddles are located right at the bottom of the spindle with a distance of 12 mm between them. Each paddle consists of two flat blades (40 mm × 13 mm × 3 mm thick) perpendicular to each other. The glass stirrer is driven by a motor, which offers stirring rates from 50 to 200 rpm.

- *Particle Micro-Electrophoresis Instrument and Timer Programme*

A particle micro-electrophoresis instrument (Rank Brothers Ltd., UK) was used to monitor particle displacement. Subject to the influence of an electric field of 80 V within a flat cell, particle displacement was timed manually under a microscope using a self written programme with QuickBASIC (Microsoft Corp.); the programme automatically calculates particle mobility according to the inputs.

- *Peristaltic Pump*

Micro Tube Pump MP-3 (EYELA Tokyo Rikakikai Co.) was used. The peristaltic pump was calibrated by measuring the flow rate relative to each dial reading using a measuring cylinder. Dial readings 2, 4, 6, 8 and 10 were tested and a trend line was fitted as shown in Figure 3.2.

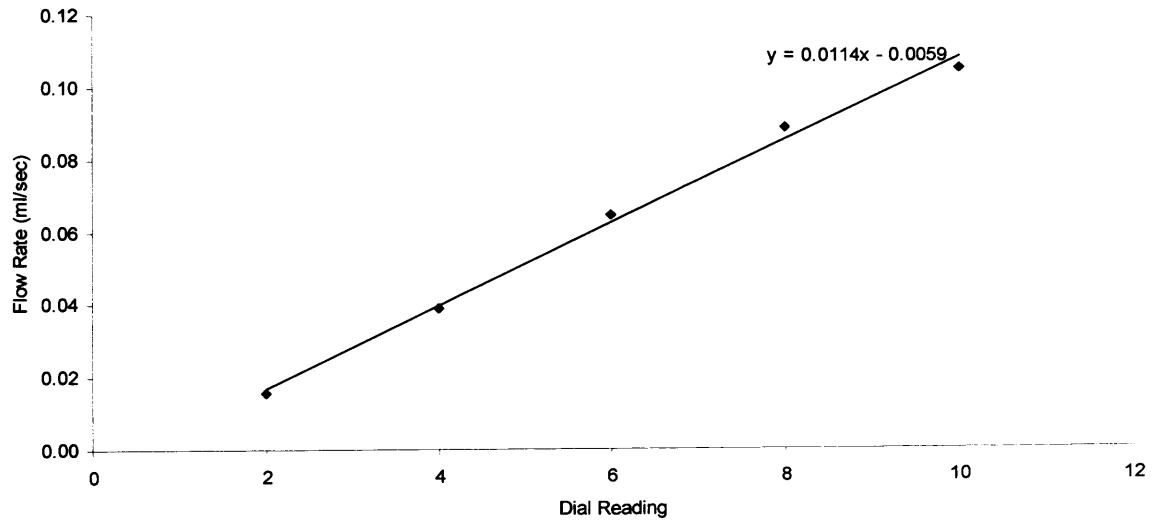

Figure 3.2 Trend line showing different flow rates offered at different dial readings.

- *pH Meter*

pH meter - HI 9812 (HANNA instruments) was used.

- *Plastic Tubing*

AlteVin Laboratory PVC tubing supplied by Altec, UK with an internal diameter of 3 mm and a wall thickness of 1 mm was used.

- *Spreadsheet and Analysis Programme*

Excel (Microsoft Corp.) was used.

- *Turbidity Meter*

Turbidity meter - Ratio/XR Turbidimeter (Hach Company) was used.

3.1.2 Arrangement

The sampling tube is placed a little above the glass stirrer in the flocculation vessel below the liquid level. A section of the sampling tube is fitted between the ends of optical fibres (see Figure 3.1), in the flocculation monitoring instrument. The suspension is carried through the tube by the peristaltic pump located downstream of the monitor at a flow rate of 6.5 ml/min. The suspension is re-circulated to the flocculating vessel. The rms and dc outputs from the monitor are connected to a laptop running the data logging software via the data logger. The data logging rate was set to every 2 seconds. A schematic diagram showing the experimental arrangement for monitoring flocculation in a stirred vessel is shown in Figure 3.3.

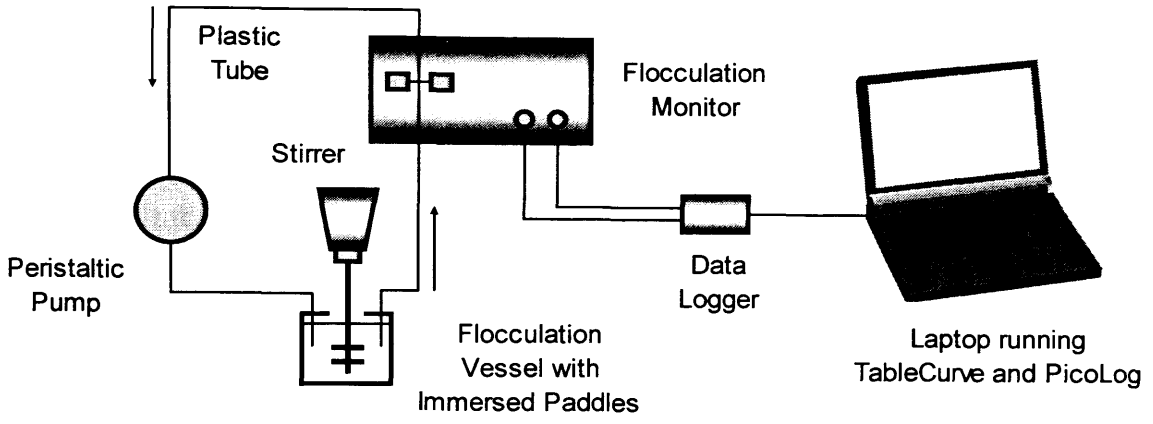

Figure 3.3 Schematic diagram of the experimental arrangement for monitoring flocculation in a stirred vessel.

3.1.3 Materials

All stock solutions and suspensions were prepared with deionised water produced by an Elgastat Option 3 Water Purifier supplied by Elga Ltd., UK. The specific conductivity of the deionised water was below 1.5 $\mu S\ cm^{-1}$.

- *Aluminium Sulphate Solution (0.1 M).*

Technical grade aluminium sulphate supplied by Fisher Scientific, UK was used.

- *Calcium Nitrate Solution (1 M)*

Analysis reagent grade calcium nitrate supplied by BDH Chemicals Ltd., UK was used.

- *Kaolin Stock Suspension (50 g/l)*

Dry kaolin was supplied by IMERYS Ltd., UK. Kaolin stock suspension was prepared by adding 200 g of the supplied dry kaolin with 500 ml of deionised water in a high-speed blender. The pH of the mixture was then raised to about 7.5 by adding 5 ml of sodium hydroxide (0.1 N) in the blender in order to fully disperse the dry kaolin. After blending at 4000 rpm for 10 minutes the kaolin suspension was diluted to 1 l with deionised water and allowed to stand overnight in a measuring cylinder.

The top 800 ml of the kaolin suspension was decanted and its concentration was determined gravimetrically to be 135 g/l. The suspension was then diluted to give a final concentration of 50 g/l. The particles were mostly below about 5 μm in size, with a mean size of about 2 μm, determined by an Elzone 280 PC particle counter supplied by Particle Data Ltd., UK.

- *Latex Stock Suspension (20 g/l)*

The latex stock suspension used was of polystyrene latex, previously prepared by emulsifier-free polymerisation of styrene with potassium persulphate as initiator. The latex has a particle size of ~ 1.5 μm and a particle density of 1.05 g/cm^3.

- *Magnafloc 1697 (poly(diallyldimethylammonium) chloride, polyDADMAC) Stock Solution (0.1% w/v)*

Magnafloc 1697 (cationic) supplied by CIBA Speciality Chemicals, UK has an intrinsic viscosity of 0.2, an estimated molecular weight of 5×10^4 and a charge density of 5.73 meq/g at pH 7 (Kam and Gregory, 2001). The liquid Magnafloc 1697 (40% w/w) supplied by the manufacturer was diluted with deionised water to give a stock solution of 0.1% w/v.

- *Sodium Carbonate Solution (0.1 N)*

Analysis reagent grade sodium carbonate supplied by Fisons Scientific Equipment, UK was sued.

- *Sodium Nitrate Solution (1 M)*

Analysis reagent grade sodium nitrate supplied by BDH Chemicals Ltd., UK was sued.

- *Zetag 64 (copolymer of acrylamide and a cationic monomer) Stock Solution (0.1% w/v)*

Zetag 64 (cationic) supplied by CIBA Speciality Chemicals, UK has an intrinsic viscosity of 12, an estimated molecular weight of several millions and a 40% cationic

charge. The granular Zetag 64 supplied by the manufacturer was wetted with 2 ml of acetone to allow better dissolution of polymer and mixed with deionised water to give a stock solution of 0.1% w/v.

3.1.4 Methods

3.1.4.1 Kaolin and Latex Particles Coagulated with Aluminium Sulphate

3 ml of sodium carbonate solution (0.1 N) and 0.5 ml of kaolin stock suspension (50 g/l) were added to the flocculation vessel. Deionised water was then added to fill the flocculation vessel up to 300 ml to give a particle mass concentration and a salt concentration of 0.08 g/l and 1 mN respectively; the mixture had a pH value of about 7.7. The mixture was stirred at 100 rpm to allow sufficient mixing.

After the brief mixing, the mixture was allowed to pump through the plastic tube passing the flocculation monitoring instrument then back into the stirring vessel before Picolog was activated. Picolog was allowed 30 seconds to run before the required amount of aluminium sulphate solution (0.1 M) was added to the mixture. Different concentrations of aluminium sulphate were tested on kaolin suspensions ranging from 6.7 to 66.7 μM in close intervals.

Each experiment took approximately 10 minutes to complete. At the end of each experiment, the stirrer was switched off and the mixture was left to settle for 15 minutes before 30 ml of the mixture was extracted for turbidity analysis and the operating pH was tested using the pH meter.

The rms data collected by Picolog were transferred to TableCurve for curve fitting then to Excel for graphical presentation. The results provided by turbidity analysis were presented graphically also using Excel. Figures 3.4 and 3.5 show a selection of experimental data points and fitted curves of kaolin suspensions coagulated at different aluminium sulphate concentrations and their operating pH values respectively and Figure 3.6 shows the corresponding results provided by turbidity analysis.

Aluminium sulphate concentration of 46.7 μM $Al_2(SO_4)_3$ was considered the optimum due to its effectiveness in turbidity removal and the enhancement of floc size as indicated by the highest rms plateau given; rms value increases with floc size.

The optimum chosen for the coagulation of kaolin particles was also regarded as the optimum for the coagulation of latex particles since the mechanism of destabilisation involved is independent of the chemical and physical nature of the primary particles.

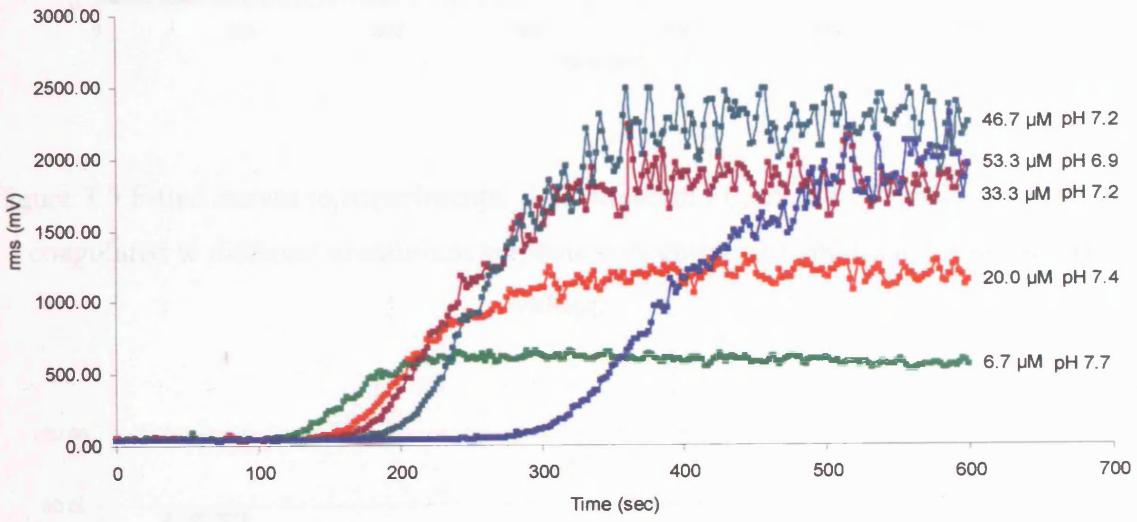

Figure 3.4 Experimental data points of kaolin suspensions coagulated at different aluminium sulphate concentrations and their operating pH values.

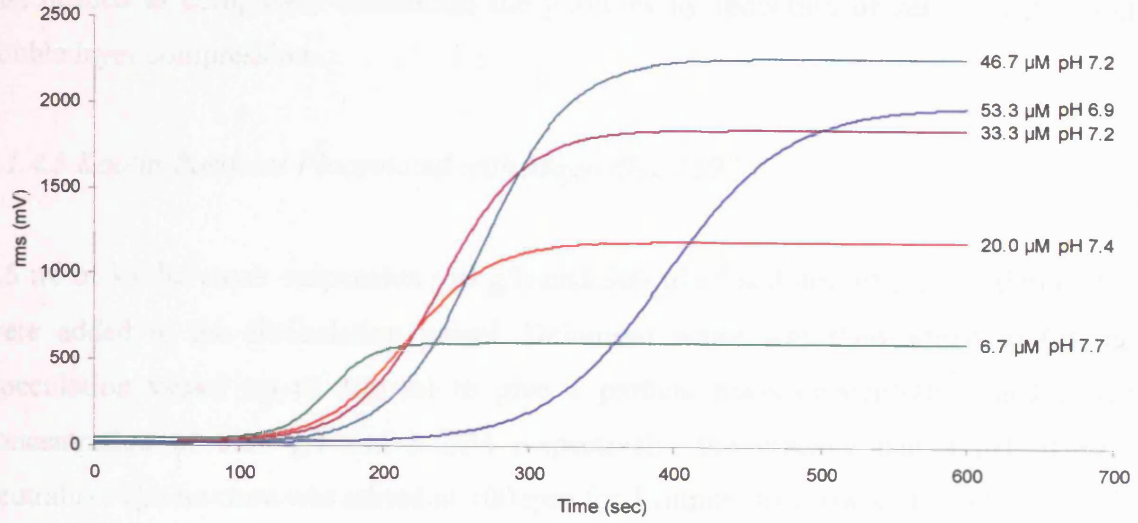

Figure 3.5 Fitted curves to experimental data points in Figure 3.4 of kaolin suspensions coagulated at different aluminium sulphate concentrations and their operating pH values.

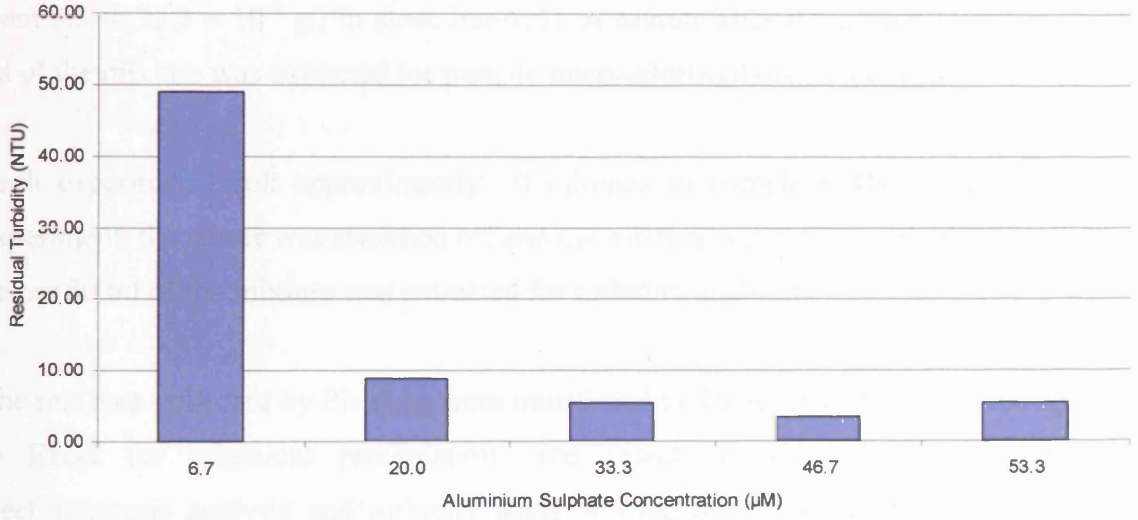

Figure 3.6 Residual turbidity of kaolin suspensions coagulated at different aluminium sulphate concentrations.

3.1.4.2 Kaolin and Latex Particles Coagulated with Calcium Nitrate

The optimal calcium nitrate concentration chosen for both the coagulation of kaolin and the coagulation of latex particles was 50 mM. The chosen salt concentration is above

that needed to completely destabilise the particles by reduction of zeta potential and double layer compression.

3.1.4.3 Kaolin Particles Flocculated with Magnafloc 1697

0.5 ml of kaolin stock suspension (50 g/l) and 300 µl of sodium nitrate solution (1 M) were added to the flocculation vessel. Deionised water was then added to fill the flocculation vessel up to 300 ml to give a particle mass concentration and a salt concentration of 0.08 g/l and 1 mM respectively; the mixture had a pH of near neutrality. The mixture was stirred at 100 rpm for 1 minute to allow sufficient mixing.

After the brief mixing, the mixture was allowed to pump through the plastic tube passing the flocculation monitoring instrument then back into the stirring vessel before Picolog was activated. Picolog was allowed 30 seconds to run before the required amount of Magnafloc 1697 stock solution (0.1 % w/v) was added to the mixture. Different concentrations of Magnafloc 1697 were tested on kaolin suspensions ranging from 3.3 to 33.3 $\times 10^{-5}$ g/l in close intervals. A minute after the dosing of polymer, 15 ml of the mixture was extracted for particle micro-electrophoresis analysis.

Each experiment took approximately 10 minutes to complete. By the end of each experiment, the stirrer was switched off and the mixture was left to settle for 15 minutes before 30 ml of the mixture was extracted for turbidity analysis.

The rms data collected by PicoLog were transferred to TableCurve for curve fitting then to Excel for graphical presentation. The results provided by particle micro-electrophoresis analysis and turbidity analysis were presented graphically also using Excel.
Magnafloc 1697 concentration of 20×10^{-5} g/l was considered the optimum due to its effectiveness in turbidity removal and the enhancement of floc size (see Section 4.1).

3.1.4.4 Kaolin Particles Flocculated with Zetag 64

Experimental procedure as described in Section 3.1.4.3 except that particle micro-electrophoresis analysis was not carried out and different concentrations of Zetag 64 were tested on kaolin suspensions ranging from 6.7 to 66.7 µM in close intervals.

Zetag 64 concentration of 60 × 10^{-5} g/l was considered the optimum due to its effectiveness in turbidity removal and the enhancement of floc size (see Section 4.1).

3.1.4.5 Latex Particles Flocculated with Magnafloc 1697

Experimental procedure as described in Section 3.1.4.3 except that particle micro-electrophoresis analysis was not carried out; 1.25 ml of latex stock suspension (20 g/l) was added to the flocculation vessel to give the same mass concentration as for kaolin; different concentrations of Magnafloc 1697 were tested on latex suspensions ranging from 1.7 to 33.3 × 10^{-5} g/l in close intervals and each experiment took approximately 30 minutes to complete.

Magnafloc 1697 concentration of 8.3 × 10^{-5} g/l was considered the optimum due to its effectiveness in turbidity removal and the enhancement of floc size (see Section 4.1).

3.1.4.6 Latex Particles Flocculated with Zetag 64

Experimental procedure as described in Section 3.1.4.3 except that particle micro-electrophoresis analysis was not carried out; 1.25 ml of latex stock suspension (20 g/l) was added to the flocculation vessel to give the same particle mass concentration as for kaolin; different concentrations of Zetag 64 were tested on latex suspensions ranging from 6.7 to 133.3 × 10^{-5} g/l in close intervals and each experiment took approximately 20 minutes to complete.

Zetag 64 concentration of 86.7 × 10^{-5} g/l was considered the optimum due to its effectiveness in turbidity removal and the enhancement of floc size (see Section 4.1).

3.2 Monitoring of Floc Formation, Breakage and Re-formation in a Stirred Vessel Based on Turbidity Fluctuations and by Microscope Photography

3.2.1 Equipment

Flocculation monitoring instrument, data logger and data logging software, flocculation vessel, mechanical glass stirrer, peristaltic pump, pH meter, plastic tubing and spreadsheet and analysis programme as described in Section 3.1.1.

- *Microscope Photography*

PhotoStudio (ArcSoft), a simple image processing software was used to capture pictures of flocs via a digital microscope camera (MODEL DMC 1 - Polaroid) using a microscope (BH2-RFCA - OLYMPUS).

- *Image Editing Programme*

Photoshop 6.0 (Adobe), an advanced image editing software was used to edit and enhance pictures captured by PhotoStudio.

3.2.2 Arrangement

Experimental arrangement as described in Section 3.1.2.

3.2.3 Materials

Aluminium sulphate (0.1 M), calcium nitrate solution (1 M), kaolin stock suspension (50 g/l), latex stock suspension (20 g/l), Magnafloc 1697 stock solution (0.1% w/v), sodium carbonate solution (0.1 N), sodium nitrate solution (1 M) and Zetag 64 stock solution (0.1% w/v) as described in Section 3.1.3.

3.2.4 Methods

3.2.4.1 Kaolin Particles Coagulated with Aluminium Sulphate

Experimental procedure as described in Section 3.1.4.1 except that only the chosen optimum was used where 140 µl of aluminium sulphate solution (0.1 M) was added to the mixture to give a salt concentration of 46.7 µM $Al_2(SO_4)_3$ and that flocs were formed and grown at 100 rpm for approximately 25 minutes, broken at 200 rpm for approximately 10 minutes and re-formed at 100 rpm for approximately 10 minutes (stirring rates were chosen specifically; according to previous trials, to promote formation, breakage and to allow possible floc reformation for the different systems under investigation). A very small amount of flocs was extracted towards the end of each stage for image analysis but turbidity analysis was not carried out.

3.2.4.2 Kaolin Particles Coagulated with Calcium Nitrate

Experimental procedure as described in Section 3.1.4.1 except that the flocculation vessel was filled with deionised water up to 285 ml and 15 ml of calcium nitrate solution (1 M) was later added to the mixture to give a salt concentration of 50 mM and that flocs were formed and grown at 100 rpm for approximately 15 minutes, broken at 200 rpm for approximately 10 minutes and re-formed at 100 rpm for approximately 15 minutes. A very small amount of flocs was extracted towards the end of each stage for image analysis but turbidity analysis was not carried out.

3.2.4.3 Kaolin Particles Flocculated with Magnafloc 1697

Experimental procedure as described in Section 3.1.4.3 except that only the chosen optimum was used where 60 µl of Magnafloc 1697 stock solution (0.1 % w/v) was added to the mixture to give a polymer concentration of 20×10^{-5} g/l and that flocs were formed and grown at 100 rpm for approximately 15 minutes, broken at 200 rpm for approximately 10 minutes and re-formed at 100 rpm for approximately 15 minutes. A very small amount of flocs was extracted towards the end of each stage for image analysis but particle micro-electrophoresis and turbidity analysis were not carried out.

3.2.4.4 Kaolin Particles Flocculated with Zetag 64

Experimental procedure as described in Section 3.1.4.4 except that only the chosen optimum was used where 180 µl of Zetag 64 stock solution (0.1 % w/v) was added to the mixture to give a polymer concentration of 60×10^{-5} g/l and that flocs were formed and grown at 100 rpm for approximately 45 minutes, broken at 200 rpm for approximately 10 minutes and re-formed at 100 rpm for approximately 45 minutes. A very small amount of flocs was extracted towards the end of each stage for image analysis but turbidity analysis was not carried out.

3.2.4.5 Latex Particles Coagulated with Aluminium Sulphate

Experimental procedure as described in Section 3.2.4.1 except that 1.25 ml of latex stock suspension (20 g/l) was added to the flocculation vessel to give the same mass concentration as for kaolin.

3.2.4.6 Latex Particles Coagulated with Calcium Nitrate

Experimental procedure as described in Section 3.2.4.2 except that 1.25 ml of latex stock suspension (20 g/l) was added to the flocculation vessel to give the same particle concentration as for kaolin and that flocs were formed and grown at 100 rpm for approximately 45 minutes, broken at 200 rpm for approximately 10 minutes and re-formed at 100 rpm for approximately 20 minutes.

3.2.4.7 Latex Particles Flocculated with Magnafloc 1697

Experimental procedure as described in Section 3.2.4.3 except that 1.25 ml of latex stock suspension (20 g/l) and 25 µl of Magnafloc 1697 stock solution (0.1% w/v) (see Section 3.1.4.5) were added to the mixture to give the same particle concentration as for kaolin and a polymer concentration of 8.3×10^{-5} g/l. In addition, flocs were formed and grown at 100 rpm for approximately 70 minutes, broken at 200 rpm for approximately 10 minutes and re-formed at 100 rpm for approximately 70 minutes.

3.2.4.8 Latex Particles Flocculated with Zetag 64

Experimental procedure as described in Section 3.2.4.4 except that 1.25 ml of latex stock suspension and 260 µl of Zetag 64 stock solution (0.1% w/v) (see Section 3.1.4.6) were added to the to give the same particle concentration as for kaolin and a polymer concentration of 86.7×10^{-5} g/l. In addition, flocs were formed and grown at 100 rpm for approximately 40 minutes, broken at 200 rpm for approximately 10 minutes and re-formed at 100 rpm for approximately 40 minutes.

3.3 New Automated Filterability Monitoring Technique

3.3.1 Equipment

Data logger, mechanical glass stirrer, plastic tubing and spreadsheet and analysis programme as described in Section 3.1.1.

- *Digital Balance*

An ACB 150 digital balance supplied by Adam Equipment Co. Ltd., UK was modified to be able to give a continuous voltage output relative to the weight of the increasing filtrate volume. The conversion from voltage to weight was achieved by calibration with known weights. The relation between voltage and weight is highly linear as shown in Figure 3.7.

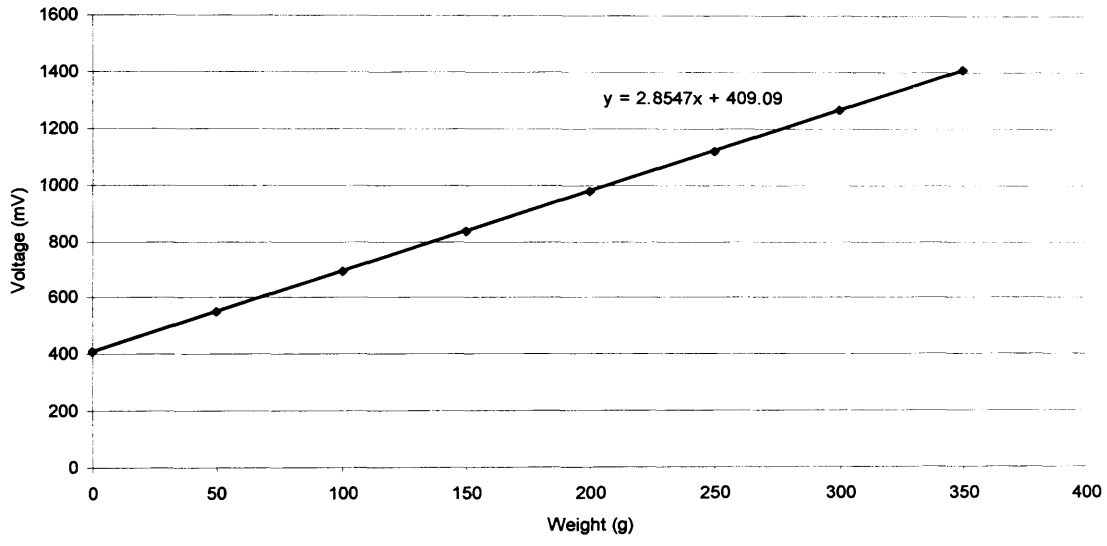

Figure 3.7 Linear relationship established between voltage and weight.

- *Plastic Membrane Filter Holder*

A Swinnex 13 filter holder supplied by Millipore, UK was used to hold 13 mm diameter cellulose nitrate membrane filters (0.45 μm) supplied by Whatman International Ltd., UK.

- *Flocculation Vessel with Valve Attachment*

A 500 ml square plastic bottle was fitted with a three-way stopcock supplied by Nipro Medical Industries Ltd., Japan.

- *Pressure Gauge*

A pressure gauge supplied by Gallenkamp, UK was used.

- *Vacuum Flask*

A 250 ml plastic vacuum flask supplied by Fisher Scientific, UK was used.

3.3.2 Arrangement

The modified plastic flocculation vessel with an adjustable plastic three-way valve attachment is filled with a test suspension. The mechanical stirrer is located right above the flocculation vessel with the stirrer immersed in the suspension. The plastic membrane filter holder is fitted to the valve and is connected to the plastic vacuum flask via a plastic tube, which the filtrate is transported through. The vacuum flask is situated on top of the digital balance and is further connected to the pressure gauge and laboratory vacuum supply. The output from the digital balance is connected to a laptop running the data acquisition software via the data logger. A schematic diagram showing the experimental arrangement for the new automated filterability monitoring technique is shown in Figure 3.8.

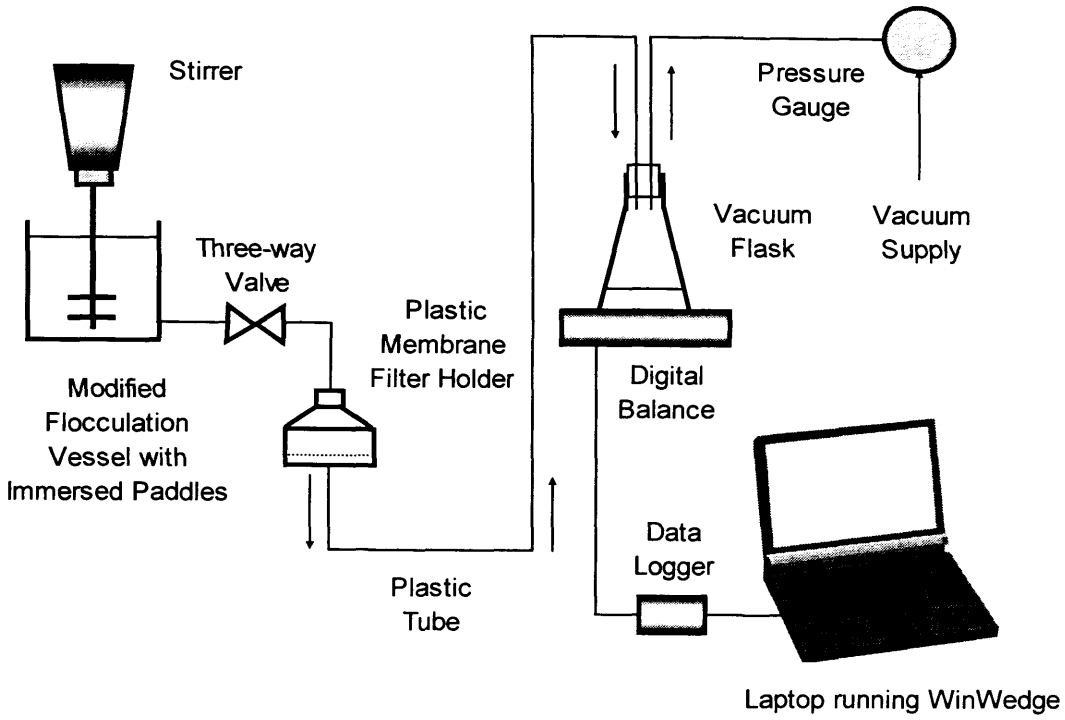

Figure 3.8 Schematic diagram of the experimental arrangement for the new automated filterability monitoring technique.

3.3.3 Materials

Calcium nitrate solution (1 M), kaolin stock suspension (50 g/l), latex stock suspension (20 g/l), Magnafloc 1697 stock solution (1% w/v), sodium nitrate solution (1 M) and Zetag 64 stock solution (0.1% w/v) as described in Section 3.1.3.

3.3.4 Methods

3.3.4.1 Kaolin Particles

1 ml of kaolin stock suspension (50 g/l) and 300 µl of sodium nitrate solution (1 M) were added to the flocculation vessel. Deionised water was then added to fill the flocculation vessel up to 300 ml to give a particle concentration and a salt concentration of 0.17 g/l and 1 mM respectively; the mixture had a pH value of near neutrality.

The mixture was stirred at 100 rpm for 1 minute to allow sufficient mixing and immediately after, WinWedge was activated as the mixture was allowed to filter through the membrane filter under constant pressure by adjustment to the valve.

The mixture was stirred at that speed throughout the filtration for approximately 10 minutes. The voltage output from the digital balance due to the weight of the increasing filtrate volume in the vacuum flask was logged every 2 seconds using WinWedge.

After completion of a filtration test, the collected data were transferred to Excel to be processed with a linear regression routine and the gradient generated (see Section 2.10.3.3) was used to compute the specific resistance to filtration.

3.3.4.2 Latex Particles

Experimental procedure as described in Section 3.3.4.1 except that 2.5 ml of latex stock suspension (20 g/l) was added to the flocculation vessel to give the same mass concentration as for kaolin before filtration.

3.3.4.3 Kaolin Particles Coagulated with Calcium Nitrate

Experimental procedure as described in Section 3.3.4.1 except that the flocculation vessel was filled with deionised water up to 285 ml and 15 ml of calcium nitrate solution (1 M) was added to the mixture after the minute of mixing at 50 rpm to give a salt concentration of 50 mM before filtration.

3.3.4.4 Kaolin Particles Flocculated with Magnafloc 1697

Experimental procedure as described in Section 3.3.4.1 except that 120 µl of Magnafloc 1697 stock solution (0.1 % w/v) was added to the mixture after the minute of mixing to give a polymer concentration of 4×10^{-4} g/l before filtration.

3.3.4.5 Kaolin Particles Flocculated with Zetag 64

Experimental procedure as described in Section 3.3.4.1 except that 360 μl of Zetag 64 stock solution (0.1 % w/v) was added to the mixture after the minute of mixing to give a polymer concentration of 1.20×10^{-3} g/l before filtration.

3.3.4.6 Latex Particles Flocculated with Magnafloc 1697

Experimental procedure as described in Section 3.3.4.2 except that 50 μl of Magnafloc 1697 stock solution (0.1 % w/v) was added to the mixture after the minute of mixing to give a polymer concentration of 1.67×10^{-4} g/l before filtration.

3.3.4.7 Latex Particles Flocculated with Zetag 64

Experimental procedure as described in Section 3.3.4.2 except that 520 μl of Zetag 64 stock solution (0.1 % w/v) was added to the mixture after the minute of mixing to give a polymer concentration of 1.73×10^{-3} g/l before filtration.

Chapter 4

Results and Discussions

4.1 Determination of Optimal Coagulant and Flocculant Concentration Using a Combination of Turbidity Fluctuations and Turbidity Analysis

Tables 4.1 and 4.2 show the selected coagulant and flocculant concentrations respectively.

Primary Particles	Aluminium Sulphate (μM)	Calcium Nitrate (mM)
Kaolin/Latex	46.7	50

Table 4.1 Selected coagulant concentrations.

Primary Particles	Magnafloc 1697 (10^{-5} g/l)	Zetag 64 (10^{-5} g/l)
Kaolin	20	60
Latex	8.3	86.7

Table 4.2 Selected flocculant concentrations.

The optimum coagulant and flocculant concentrations chosen for different systems as shown in Tables 4.1 and 4.2 were based on results from turbidity fluctuations and turbidity analysis. For example, 8.3×10^{-5} g/l was considered the optimum Magnafloc 1697 concentration for flocculating latex particles because of the significant increase in relative rms (see Figure 4.1) and the outstanding percentage turbidity removal observed (see Figure 4.2). Results from turbidity fluctuations tend to cohere with results from turbidity analysis and therefore the determination of optimum concentration is usually fairly straightforward. In the case of flocculating kaolin particles with different concentrations of Magnafloc 1697, the optimum concentration chosen (20×10^{-5} g/l) was based mainly on the results from turbidity fluctuations (see Figure 4.4). The uncertainty incurred from turbidity analysis (see Figure 4.3) could have been avoided by

using a more sensitive turbidity meter or by shortening the floc settling time after each experiment.

When flocculating latex particles with Magnafloc 1697, an optimal concentration was found to be rather difficult to establish. An optimum was only observed after testing different concentrations of Magnafloc 1697 with latex particles in small increments. Figure 4.1 shows the rms values (size) of flocs formed at different concentrations of Magnafloc 1697 relative to the size of the primary particles, before aggregation begins. As shown in Figures 4.1 and 4.2, the optimum is very sharp and is instantly followed by a drop in floc size and turbidity removal, which are indications of particle restabilisation. The optimum observed for Magnafloc 1697 flocculated kaolin particles, on the other hand, is not affected by yet higher polymer dosage as shown in Figure 4.3.

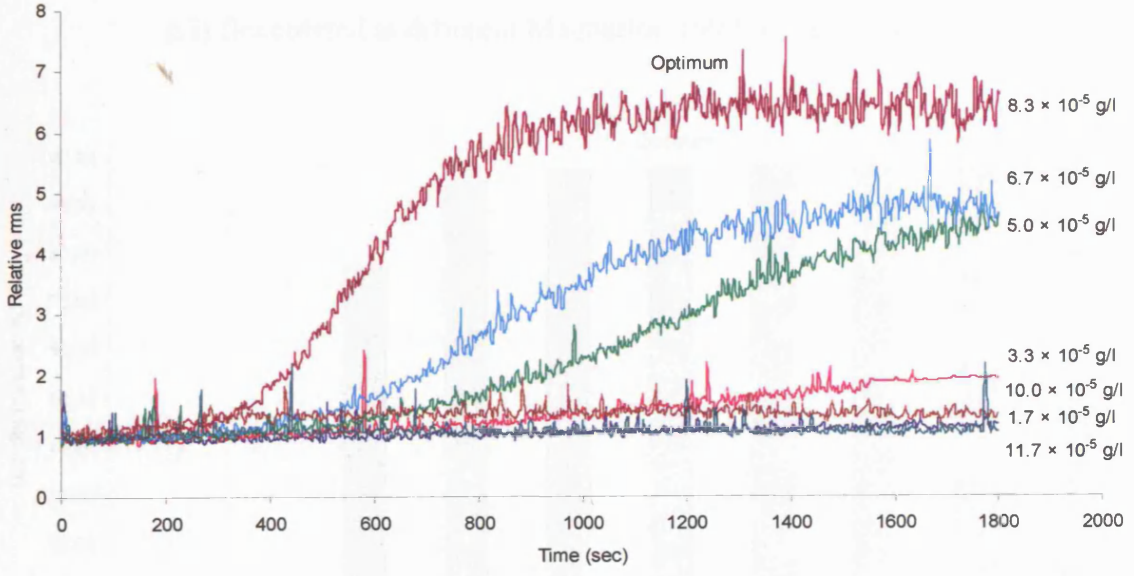

Figure 4.1 Flocculation curves of latex suspensions (particle mass concentration ≈ 0.08 g/l) flocculated at different Magnafloc 1697 concentrations.

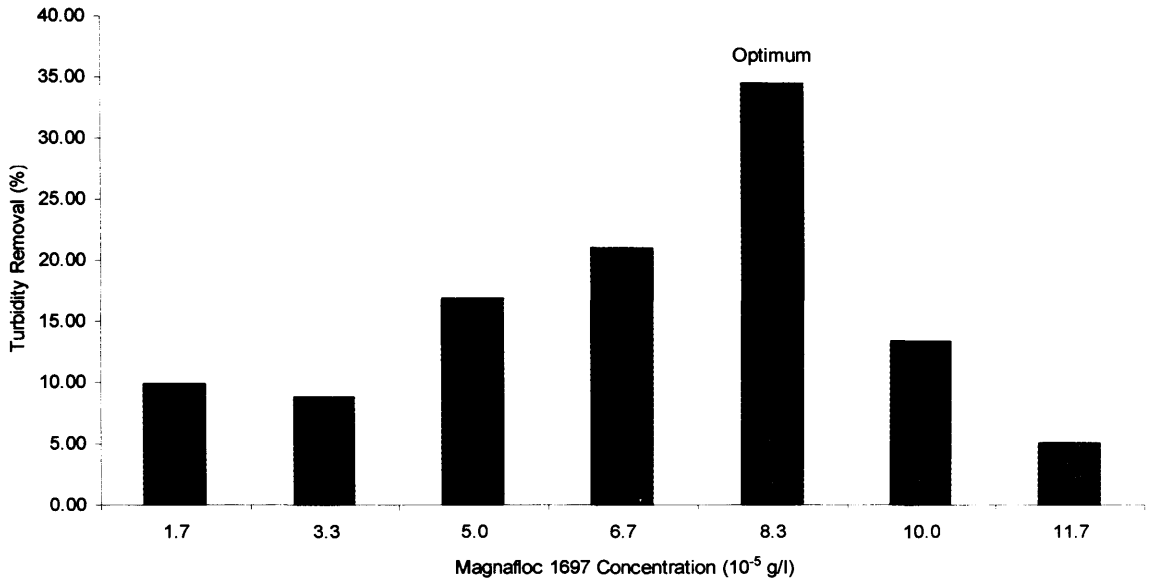

Figure 4.2 Turbidity removal of latex suspensions (particle mass concentration ≈ 0.08 g/l) flocculated at different Magnafloc 1697 concentrations.

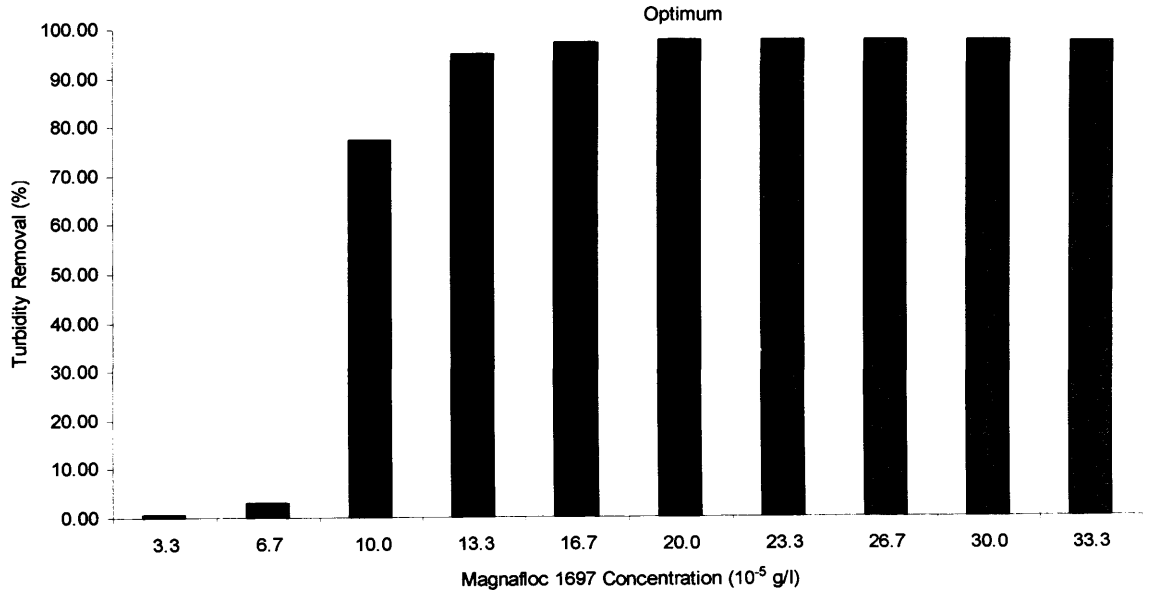

Figure 4.3 Turbidity removal of kaolin suspensions (particle mass concentration ≈ 0.08 g/l) flocculated at different Magnafloc 1697 concentrations.

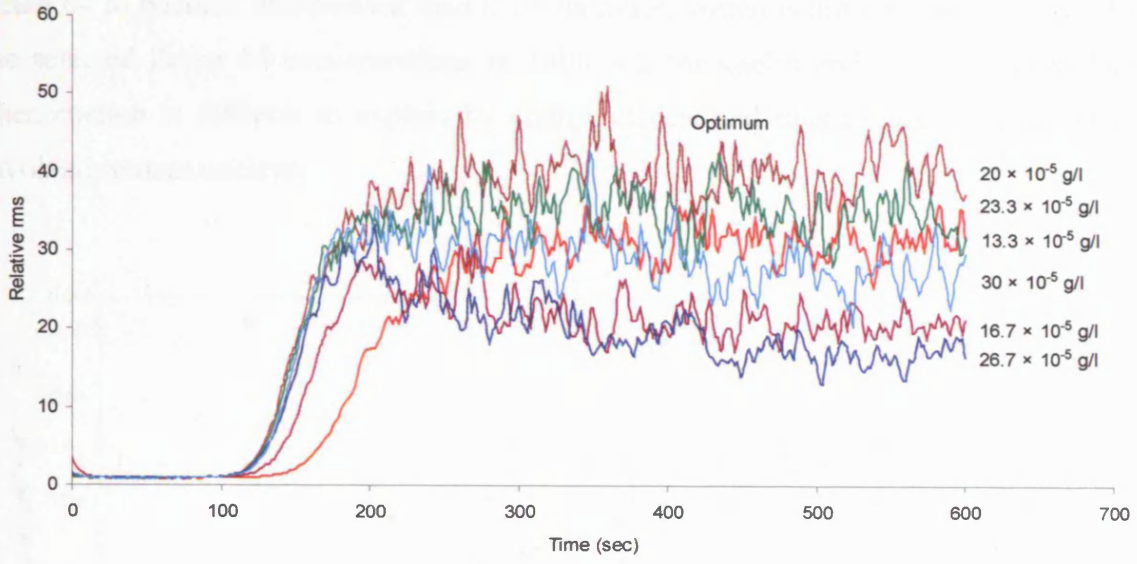

Figure 4.4 Flocculation curves of kaolin suspensions (particle mass concentration ≈ 0.08 g/l) flocculated at different Magnafloc 1697 concentrations.

This phenomenon can be attributed to the difference in charge density between the latex particles and Magnafloc 1697. Since Magnafloc 1697 is a highly charged polymer, without appropriate dilution and careful addition of the stock solution, latex particles with much lower charge density could easily become overdosed or underdosed instead of destabilised, hence the sharp optimum observed. An optimal concentration for flocculating kaolin particles with Magnafloc 1697, on the other hand, was easily established without having to trial different concentrations of Magnafloc 1697 in small increments.

This suggests that kaolin particles have a comparatively higher charge density than latex particles and are able to adsorb highly charged polymers like Magnafloc 1697 without missing the optimum or becoming restabilised easily, which agrees with the results given by particle micro-electrophoresis analysis as shown in Figure 4.5 and the estimated charge density values of 86.85 $\mu C/cm^2$ and 14.51 $\mu C/cm^2$ for kaolin and latex particles respectively; assuming that kaolin has a cation exchange capacity of 0.09 meq/g (Grim, 1968; Elfarissi and Pefferkorn, 2000) and a specific area of 10 m^2/g (Yong et al., 1992; Zbik and Smart, 2002).

However, if the above findings were true that kaolin particles had a comparatively higher charge density than latex particles, kaolin particles should in theory require more

Zetag 64 to become destabilised than latex particles, which is not the case as shown by the selected Zetag 64 concentrations in Table 4.2 for kaolin and latex particles. This phenomenon is difficult to explain by charge effects and thus the exact mechanisms involved remain unclear.

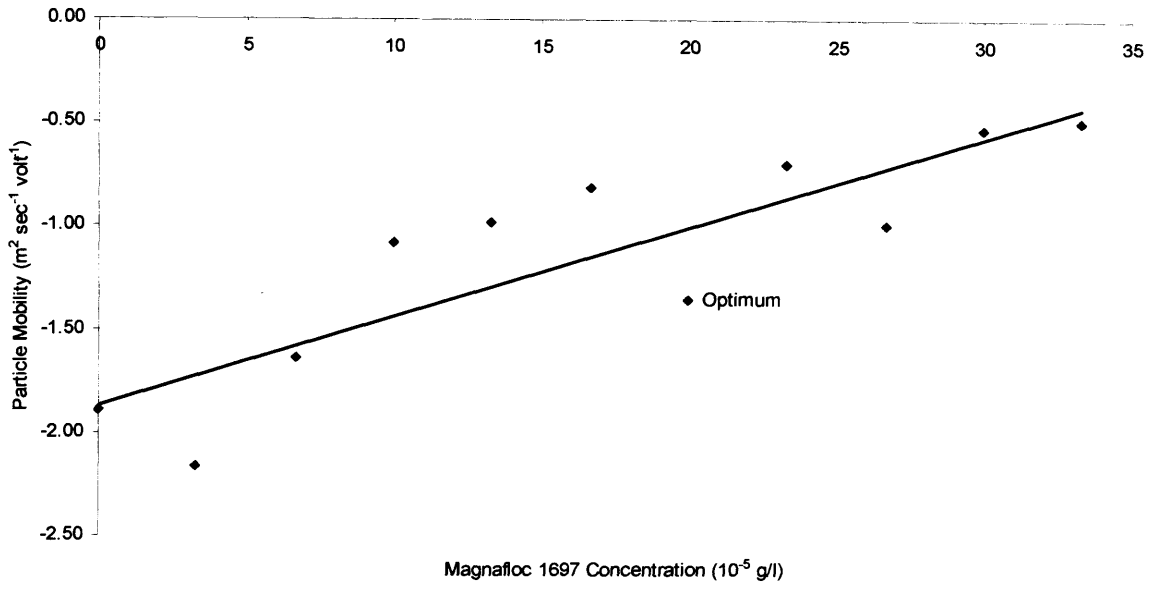

Figure 4.5 Electrophoretic mobility of kaolin particles coagulated at different concentrations of Magnafloc 1697.

The comparatively poor turbidity removal observed for Magnafloc 1697 flocculated latex suspensions as shown in Figure 4.2 to Magnafloc 1697 flocculated kaolin suspensions can be attributed to ineffective particle destabilisation as pointed out earlier.

Flocs tend not to grow into larger sizes (see Figure 4.1) when their constituent particles are not properly destabilised, either due to insufficient polymer adsorption or particle restabilisation, which result in small weak structures that take a long time to settle, hence the poor turbidity removal observed for Magnafloc 1697 flocculated latex suspensions.

In addition, apart from ineffective particle destabilisation, the low density of the employed latex particles (1.05 g/cm^3) may also be a contributing factor towards the poor turbidity removal observed. Kaolin particles have higher density (~ 2.5 g/cm^3) and are more effectively destabilised by Magnafloc 1697, thus result in larger, heavier flocs (see

Figure 4.4) that settle faster to give more satisfactory turbidity removal as shown in Figure 4.3.

Moreover, Figure 4.5 shows that particle destabilisation does not necessarily occur at high polymer coverage, which agrees with findings by researchers such as Healy and La Mer (1964) and that particle neutralisation is not a priority when particles are destabilised under electrostatic patch mechanism (see Section 4.4.3.2).

4.2 Monitoring of Floc Formation, Breakage and Re-formation in a Stirred Vessel Based on Turbidity Fluctuations and by Microscope Photography

Figures 4.6 and 4.7 show the formation, breakage and re-formation of aluminium sulphate coagulated kaolin and latex flocs respectively. Flocs were formed under conditions of precipitate entrapment (sweep coagulation), where particles are enmeshed in a growing hydroxide precipitate (see Section 2.3.1).

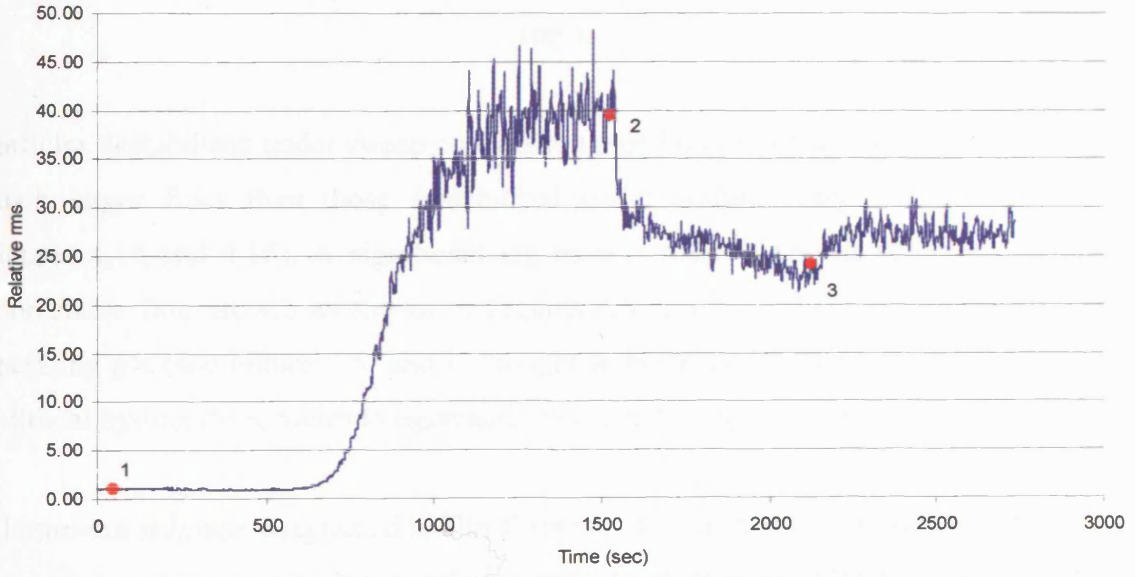

Figure 4.6 Flocculation curve showing the formation, breakage and re-formation of aluminium sulphate coagulated kaolin flocs. 1. Aluminium sulphate addition followed by an approximately 25 minute formation (100 rpm), 2. Onset of an approximately 10 minute breakage (200 rpm), 3. Onset of an approximately 10 minute re-formation (100 rpm).

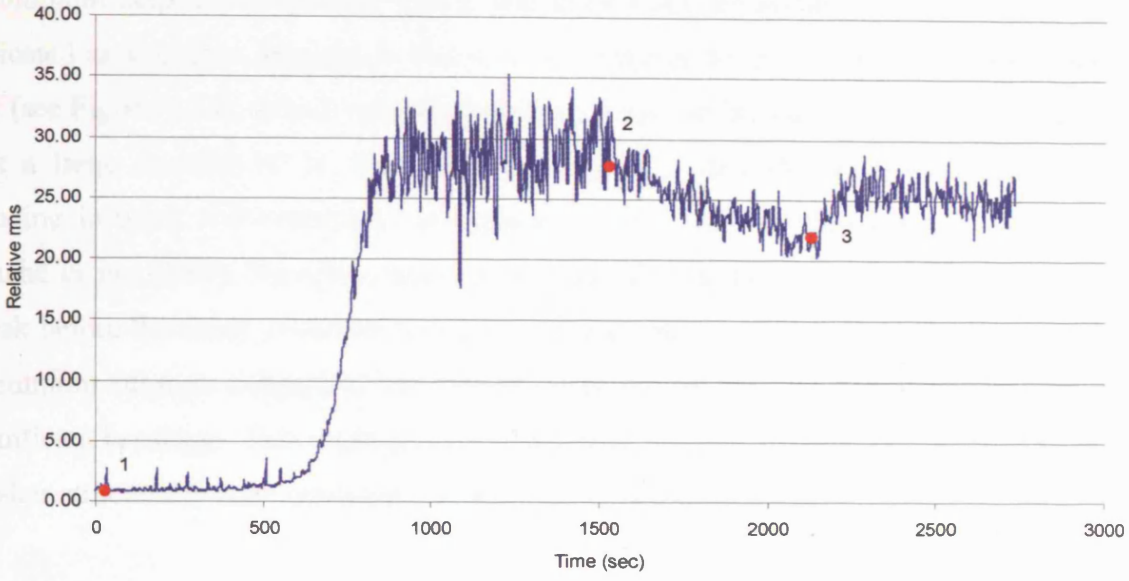

Figure 4.7 Flocculation curve showing the formation, breakage and re-formation of aluminium sulphate coagulated latex flocs. 1. Aluminium sulphate addition followed by an approximately 25 minute formation (100 rpm), 2. Onset of an approximately 10 minute breakage (200 rpm), 3. Onset of an approximately 10 minute re-formation (100 rpm).

Particles destabilised under sweep coagulation (see Figures 4.6 and 4.7) tend to result in much larger flocs than those destabilised under simple charge neutralisation (see Figures 4.14 and 4.15). A significant lag time is often observed before the onset of appreciable floc growth as shown in Figures 4.6 and 4.7, which is influenced by the operating pH (see Figure 3.5) and is thought to be related to the time required for the colloidal hydroxide particles to aggregate (Duan and Gregory, 2003).

Aluminium sulphate coagulated kaolin flocs are similar in size; floc size is indicated as a primary particle size multiple (relative rms), to aluminium sulphate coagulated latex flocs during formation, breakage and re-formation as shown in Figures 4.6 and 4.7, which indicates that particle destabilisation under conditions of precipitate entrapment is independent of the chemical and physical nature of the particles involved (Packham, 1963), although the slight difference in floc size observed, during formation in particular, may be a result of primary particles incorporating themselves differently within the hydroxide precipitate according to their shapes.

Aluminium sulphate coagulated kaolin and latex flocs are subject to surface erosion; indicated as a gradual decrease in floc size (see Figures 4.6 and 4.7) rather than a sharp fall (see Figure 4.14), which indicates breakage. This can be attributed to the possibility that a large fraction of the floc mass consists of hydroxide precipitate, which the bonding is weak and vulnerable to surface erosion despite being naturally cohesive (Bache et al., 1999). However, aluminium sulphate coagulated kaolin flocs appear to break before the onset of surface erosion; indicated as a sudden drop in floc size, while aluminium sulphate coagulated latex flocs erode all the way through with no signs of significant breakage. This suggests that aluminium sulphate coagulated kaolin flocs are weaker structurally than aluminium sulphate coagulated latex flocs.

Moreover, the surface erosion of flocs observed suggests that aluminium sulphate coagulated latex flocs are smaller than the Kolmogoroff microscale (see Section 2.7.1). The observation that aluminium sulphate coagulated kaolin flocs break before surface erosion occurs indicates approximately the point where the Kolmogoroff microscale lies. However, due to the lack of power input information from the mechanical glass stirrer, Kolmogoroff microscale could not be determined for this system.

Limited re-formation of flocs was observed for both aluminium sulphate coagulated kaolin and latex flocs after breakage, where flocs do not completely re-form when the original stirring rates are restored, which agrees with studies by researchers such as Francois (1987) and Yukselen and Gregory (2002 and 2004). Despite the generalisation that floc breakage is irreversible when the destabilising agent involved is either a polymer or a precipitated solid (Spicer at al, 1998), such observation is well known in practice but the underlying mechanisms involved remain unclear (Francois, 1987). However, since aluminium sulphate coagulated kaolin and latex flocs tend to erode during breakage, the resulting fragments are likely to be very small units, which may penetrate some way into a cluster during re-formation, facilitating the recovery of floc size as shown in Figures 4.6 and 4.7.

Figures 4.8 to 4.13 show images of aluminium sulphate coagulated kaolin and latex flocs during formation, breakage and re-formation. Aluminium sulphate coagulated latex flocs appear to be more compact and denser than aluminium sulphate coagulated kaolin flocs, which are characteristics typically associated with stronger flocs.

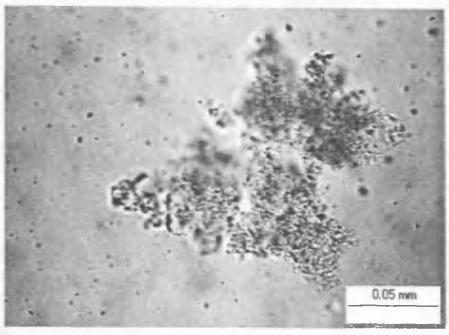

Figure 4.8 Aluminium sulphate coagulated kaolin floc formed at 100 rpm.

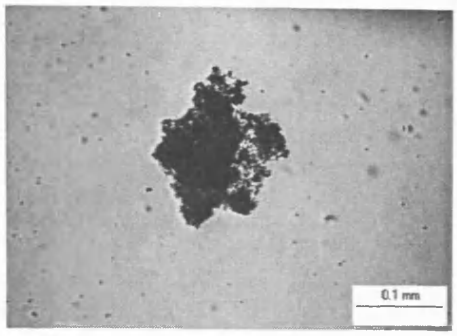

Figure 4.9 Aluminium sulphate coagulated latex floc formed at 100 rpm.

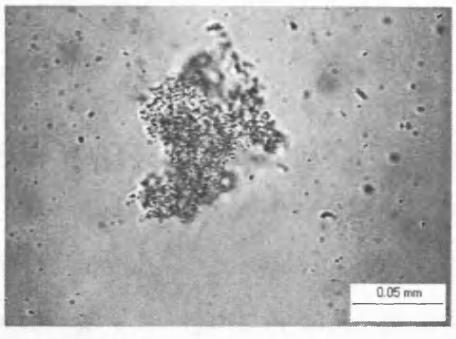

Figure 4.10 Aluminium sulphate coagulated kaolin floc broken at 200 rpm.

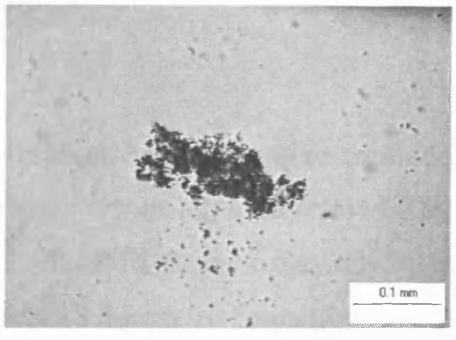

Figure 4.11 Aluminium sulphate coagulated latex floc eroded at 200 rpm.

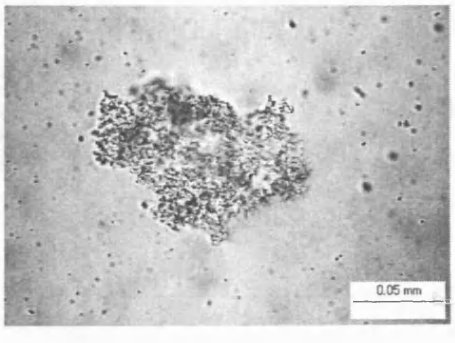

Figure 4.12 Aluminium sulphate coagulated kaolin floc re-formed at 100 rpm.

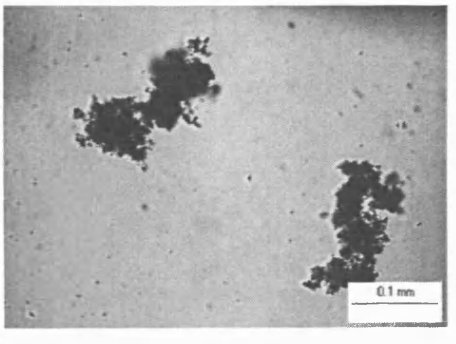

Figure 4.13 Aluminium sulphate coagulated latex floc re-formed at 100 rpm.

Figures 4.14 and 4.15 show the formation, breakage and re-formation of calcium nitrate coagulated kaolin and latex flocs respectively. Flocs were formed under both double layer compression and charge neutralisation through adsorption (See Section 2.3.1).

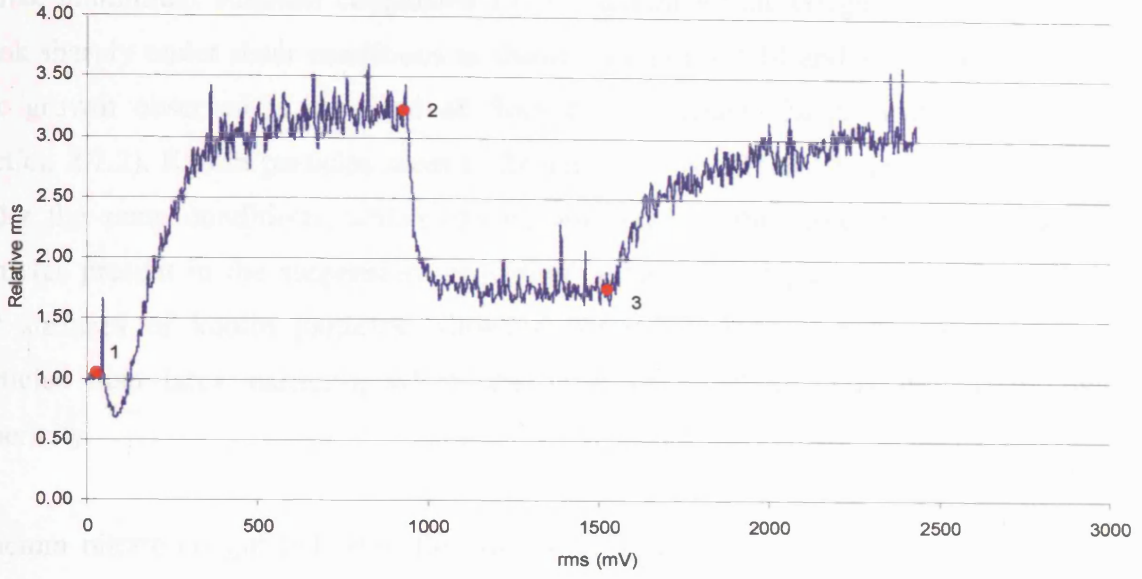

Figure 4.14 Flocculation curve showing the formation, breakage and re-formation of calcium nitrate coagulated kaolin flocs. 1. Calcium nitrate addition followed by an approximately 15 minute formation (100 rpm), 2. Onset of an approximately 10 minute breakage (200 rpm), 3. Onset of an approximately 15 minute re-formation (100 rpm).

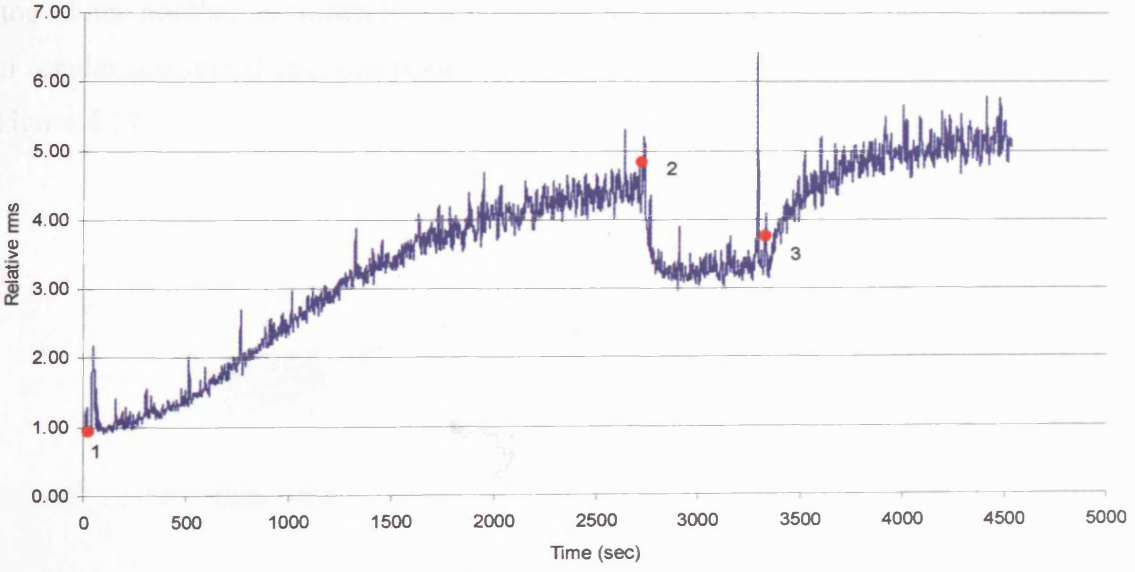

Figure 4.15 Flocculation curve showing the formation, breakage and re-formation of calcium nitrate coagulated latex flocs. 1. Calcium nitrate addition followed by an approximately 45 minute formation (100 rpm), 2. Onset of an approximately 10 minute breakage (200 rpm), 3. Onset of an approximately 20 minute re-formation (100 rpm).

Unlike aluminium sulphate coagulated flocs, calcium nitrate coagulated flocs tend to break sharply under shear conditions as shown in Figures 4.14 and 4.15. The reversible floc growth observed is expected of flocs formed under charge neutralisation (see Section 2.7.2). Kaolin particles seem to flocculate more effectively than latex particles under the same conditions, which can be attributed to the larger number of kaolin particles present in the suspension, providing better rates of particle collision and the flat surfaces of kaolin particles, allowing better attachments between destabilised particles than latex particles, which the level of attachments is limited by their sphericity.

Calcium nitrate coagulated latex flocs are slightly larger in size than calcium nitrate coagulated kaolin flocs during formation, breakage and re-formation as shown in Figures 4.14 and 4.15, which can be attributed to the ways the different primary particles were bonded together.

Kaolin particles are plate-like and they tend to bond face to face to each other due to the larger surfaces available for bonding under normal circumstances. This arrangement limits the overall increase in floc size despite the increasing number of particles piling on top of one another as shown in Figure 4.16. Latex particles, on the other hand, due to their regular size and shape, contribute to the overall floc size more effectively as shown in Figure 4.17.

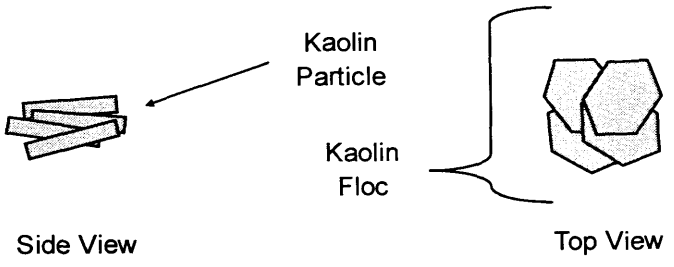

Figure 4.16 Side and top views of a kaolin floc consists of four kaolin particles.

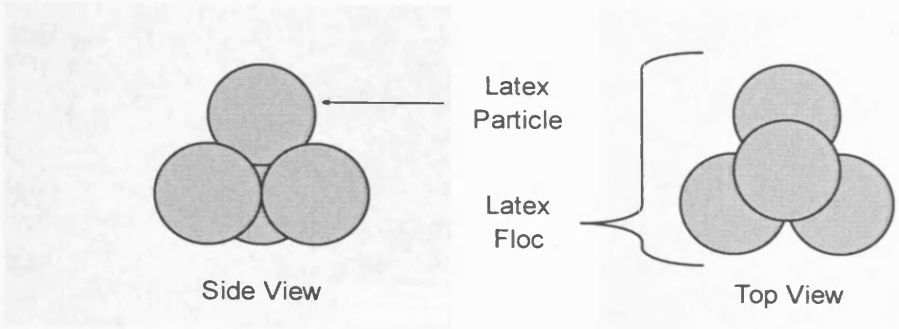

Figure 4.17 Side and top views of a latex floc consists of four latex particles.

Figures 4.18 to 4.23 show images of calcium nitrate coagulated kaolin and latex flocs during formation, breakage and re-formation. Calcium nitrate coagulated latex flocs appear to be more compact and denser than calcium nitrate coagulated kaolin flocs. Figure 4.20 shows small clusters of kaolin particles resulting from the breakage of calcium nitrate coagulated kaolin flocs. Although large open flocs tend to occur as a result of cluster-cluster encounters, such flocs are not apparent during re-formation as shown in Figure 4.22. Although flocs re-formed at 100 rpm (see Figure 4.23) appear to be larger in size than those formed during the formation stage (see Figure 4.19), this observation should be disregarded due to possible unwanted flocculation imposed on flocs during extraction and transfer from the flocculation vessel to the microscope for image analysis (see Section 3.2.4.2). Figure 4.22 also shows re-formed flocs that are larger in size than those broken at 200 rpm, once again this should not be regarded as a reliable size observation due to the above justification.

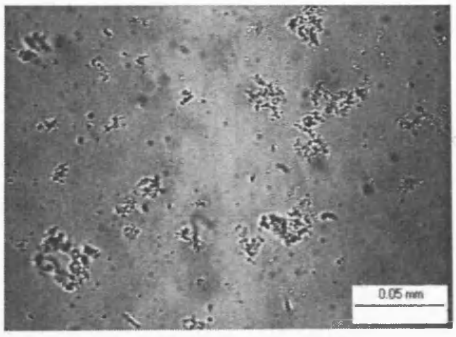

Figure 4.18 Calcium nitrate coagulated kaolin floc formed at 100 rpm.

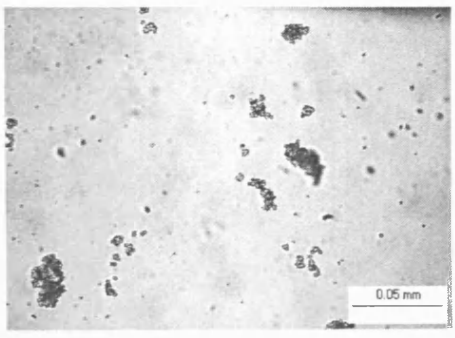

Figure 4.19 Calcium nitrate coagulated latex floc formed at 100 rpm.

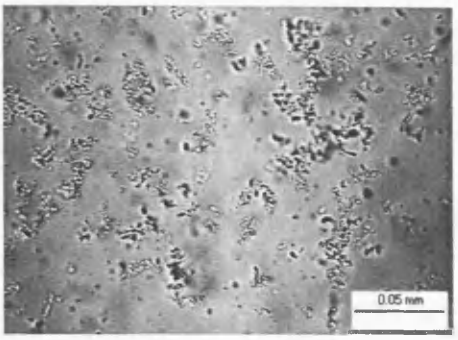

Figure 4.20 Calcium nitrate coagulated kaolin floc broken at 200 rpm.

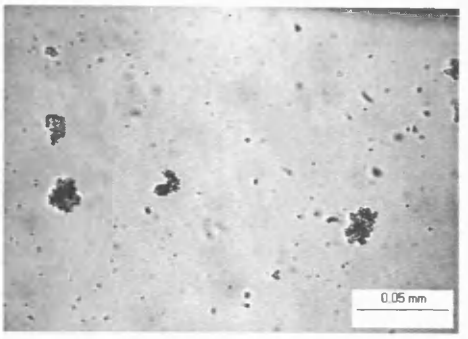

Figure 4.21 Calcium nitrate coagulated latex floc broken at 200 rpm.

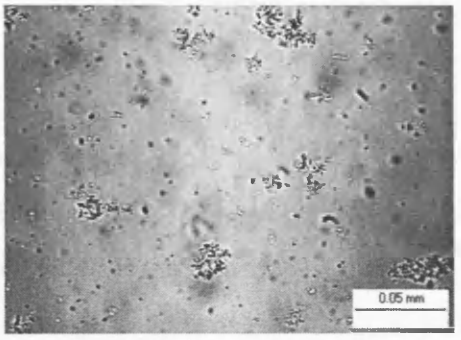

Figure 4.22 Calcium nitrate coagulated kaolin floc re-formed at 100 rpm.

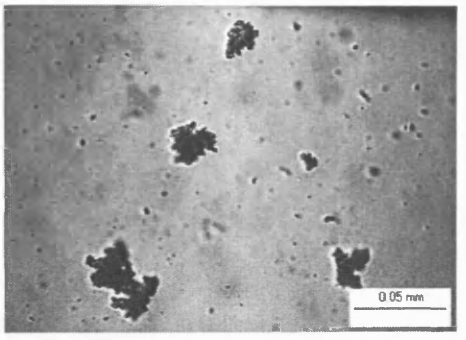

Figure 4.23 Calcium nitrate coagulated latex floc re-formed at 100 rpm.

Figures 4.24 and 4.25 show the formation, breakage and re-formation of Magnafloc 1697 flocculated kaolin and latex flocs respectively. Flocs were formed under electrostatic patch mechanism, where particles align according to their alternating surface charge to form flocs (see Section 2.4.3.2).

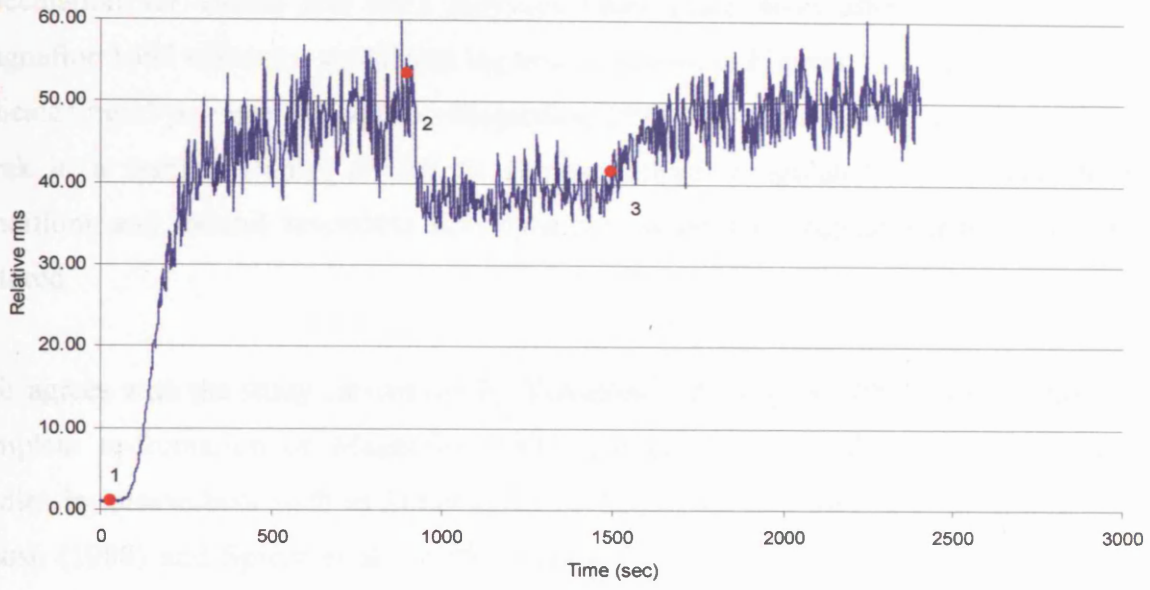

Figure 4.24 Flocculation curve showing the formation, breakage and re-formation of Magnafloc 1697 flocculated kaolin flocs. 1. Magnafloc 1697 addition followed by an approximately 15 minute formation (100 rpm), 2. Onset of an approximately 10 minute breakage (200 rpm), 3. Onset of an approximately 15 minute re-formation (100 rpm).

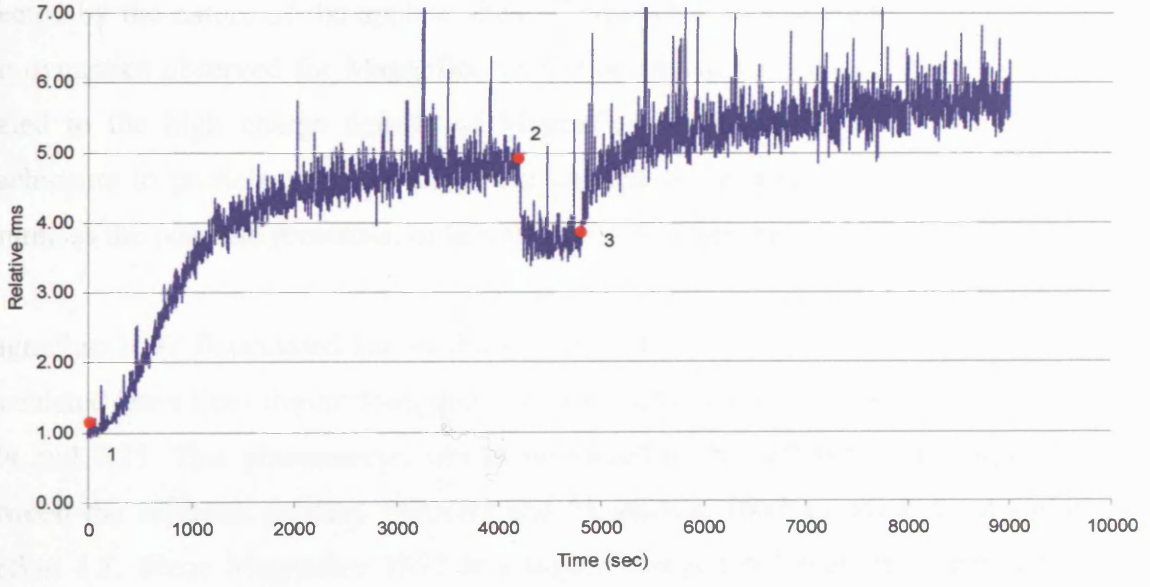

Figure 4.25 Flocculation curve showing the formation, breakage and re-formation of Magnafloc 1697 flocculated latex flocs. 1. Magnafloc 1697 addition followed by an approximately 70 minute formation (100 rpm), 2. Onset of an approximately 10 minute breakage (200 rpm), 3. Onset of an approximately 70 minute re-formation (100 rpm).

Flocculation for kaolin and latex particles takes place soon after the addition of Magnafloc 1697 without a significant lag time as shown in Figures 4.24 and 4.25, which indicates rapid polymer adsorption. Magnafloc 1697 flocculated kaolin and latex flocs break in a fashion similar to that of calcium nitrate coagulated flocs under shear conditions and exhibit reversible floc dynamics when the original stirring rates are restored.

This agrees with the study carried out by Yukselen and Gregory (2002), which showed complete re-formation of Magnafloc 1697 flocculated kaolin flocs but contradicts studies by researchers such as Ditter et al. (1982), Horn and Merrill (1984), Leu and Ghosh (1988) and Spicer et al. (1998), who attributed the irreversible floc dynamics observed to the detachment of polymer chains from kaolin particles and the reduced ability of the resulting fragments to bond to one another after intense fragmentation.

Apart from the different materials and experimental specifications employed by different researchers to consider, it is possible that reversible floc dynamics is directly related to the shear conditions applied, since the mixing of added polymer, adsorption of polymer to particles and the formation and breakage of particle-particle bonds are all affected by the nature of the applied shear (Gregory, 1988). In addition, the reversible floc dynamics observed for Magnafloc 1697 flocculated kaolin and latex flocs can be related to the high charge density of Magnafloc 1697, which allows firm polymer attachments to particle surfaces under the applied shear conditions and subsequently minimises the possible formation of less adhesive polymer fragments.

Magnafloc 1697 flocculated kaolin flocs are significantly larger than Magnafloc 1697 flocculated latex flocs during formation, breakage and re-formation as shown in Figures 4.24 and 4.25. This phenomenon can be attributed to the difference in charge density between the different primary particles and Magnafloc 1697 as pointed out earlier in Section 4.1. Since Magnafloc 1697 is a highly charged polymer, latex particles with much lower charge density are prone to overdose or underdose by polymer instead of being destabilised, which results in minimum floc growth. In addition, due to their larger surface areas and higher particle number concentration, kaolin particles are likely to collide and attach to one another more effectively and result in much larger flocs than latex particles, which the level of attachments is limited by their sphericity.

In addition, Magnafloc 1697 flocculated kaolin particles tend to form a highly irregular and voluminous floc structure similar to the card house structure as shown earlier in Figure 2.21 through regions of alternative charge on the edges and surfaces of kaolin particles. Magnafloc 1697 flocculated latex particles, on the other hand, form a comparatively smaller and more uniform floc structure restricted by the sphericity of the latex particles. Furthermore, kaolin particles are more reactive than latex particles due to their larger surface area, which may be a contributing factor to the superior floc growth observed for Magnafloc 1697 flocculated kaolin flocs.

Despite the fact that there is a higher particle number concentration for the kaolin systems studied, this should not be considered the primary factor for the dramatic difference in floc size observed between the two systems since maximum floc size is governed by the power input P, which is related to the effective shear rate (mean velocity gradient) $\overline{G}$ and not the particle number concentration of a system (see Section 2.7).

Figures 4.26 to 4.31 show images of Magnafloc 1697 flocculated kaolin and latex flocs during formation, breakage and re-formation. Magnafloc 1697 flocculated latex flocs appear to be slightly more compact and denser than Magnafloc 1697 flocculated kaolin flocs. Magnafloc 1697 flocculated kaolin flocs appear to have fine pores incorporated within the structure, which may be regarded as an indication of the card house structure mentioned earlier. The significant difference in floc size as seen here, may explain the low turbidity removal observed for latex suspensions flocculated with Magnafloc 1697 as shown earlier in Figure 4.2.

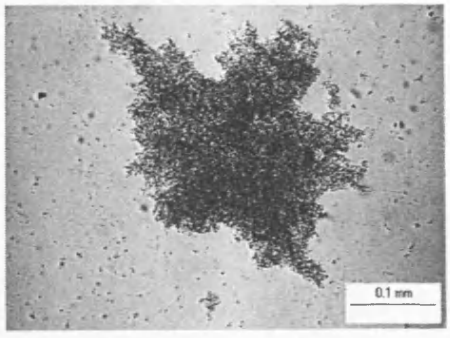

Figure 4.26 Magnafloc 1697 flocculated kaolin floc formed at 100 rpm.

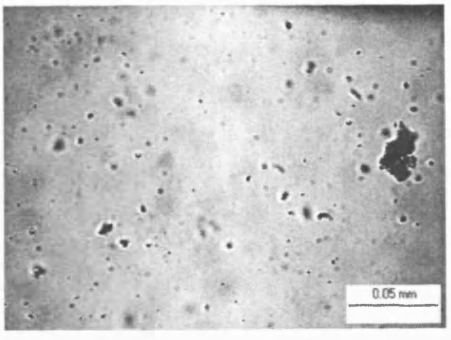

Figure 4.27 Magnafloc 1697 flocculated latex floc formed at 100 rpm.

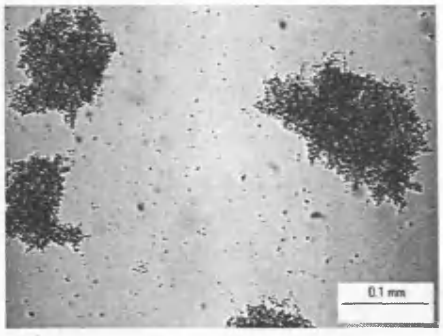

Figure 4.28 Magnafloc 1697 flocculated kaolin floc broken at 200 rpm.

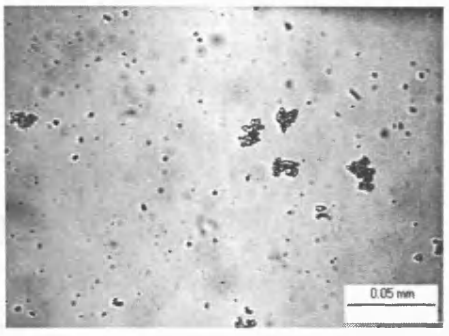

Figure 4.29 Magnafloc 1697 flocculated latex floc broken at 200 rpm.

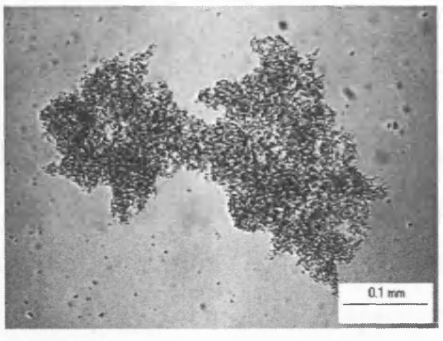

Figure 4.30 Magnafloc 1697 flocculated kaolin floc re-formed at 100 rpm.

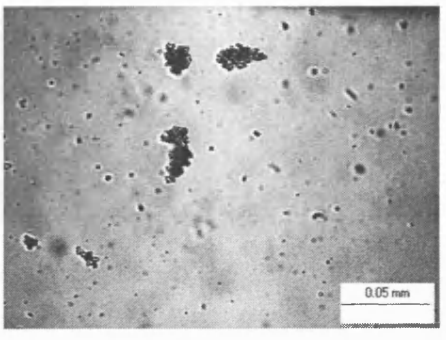

Figure 4.31 Magnafloc 1697 flocculated latex floc re-formed at 100 rpm.

Figures 4.32 and 4.33 show the formation, breakage and re-formation of Zetag 64 flocculated kaolin and latex flocs respectively. Unlike Magnafloc 1697, Zetag 64 destabilises particles via polymer bridging and charge neutralisation (see Section 2.4.3.1).

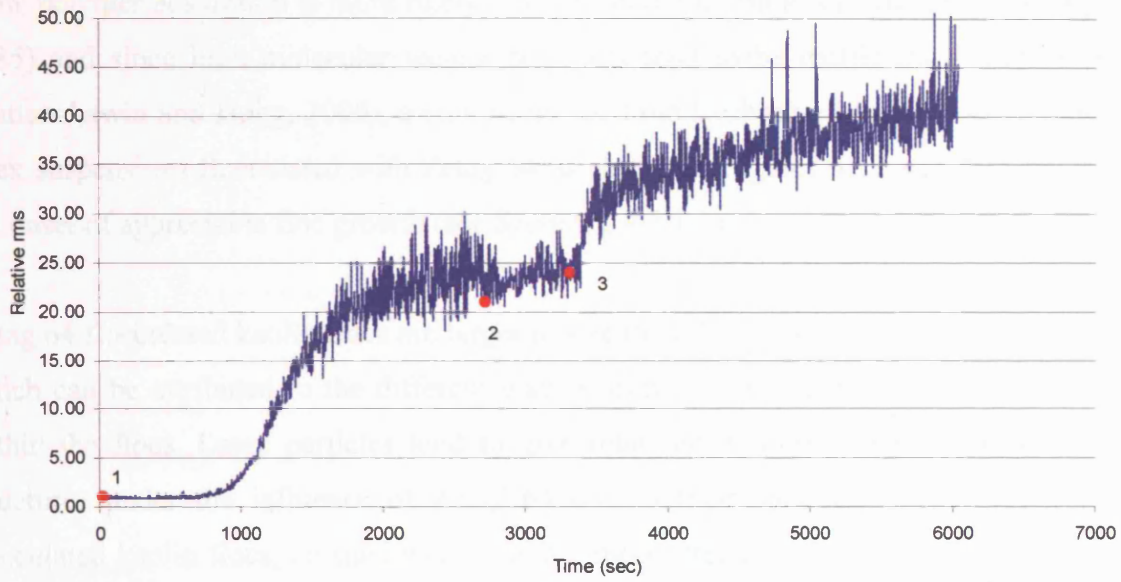

Figure 4.32 Flocculation curve showing the formation, breakage and re-formation of Zetag 64 flocculated kaolin flocs. 1. Zetag 64 addition followed by an approximately 45 minutes formation (100 rpm), 2. Onset of an approximately 10 minutes breakage (200 rpm), 3. Onset of an approximately 45 minutes re-formation (100 rpm).

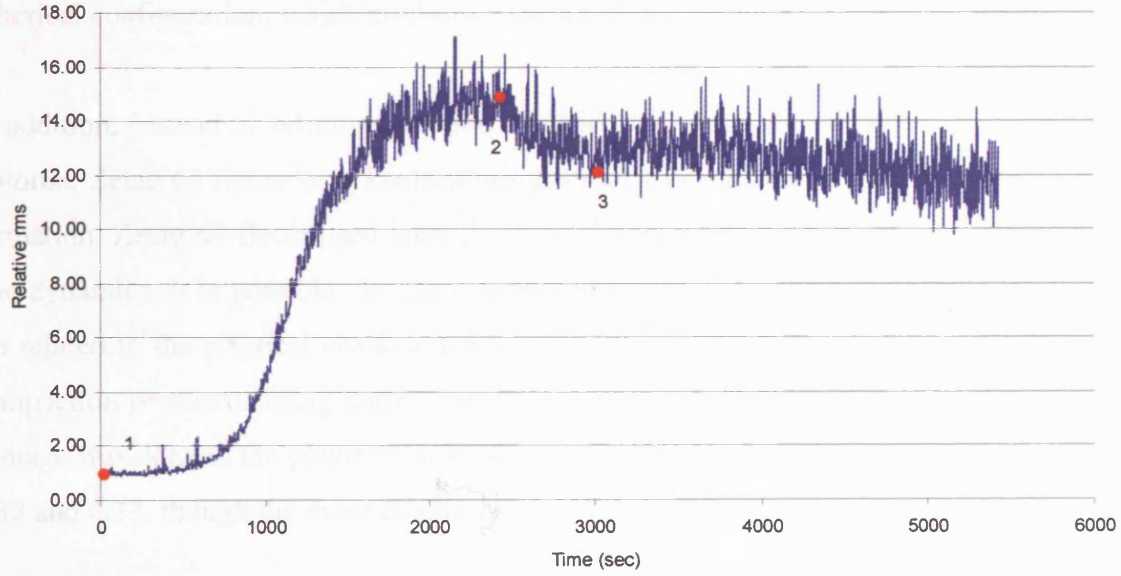

Figure 4.33 Flocculation curve showing the formation, breakage and re-formation of Zetag 64 flocculated latex flocs. 1. Zetag 64 addition followed by an approximately 40 minutes formation (100 rpm), 2. Onset of an approximately 10 minutes breakage (200 rpm), 3. Onset of an approximately 40 minutes re-formation (100 rpm).

Slow polymer adsorption is more likely to be observed in dilute suspensions (Gregory, 1985) and since high molecular weight polymers tend to be inefficient destabilisers (Rattanakawin and Hogg, 2000), a significant lag time is observed for both kaolin and latex suspensions flocculated with Zetag 64 as shown in Figures 4.32 and 4.33 before the onset of appreciable floc growth (see Section 2.4.3.1.1).

Zetag 64 flocculated kaolin flocs are larger in size than Zetag 64 flocculated latex flocs, which can be attributed to the different ways kaolin and latex particles are structured within the flocs. Latex particles tend to give relatively uniform, more compact floc structures under the influence of Zetag 64 due to their spherical shape. Zetag 64 flocculated kaolin flocs, on the other hand, are more irregular and porous in structure, hence their larger size, and are susceptible to a higher level of compaction or restructuring during breakage.

Contrary to the systems already discussed, limited floc breakage was observed for both Zetag 64 flocculated kaolin and latex flocs under shear conditions. This suggests that suspensions flocculated with polymers of low charge density and high molecular weight tend to give stronger flocs (Gregory, 2000), possibly due to their coiled, almost spherical configuration, which minimises the forces imposed under shear conditions.

In addition, instead of returning to their original size when the original stirring rate is restored, Zetag 64 flocculated kaolin flocs grow further into larger size flocs during re-formation. Zetag 64 flocculated latex flocs, on the other hand, do not exhibit reversible floc dynamics. It is possible that the different behaviours observed during re-formation are related to the physical characteristics of the primary particles and the level of floc compaction or restructuring during breakage rather than the polymer itself, since little damage was done to the polymer molecules during floc breakage as indicated in Figures 4.32 and 4.33, though the exact mechanisms involved remain unclear.

Figures 4.34 to 4.39 show images of Zetag 64 flocculated kaolin and latex flocs during formation, breakage and re-formation. Zetag 64 flocculated kaolin flocs appear to be slightly less compact and dense than Zetag 64 flocculated latex flocs. Zetag 64 flocculated kaolin flocs become larger than their original size during re-formation, which shows that floc compaction or restructuring during breakage can promote further floc growth for some systems.

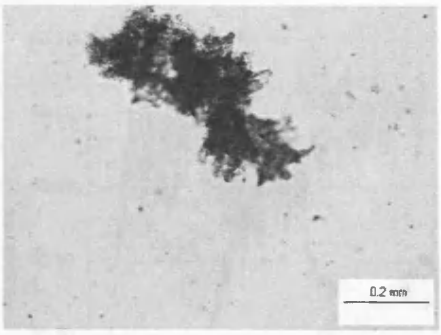

Figure 4.34 Zetag 64 induced kaolin floc formed at 100 rpm.

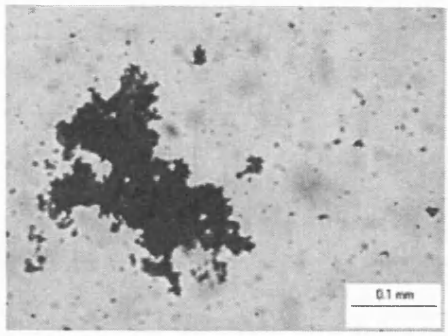

Figure 4.35 Zetag 64 induced latex floc formed at 100 rpm.

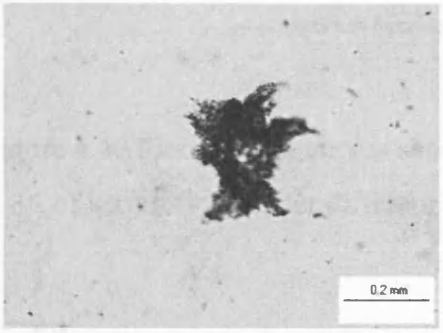

Figure 4.36 Zetag 64 induced kaolin floc broken at 200 rpm.

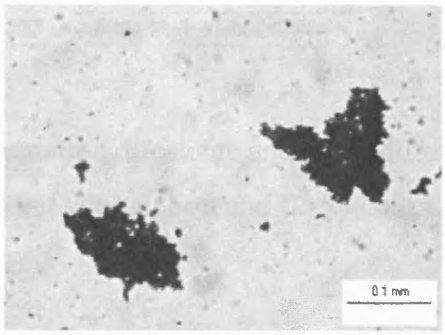

Figure 4.37 Zetag 64 induced latex floc broken at 200 rpm.

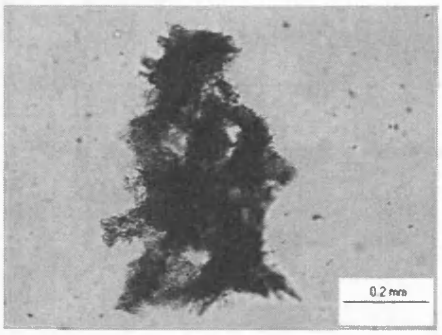

Figure 4.38 Zetag 64 induced kaolin floc re-formed at 100 rpm.

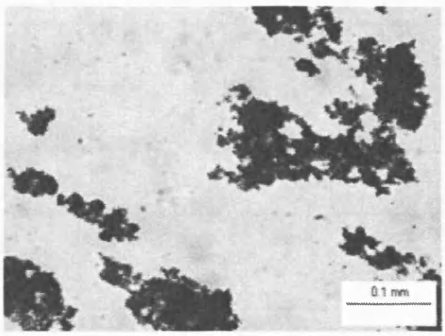

Figure 4.39 Zetag 64 induced latex floc re-formed at 100 rpm.

Figures 4.40 and 4.41 show the formation, breakage and the re-formation of kaolin and latex flocs under different mechanisms of coagulation and flocculation respectively.

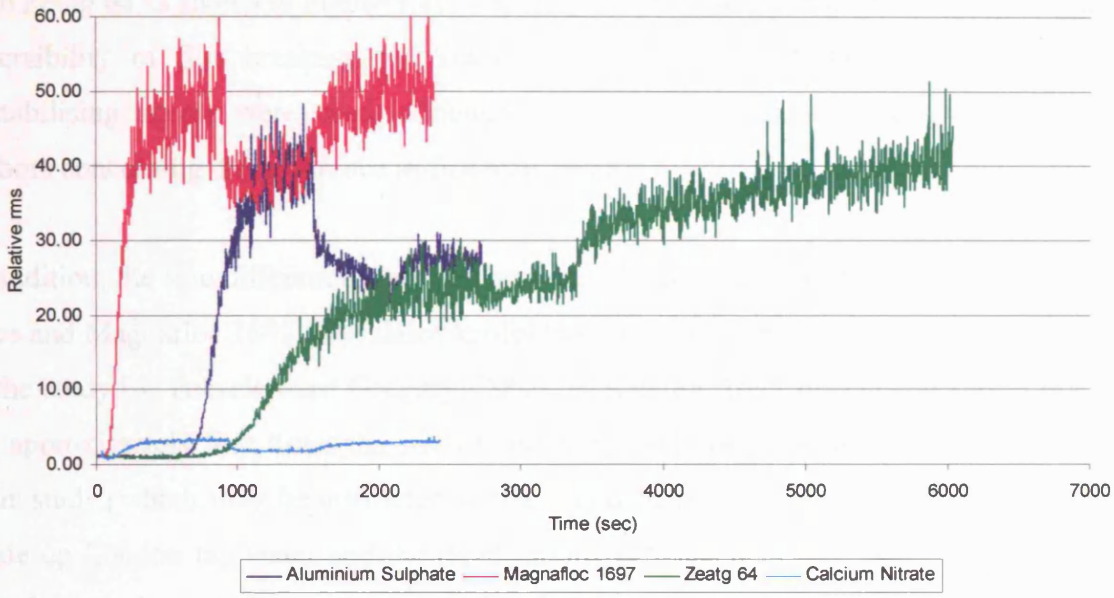

Figure 4.40 Flocculation curves showing the formation, breakage and the re-formation of kaolin flocs under different mechanisms of coagulation and flocculation.

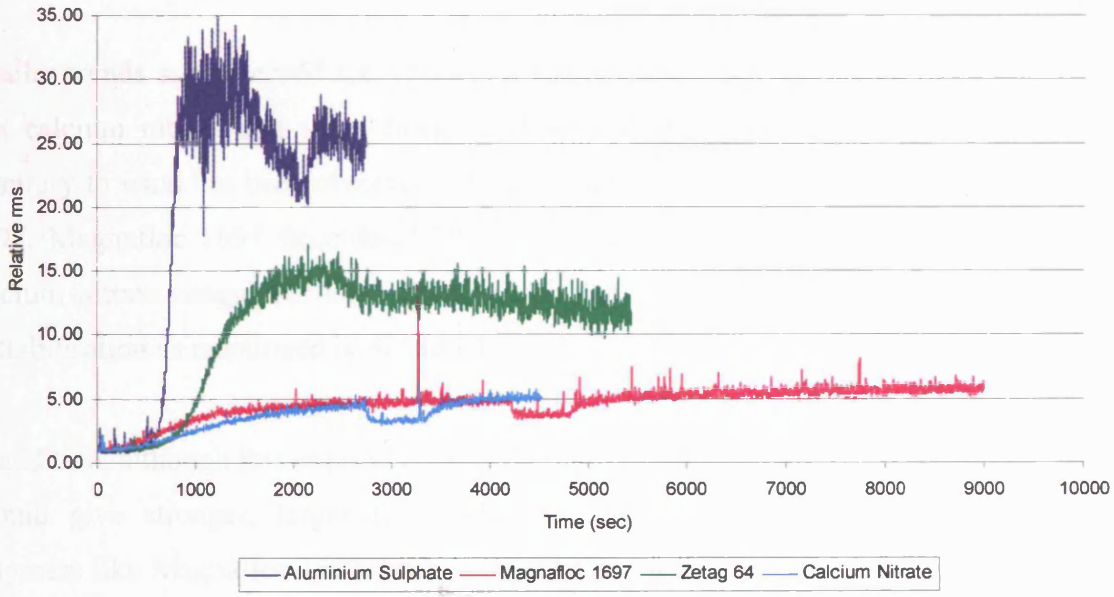

Figure 4.41 Flocculation curves showing the formation, breakage and the re-formation of latex flocs under different mechanisms of coagulation and flocculation.

Among the different destabilising agents tested with kaolin suspensions, those flocculated with Magnafloc 1697 produce the largest flocs; probably due to the high charge density of the polymer, followed by those coagulated with aluminium sulphate; floc size likely to be contributed mainly by precipitated materials, and those flocculated

with Zetag 64 as shown in Figure 4.40. These agree with the findings in the study on the reversibility of floc breakage by Yukselen and Gregory (2004), which the same destabilising agents were used, although no clear explanations were given by the authors concerning the difference in floc size observed.

In addition, the size difference observed between aluminium sulphate coagulated kaolin flocs and Magnafloc 1697 flocculated kaolin flocs are not as significant as that observed in the study by Yukselen and Gregory (2002); Magnafloc 1697 flocculated kaolin flocs are approximately four times the size of aluminium sulphate coagulated kaolin flocs in their study, which may be attributed to the added humic acid in their test suspension made up London tap water and the rapid mixing (15 seconds) (see Section 2.6.1) and low slow stirring rate (30 rpm) employed in their study.

Kaolin suspensions coagulated with calcium nitrate, on the other hand, produce the smallest flocs as shown in Figure 4.40, which is expected of the type of destabilising mechanism that is involved (Gregory, 2000).

Similar trends are observed for latex suspensions coagulated with aluminium sulphate and calcium nitrate and those flocculated with Zetag 64 as shown in Figure 4.41. Contrary to what has been observed for kaolin suspensions flocculated with Magnafloc 1697, Magnafloc 1697 flocculated latex flocs have the smallest floc size along with calcium nitrate coagulated latex flocs, which can be attributed to ineffective particle destabilisation as mentioned in Section 4.1.

In addition, although it is expected that higher molecular weight polymers, like Zetag 64 should give stronger, larger flocs (Gregory, 1996) than lower molecular weight polymers like Magnafloc 1697, both Zetag 64 flocculated kaolin and latex flocs fail to give larger floc sizes, which may be explained by the difference in charge density between the polymers employed.

4.3 New Automated Filterability Monitoring Technique

Figure 4.42 shows the mean specific resistance to filtration values given by different suspensions under the same filtration technique as described in Section 3.3. Kaolin suspension shows the highest mean specific resistance to filtration among the different

suspensions under test and is approximately nine times higher than that of latex suspension.

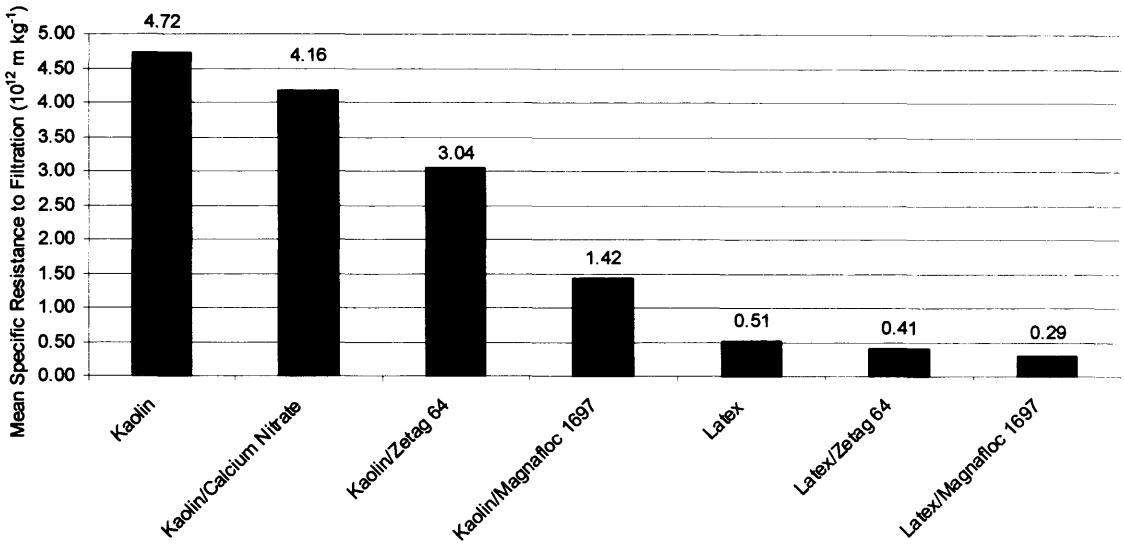

Figure 4.42 Mean specific resistance to filtration values given by different suspensions under the new automated filterability monitoring technique.

This can be explained by the work of Besra et al. (2000) regarding the effect of particle characteristics on the dewatering and filtration behaviour of kaolin, calcite and quartz suspensions. They attributed the poor dewaterability and filterability of kaolin observed to its fineness, high water retaining capacity and plate-like shape of its particles having low sphericity.

The effect of particle size and shape on filter cake permeability has long been recognised (Krubien and Monk, 1943). Sharma and Zongming (1991) studied the properties of clay filter cakes by means of a structural network model and they found that cake permeability decreases with mean particle diameter. They attributed the exceptionally low permeability of clay filter cakes observed to the small, flat and filmy clay platelets which agrees with the observation by Bersa at al. (2000).

The understanding of the way particles are packed together to form a filter cake relative to their physical characteristics is important to define permeability and dewaterability (Mota et al., 2003). The structure of a filter cake consisting of latex particles is somewhat uniform due to the spherical shape of the particles as shown in Figures 4.43

and 4.44. Water channels are formed within the regular structure facilitating the drainage of liquid. Plate-like particles like kaolin, on the other hand, are likely to pile on top of each other (Ozcan et al., 2000) as shown in Figures 4.45 and 4.46 allowing minimal formation of water channels, which leads to a substantial decrease in permeability.

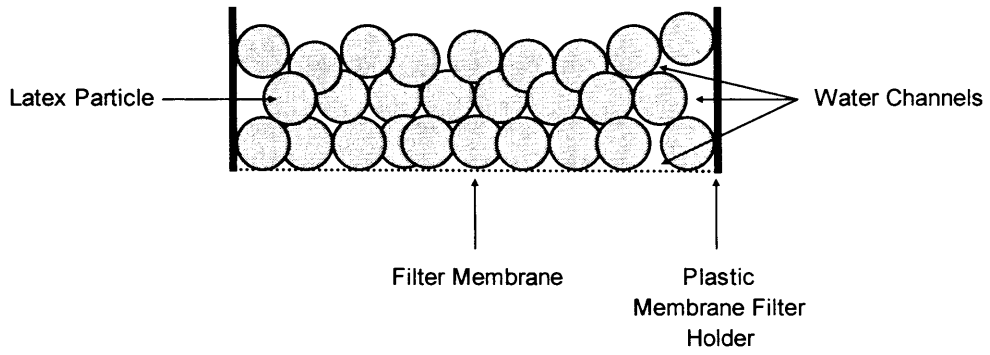

Figure 4.43 Cross-sectional structure of a filter cake consisting of spherical latex particles.

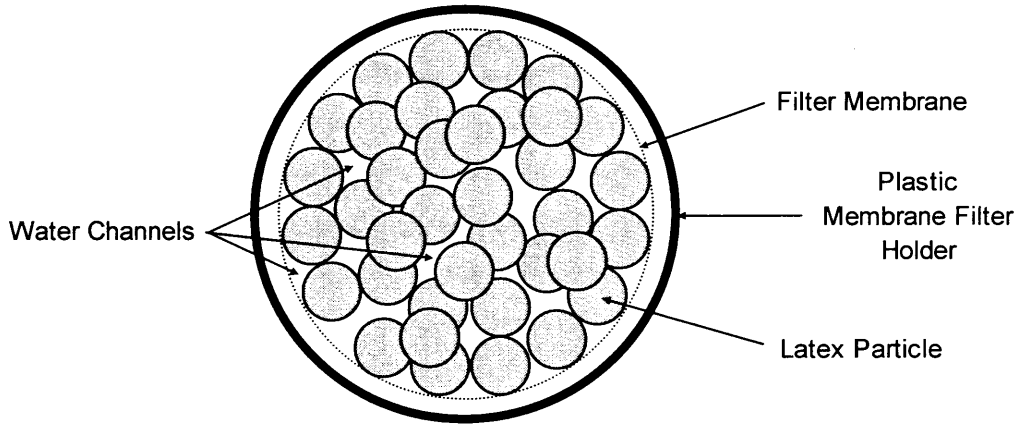

Figure 4.44 Top view of a filter cake consisting of latex particles.

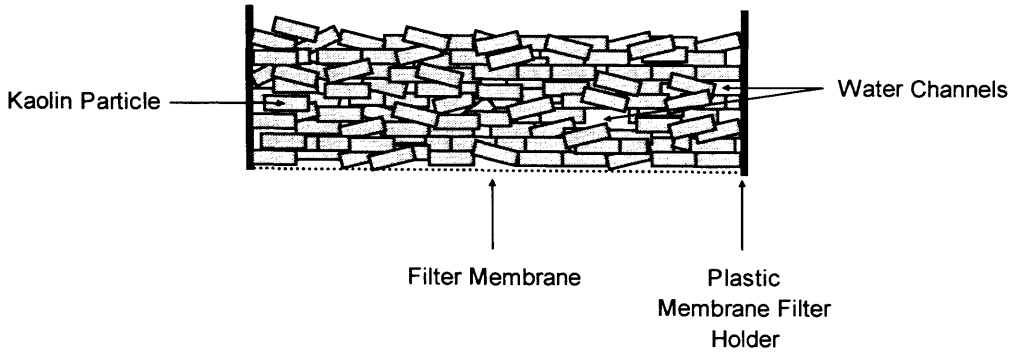

Figure 4.45 Cross-sectional structure of a filter cake consisting of plate-like kaolin particles.

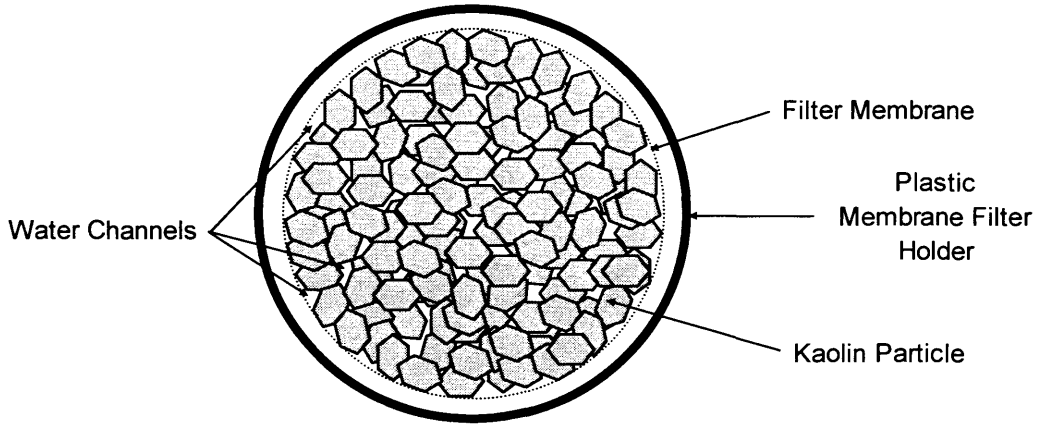

Figure 4.46 Top view of a filter cake consisting of kaolin particles.

Magnafloc 1697 is more effective in enhancing filterability than Zetag 64 for both kaolin and latex suspensions as shown in Figure 4.42. This can be explained by the ways these polymers are distributed over and attached to the different particles.

The amount of Magnafloc 1697 required to destabilise kaolin particles is comparatively smaller than that of Zetag 64 (see Table 4.2) probably due to its high charge density. In such a small amount, Magnafloc 1697 molecules are unlikely to be distributed evenly over the edges and surfaces of the kaolin particles. The kaolin particles under test are negatively charged overall (see Section 2.11.1), cationic polymers of high charge density and low molecular weight like Magnafloc 1697 tend to adsorb onto the edges

and surfaces of kaolin particles in a completely flat configuration forming regions of alternative charges. These regions align accordingly to form a porous floc structure similar to the card house structure as shown in Figure 4.47, which allows the passage of liquid through the water channels created within (see Section 2.10.4). The structure of a filter cake consisting of Magnafloc 1697 flocculated kaolin flocs is shown in Figure 4.48.

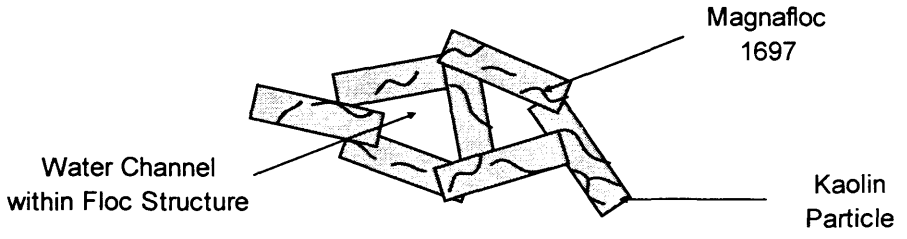

Figure 4.47 Structure of a Magnafloc 1697 flocculated kaolin floc.

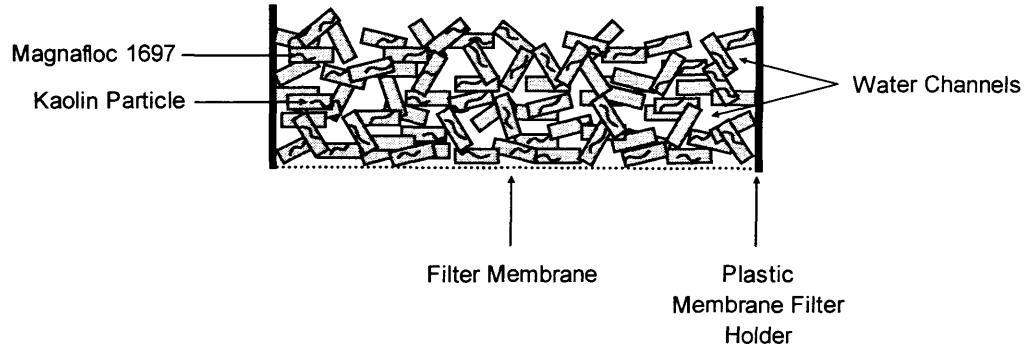

Figure 4.48 Cross-sectional structure of a filter cake consisting of Magnafloc 1697 flocculated kaolin flocs.

Cationic polymers of low charge density and high molecular weight like Zetag 64, on the other hand, assume a coiled, almost spherical configuration (see Section 2.4.2) and they tend to tangle (see Sections 2.4.4) and have a high value of hydrodynamic radius or adsorbed layer thickness, which is detrimental to flocculation because of hindrance to close approach of polymer coated particles to each other (Besra, et al., 2004).

Since a larger amount of Zetag 64 is required to destabilise the same amount of kaolin particles, the card house structure becomes unlikely due to higher polymer coverage. Instead, kaolin particles are neutralised and bridged together by Zetag 64 molecules in a face to face configuration due to the larger attractive surfaces to the edges (see Figure 4.49), leading to a more compact filter cake structure under pressure, which subsequently minimises liquid flow as shown in Figure 4.50. In addition, due to the larger amounts of Zetag 64 required to destabilise kaolin and latex particles (see Table 4.2), the polymer itself may add resistance to the flow; high molecular weight polymers tend to entrap water within their structures (Besra et al., 2002) and fill in pores within the filter cake structure (Li and Ganczarczyk, 1992 and 1998).

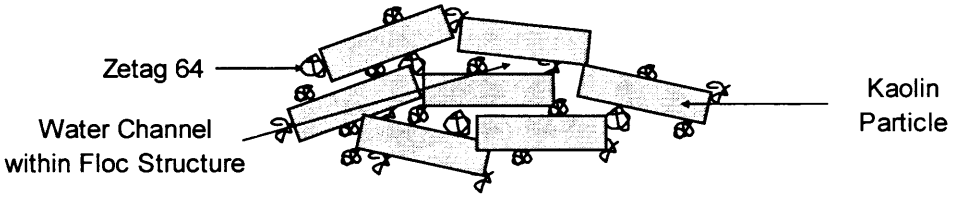

Figure 4.49 Structure of a Zetag 64 flocculated kaolin floc.

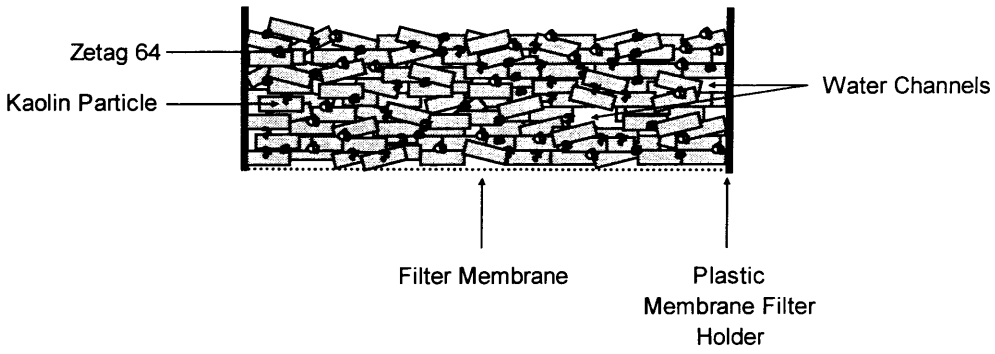

Figure 4.50 Cross-sectional structure of a filter cake consisting of Zetag 64 flocculated kaolin flocs.

No matter how polymers are distributed on the spherical latex particles, they tend to bond more or less the same way they are packed together without the influence of a polymer due to their shape. Therefore, the mean specific resistance to filtration values given by a latex suspension flocculated with Magnafloc 1697 or Zetag 64 are very

similar to that of a latex suspension as shown in Figure 4.42. The slight difference observed between the two can be attributed to the different floc structures created relative to the physical characteristics of the different polymers employed.

As mentioned earlier in Section 4.1 that latex particles are prone to overdose or underdose by Magnafloc 1697, this may lead to repulsion between flocs and ineffectively destabilised latex particles (see Figure 4.51). Water channels are created within the filter cake structure as a result, facilitating the drainage of liquid as shown in Figure 4.52. Zetag 64, on the other hand, neutralises and bridges latex particles together (see Figure 4.53) forming a slightly more compact filter cake structure under pressure as shown in Figure 4.54.

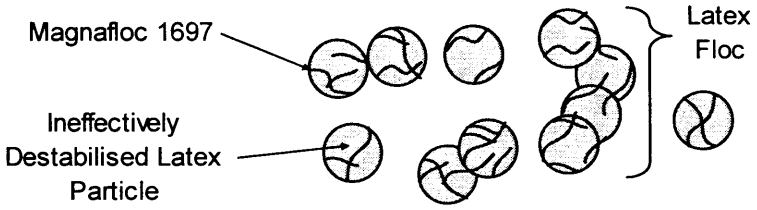

Figure 4.51 Electrostatic repulsion between Magnafloc 1697 flocculated latex flocs and ineffectively destabilised latex particles.

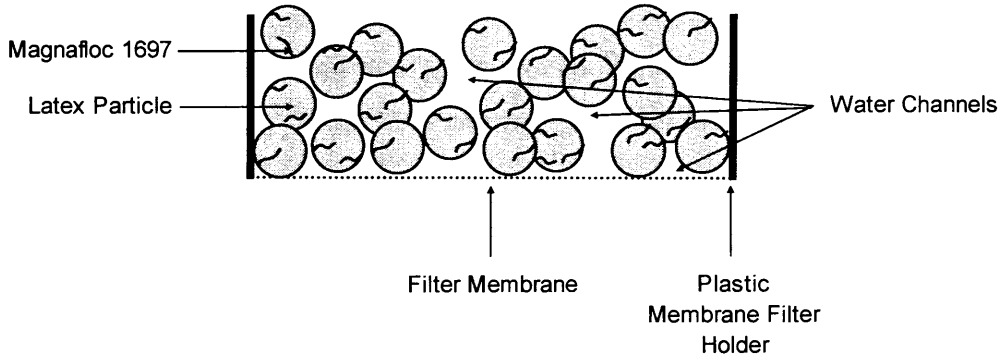

Figure 4.52 Cross-sectional structure of a filter cake consisting of Magnafloc 1697 flocculated latex flocs and ineffectively destabilised latex particles.

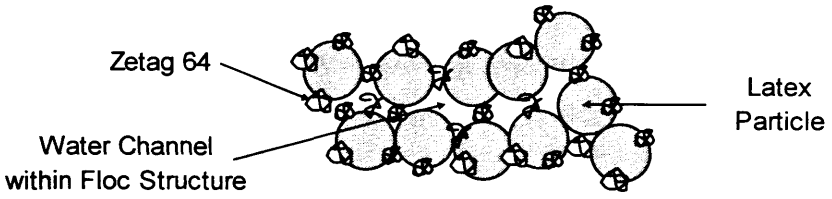

Figure 4.53 Structure of a Zetag 64 flocculated latex floc.

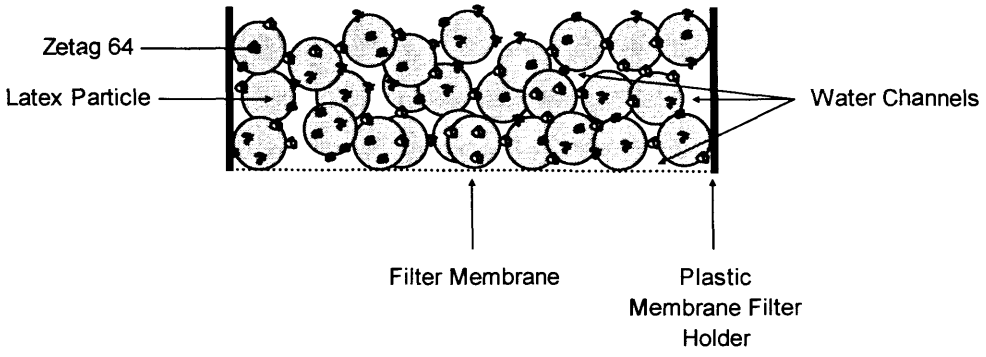

Figure 4.54 Cross-sectional structure of a filter cake consisting of Zetag 64 flocculated latex flocs.

The mean specific resistance to filtration values obtained from filtering polymer flocculated suspensions are apparently dependent on the physical characteristics of the different primary particles employed as shown in Figure 4.42. This agrees with the observation by Mikkelsen (2001) that primary particles have a dominant effect on filterability and suggests that polymers do not contribute significantly to the filterability of flocs if the primary particles involved possess high sphericity.

Magnafloc 1697 flocculated kaolin flocs are significantly larger than Magnafloc 1697 flocculated latex flocs as shown earlier in Figures 4.24 and 4.25. Since fractal aggregates increase in porosity as their size increases (Meakin, 1988; Jiang and Logan, 1991; Gregory, 1997), Magnafloc 1697 flocculated kaolin flocs should in theory possess a significantly higher permeability than Magnafloc 1697 flocculated latex flocs (see Section 2.10.4) which is contrary to what has been observed as shown in Figure 4.42.

The higher mean specific resistance to filtration value obtained from filtering Magnafloc 1697 flocculated kaolin suspensions suggests that the drainage of liquid from the filter cake is not solely determined by the fractal dimension (Li and Logan, 2001) or its porosity but also by some other factors, which may include the distribution of primary particles within the flocs (Li and Logan, 2001) and the presence of blocked pores within the cake structure that actually do not take part in the drainage of liquid (Besra et al., 2000).

Although it is not clear exactly what contributed to the low permeability observed despite the size of the kaolin flocs, a similar phenomenon was encountered by researchers such as Besra et al. (2000) and they suggested that the low permeability of kaolin may probably be a result of its swelling tendency and high water retaining capacity.

Despite an increase in floc size as shown earlier in Figure 4.14, the mean specific resistance to filtration value obtained from filtering calcium nitrate coagulated kaolin suspensions at 100 rpm was essentially identical to the mean value obtained from filtering kaolin suspensions at the same stirring rate using the employed filtration technique. A lower stirring rate at 50 rpm was later adopted as described earlier in Section 3.3.4.3, which a larger floc size and a small decrease in mean specific resistance to filtration (see Figure 4.42) were observed.

Kaolin particles coagulated with calcium nitrate are bonded together by weak van der Waals forces through double layer compression as described earlier in Section 2.3.1. Despite the higher particle collision rates offered by higher mixing conditions, firm attachments between particles may be difficult to establish when the means of particle attachment depends solely on weak attractive forces. In addition, excessive mixing can lead to the formation of underdeveloped flocs with undesirable physical characteristics.

Kaolin particles destabilised with calcium nitrate tend to bond face to face due to the larger attractive surfaces to the edges. Flocs become increasingly irregular in shape as they grow larger and pack less effectively as they are being filtered. Kaolin particles and the small flocs formed at 100 rpm may pack together and interpenetrate more effectively than the larger flocs formed at 50 rpm, leading to a more restricted liquid

flow. Kaolin particles and the small flocs having similar filterability can be attributed to similarities in filter cake structure and compactness.

The specific resistance to filtration of a coagulated or flocculated suspension under continuous filtration and mixing tends not to change significantly despite continuous floc growth. Figure 4.55 shows a linearised plot for a Magnafloc 1697 flocculated kaolin suspension and as mentioned earlier in Section 2.10.3.3 that the slope of which can be used to calculate the specific resistant to filtration of the suspension, it is also an indication to whether floc growth has an impact on specific resistance to filtration.

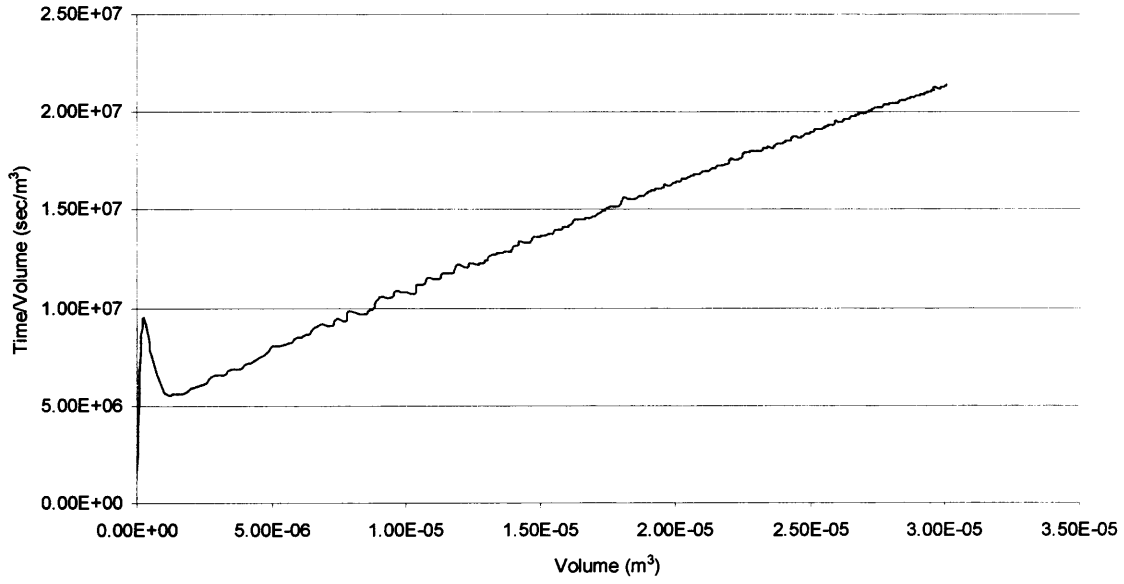

Figure 4.55 Time/Volume against Volume plot for a Magnafloc 1697 flocculated kaolin suspension.

Among the different systems under test, kaolin suspensions flocculated with Magnafloc 1697 have the most significant floc growth and the largest floc size (see Figure 4.40) and yet it is apparent from Figure 4.55 that as soon as a resistance is established within the membrane filter, which takes approximately 10 seconds, the plot remains linear since despite the significant floc growth that follows. This indicates that filterability may not to be greatly dependent on floc size, which agrees with the observation by Gregory and de Moor (1984) and supported by the work of Hogg (2000) which suggests that floc size, in itself, has only secondary effects to filtration.

The breakage and re-formation of flocs coagulated and flocculated with different destabilising agents were initially incorporated as parts of the experimental procedures in order to assess the effect of floc breakage and re-formation on specific resistance to filtration. However, early results obtained suggest that breakage and re-formation of flocs have no significant effects on specific resistance to filtration. Therefore, further trials were abandoned and the results obtained are not presented in this work.

Such behaviour can be explained by the concept that flocs consist of micro-flocs (Michaels and Bolger, 1962; Van de Ven and Hunter, 1977; Higashitani and Shibata, 1987; Hogg, 2000 and Kan et al., 2002), which determine the overall filterability of a floc (see Section 2.10.4).

Micro-flocs are formed during the initial mixing of primary particles with a destabilising agent and their size is dependent on the shear conditions applied. During the further mixing that follows, micro-flocs collide and aggregate to form larger flocs (Gregory and de Moor, 1984). Whether flocs are being grown, broken or re-formed, as long as the structure of the micro-flocs are not subject to significant alterations, the overall filterability of a floc should be based on its constituent micro-flocs.

Furthermore, all filtration curves obtained using the proposed automated filterability monitoring technique are linearised adequately and show no obvious signs of filter cake compression or deformation and the specific resistance to filtration valves obtained are reproducible with the new automated filterability monitoring technique as shown in Table 4.3.

Suspension	Mean Specific Resistance to Filtration (10^{12} m kg^{-1})	Standard Deviation (10^{12} m kg^{-1})	95% Confidence (10^{12} m kg^{-1})
Kaolin	4.72	1.19	±0.67
Kaolin/Calcium Nitrate	4.16	1.12	±0.64
Kaolin/Zetag 64	3.04	0.76	±0.43
Kaolin/Magnafloc 1697	1.42	0.44	±0.25
Latex	0.51	0.07	±0.04
Latex/Zetag 64	0.41	0.13	±0.07
Latex/Magnafloc 1697	0.29	0.04	±0.02

Table 4.3 Reproducibility of the new automated filterability monitoring technique.

Chapter 5

Conclusions

Conclusions drawn below apply only to experiments carried out following the stated experimental specifications in Sections 3.1, 3.2 and 3.3. A concise summary of experimental findings is presented in Table 5.1.

Floc Size	System	Lag Time	Flocculation Rate	Floc Erosion	Floc Breakage	Floc Reformation	Filterability	*Other
Large	Kaolin/Magnafloc 1697	No	High	No	Yes	Yes	Medium/High	-
	Kaolin/Aluminium Sulphate	Significant	High	Yes	Yes*	No	-	Flocs break before erosion begins
	Latex/Aluminium Sulphate	Significant	High	Yes	No	No	-	-
	Kaolin/Zetag 64	Significant	Medium	No	Yes*	Yes*	Medium/Low	Floc breakage is not significant and further floc growth is observed during reformation
	Latex/Zetag 64	Significant	Medium	No	Yes*	No	High	Limited floc breakage
	Latex/Magnafloc 1697	No	Low	No	Yes	Yes	High	-
	Latex/Calcium Nitrate	No	Low	No	Yes	Yes	-	-
Small	Kaolin/Calcium Nitrate	No	High	No	Yes	Yes	Low	-

Table 5.1 Concise summary of experimental findings.

5.1 Kaolin and Latex Particles Flocculated with Magnafloc 1697

Polymers with high charge density and low molecular weight like Magnafloc 1697 are not suitable for flocculating low charge density latex particles (~ 14 $\mu C/cm^2$) due to the high possibility of ineffective particle destabilisation as a result of significant charge density difference between the latex particles and the polymer (see Section 4.1).

Magnafloc 1697 effects flocculation for kaolin and latex particles at approximately the same time but kaolin particles seem to flocculate much more rapidly than latex particles (see Figures 4.24 and 4.25) under the same conditions, which may be a result of more effective particle destabilisation and kaolin particles being more reactive by having larger surface areas.

Magnafloc 1697 has the ability to promote significant floc growth but only if the particles are effectively destabilised. Fine, plate-like particles like kaolin tend to form large, porous floc structures under the influence of Magnafloc 1697 (see Figure 4.24). Magnafloc 1697 flocculated kaolin and latex flocs tend to break sharply under the applied shear conditions (Figures 4.24 and 4.25).

Magnafloc 1697 flocculated flocs exhibit reversible floc breakage (see Figures 4.24 and 4.25), which may be related to the high charge density of Magnafloc 1697 allowing firm polymer attachments to particle surfaces under the applied shear conditions and subsequently minimising the possible formation of less adhesive polymer fragments for reformation.

Magnafloc 1697 flocculated latex flocs appear to be more compact and denser than Magnafloc 1697 flocculated kaolin flocs (see Figures 4.26 and 4.27), which possess a distinctive mass perforated structure (card house structure).

Magnafloc 1697 is effective in enhancing filterability for kaolin suspensions by promoting the formation of large, porous floc structures (see Figure 4.42), which allow the passage of fluid through them as well as around them within the filter cake (see Section 2.10.4). A slight improvement in filterability is observed for latex suspensions flocculated with Magnafloc 1697 (see Figure 4.42). However, this is likely to be an effect of the repulsive forces exist between the small flocs and the primary particles as a result of ineffective particle destabilisation (see Figure 4.51), which allows better liquid flow around them within the filter cake (see Figure 4.52).

5.2 Kaolin and Latex Particles Flocculated with Zetag 64

Comparatively larger amounts of Zetag 64 are usually required for particle destabilisation than Magnafloc 1697 (see Table 4.2), which may be related to its low charge density.

Zetag 64 adsorbs onto kaolin and latex particles comparatively slower than Magnafloc 1697 (see Figures 4.32 and 4.33), which is probably due to its low charge density and high molecular weight (Ouali and Pefferkorn, 1994; Rattanakawin and Hogg, 2000). Kaolin and latex particles flocculate at similar rates under the influence of Zetag 64 but

larger flocs are formed with kaolin particles (see Figures 4.32 and 4.33). This is likely to be related to the different ways kaolin and latex particles are structured according to their shapes within the flocs.

Although Zetag 64 flocculated kaolin and latex flocs do not grow to the same extent as Magnafloc 1697 flocculated kaolin flocs, they seem to have better floc strength as they do not break significantly under the applied shear conditions (See Figures 4.32 and 4.33). This suggests better floc strength provided by the polymer (Gregory, 2000), possibly due to its coiled and almost spherical configuration, which minimises the forces imposed under the applied shear conditions.

Zetag 64 flocculated kaolin flocs grow further into larger size flocs, while Zetag 64 flocculated latex flocs remain more or less the same size during reformation after breakage. Although the exact mechanisms involved remain unclear, it is possible that the different behaviours observed during reformation are related to the physical characteristics of the primary particles and the level of floc compaction or restructuring during breakage. The behaviour observed during reformation for Zetag 64 flocculated kaolin shows that breakage can promote further floc growth for some systems.

Zetag 64 flocculated kaolin flocs appear to be less compact and dense than Zetag 64 flocculated latex flocs (see Figures 4.34 and 4.35).

Zetag 64 is not as effective as Magnafloc 1697 in enhancing filterability for kaolin and latex suspensions (see Figure 4.42) as it does not promote the formation of porous floc structures and may add resistance to fluid flow itself since high molecular weight polymers tend to entrap water within their structures (Besra et al., 2002) and fill in pores within the filter cake structure (Li and Ganczarczyk, 1992 and 1998).

5.3 Kaolin and Latex Particles Coagulated with Aluminium Sulphate

For kaolin and latex particles coagulated with aluminium sulphate, a significant lag time is observed before the onset of appreciable floc growth (see Figures 4.6 and 4.7), which may be related to the time required for the colloidal hydroxide particles to aggregate (Duan and Gregory, 2003). Kaolin and latex particles flocculate at approximately the

same time and at similar rates after being coagulated with aluminium sulphate (see Figure 4.6 and 4.7).

Aluminium sulphate coagulated kaolin flocs are slightly larger in size than aluminium sulphate coagulated latex flocs (see Figures 4.6 and 4.7), which may be a result of primary particles incorporating themselves differently within the hydroxide precipitate according to their shapes.

Aluminium sulphate coagulated latex flocs are subject to surface erosion under shear conditions (Figure 4.7). This is possibly due to the weak bonding between colloidal hydroxide particles, which account for a large fraction of the floc mass (Bache et al., 1999). Aluminium sulphate coagulated kaolin flocs, on the other hand, are also subject to surface erosion but this only occurs after a small breakage of flocs (Figure 4.6), which suggests that aluminium sulphate coagulated kaolin flocs are weaker structurally than aluminium sulphate coagulated latex flocs.

Aluminium sulphate coagulated kaolin and latex flocs do not completely reform when the original stirring rates are restored after breakage (See Figures 4.6 and 4.7). The limited reformation of flocs observed may be a result of eroded fragments penetrating some way into floc clusters.

Aluminium sulphate coagulated latex flocs appear to be more compact and denser than aluminium sulphate coagulated kaolin flocs (Figures 4.8 and 4.9).

5.4 Kaolin and Latex Particles Coagulated with Calcium Nitrate

Kaolin and latex particles coagulated with calcium nitrate flocculate at approximately the same time but at different rates (see Figures 4.14 and 4.15). Kaolin particles flocculate at a faster rate than latex particles after being coagulated with calcium nitrate. This is possibly due to the larger number of kaolin particles present in the suspension, providing better rates of particle collision and the flat surfaces of kaolin particles, allowing better attachments than latex particles, which the level of attachments is limited by their sphericity.

Calcium nitrate coagulated latex flocs are slightly larger in size than calcium nitrate coagulated kaolin flocs (see Figures 4.14 and 4.15), which may be a result of primary particles incorporating themselves differently according to their shapes; particles with increasing sphericity contribute to overall floc size more effectively (see Figures 4.16 and 4.17). Calcium nitrate coagulated kaolin and latex flocs break sharply under the applied shear conditions (see Figures 4.14 and 4.15) and show reversibility during reformation after breakage.

Calcium nitrate coagulated latex flocs appear to be more compact and denser than calcium nitrate coagulated kaolin flocs (see Figures 4.18 and 4.19).

Calcium nitrate is not very effective in enhancing the filterability of kaolin suspensions (see Figure 4.42). This is possibly due to the face to face configuration that kaolin particles are bonded together (see Figure 4.16), which limits fluid flow through flocs. In addition, kaolin particles are held together by weak van der Waals forces as flocs, which are subject to compaction under pressure during filtration, limiting fluid flow as a result.

5.5 Floc Size Promoted by Different Destabilising Agents

Among the different destabilising agents tested with kaolin suspensions, those flocculated with Magnafloc 1697 produce the largest flocs followed by those coagulated with aluminium sulphate and those flocculated with Zetag 64 (see Figure 4.40). Kaolin suspensions coagulated with calcium nitrate, on the other hand, produce the smallest flocs. Similar trends are observed for latex suspensions coagulated with aluminium sulphate and calcium nitrate and those flocculated with Zetag 64 (see Figure 4.41). Magnafloc 1697 flocculated latex flocs have the smallest floc size along with calcium nitrate coagulated latex flocs.

5.6 Filterability of Flocs

Kaolin suspensions do not filter as well as latex suspensions even when they are treated with polymers (Figure 4.42). This is due to the plate-like kaolin particles having high water retaining capacity and low sphericity (Besra et al., 2000) and that primary particles with high sphericity like latex particles are not influenced significantly by polymers in terms of filterability (Mikkelsen, 2001).

Magnafloc 1697 flocculated kaolin flocs are significantly larger than Magnafloc 1697 flocculated latex flocs (see Figures 4.24 and 4.25) but they do not filter as well as the smaller Magnafloc 1697 flocculated latex flocs (see Figure 4.42), despite the fact that fractal aggregates increase in porosity as their size increases (Meakin, 1988; Jiang and Logan, 1991; Gregory, 1997). The higher mean specific resistance to filtration value obtained from filtering Magnafloc 1697 flocculated kaolin suspensions suggests that the drainage of liquid from the filter cake is not solely determined by the fractal dimension (Li and Logan, 2001) or its porosity but also by some other factors, which may include the shape of the primary particles, the distribution of primary particles within the flocs (Li and Logan, 2001) and the presence of blocked pores within the cake structure that actually do not take part in the drainage of liquid. The low permeability of Magnafloc 1697 flocculated kaolin flocs may also be a result of the swelling tendency and high water retaining capacity of kaolin particles (Besra et al., 2000).

The specific resistance to filtration of a coagulated or flocculated suspension under continuous filtration and mixing tends not to change significantly despite continuous floc growth. This phenomenon is most apparent when filtering kaolin suspensions flocculated with Magnafloc 1697, where floc growth and the large flocs that result seem to have no effects on specific resistance to filtration (see Figure 4.55). This indicates that filterability may not to be greatly dependent on floc size (Gregory and de Moor, 1984) and that floc size, in itself, has only secondary effects to filtration (Hogg, 2000).

5.7 New Automated Filterability Monitoring Technique

The proposed automated filterability monitoring technique proves to be an effective means of determining the filterability of dilute suspensions under the influence of a variety of destabilising agents. All filtration curves obtained from using this new technique are linearised adequately and show no obvious signs of filter cake compression or deformation and the specific resistance to filtration valves obtained are reproducible (see Table 4.3). The experimental set-up and procedures are simple to recreate and follow and the equipment involved is inexpensive (see Section 3.3).

5.8 Other Findings

Flocs consisting of spherical latex particles tend to be more compact and denser than those consisting of kaolin particles, which are plate-like and irregular in shape (see Figures 4.8, 4.9, 4.18, 4.19, 4.26, 4.27, 4.34 and 4.35).

Although not presented in this work, the small number of experiments that were carried out regarding the effects of floc breakage and reformation have on specific resistance to filtration show that the structure of micro-flocs may be the crucial factor in determining the overall filterability of a floc as long as the structure of the micro-flocs are not subject to significant alterations during breakage and reformation (Gregory and de Moor, 1984).

Microscope photography proves to be useful in providing information on floc compaction and density and other distinctive structural features. Microscope photography may be used as a method to determine floc size, however, due to the possible interference imposed on flocs during extraction and transfer from the flocculation vessel to the microscope (see Section 3.2.4), microscope photography was not used in this way.

5.9 Suggestions for Further Work

- Redesign the experimental set-up so that turbidity fluctuations, microscope photography and filtration can be performed on the same sample simultaneously to provide readily comparable results.

- Apply turbidity fluctuations to a column of settling flocs to assess their density, as the current setting does not provide this information directly.

- Investigate the effects anionic and non-ionic polymers on floc formation, breakage, reformation and filterability and compare them with the current findings.

- Look for other possible mechanisms behind the further floc growth observed during reformation for Zetag 64 flocculated kaolin flocs.

References

Akers, R. J. (1975), In: *The Scientific Basis of Flocculation*, (Ives, K. J., ed.), Alphen aan den Rijn (The Netherlands): Noordhoff International Publishers B.V.

Amirtharajah, A., and Jones, S. C. (1996), *Mixing for Coagulation: Organic Polymers, Static Mixers and Modelling*, Chemical Water and Wastewater treatment IV, (H. H. Hermann et al., ed.), Springer-Verlag, Berlin, 3-15.

Amirtharajah, A., and Mills, K. M. (1982), *Rapid-Mix Design for Mechanisms of Alum Coagulation*, J. AWWA 74 (4), 210-216.

Argaman, Y., and Kaufman, W. J. (1970), *Turbulence and Flocculation*, J. San. Engr. Div., ASCE, 96, SA2, 223-241, April.

Bache, D. H., Johnson, C., Papavasilopoulos, E., Rasool, E., and McGilligan, F. J. (1999), *Sweep Coagulation: Structures, Mechanisms and Practice*, J. Water SRT - Aqua 48, 201-210.

Bache, D. H., Rasool, E, Johnson, C., and McGilligan, J. F. (1996), *Temperature and Coagulant Control in the Sweep Floc Domain*, J. Water SRT - Aqua 45, 195-206.

Bangs, L. B. (1984), *Uniform Latex Particles*, Indiana (USA): Seragen Diagnostics Inc.

Barnes, D., and Wilson, F. (1983), *Chemistry and Unit Operations in Water Treatment*, Barking (UK): Applied Science Publishers, Ltd.

Besra, L., Sengupta, D. K., and Roy, S. K. (2000), *Particle Characteristics and Their Influence on Dewatering of Kaolin, Calcite and Quartz Suspensions*, Int. J. Miner. Process. 59, 89-112.

Besra, L., Sengupta, D. K., Roy, S. K., and Ay, P. (2002), *Flocculation and Dewatering of Kaolin Suspensions in the Presence of Polyacrylamide and Surfactants*, Int. J. Miner. Process. 66, 203-232.

Besra, L., Sengupta, D. K., Roy, S. K., and Ay, P. (2004), *Influence of Polymer Adsorption and Conformation on Flocculation and Dewatering of Kaolin Suspension*, Separation and Purification Technology 37 (3), 231-264.

Bickmore, B. R., Nagy, K. L., Sandlin, P. E., and Crater, T. S. (2002), *Quantifying Surface Areas of Clays by AFM*, American Mineralogist 87, 780-783.

Biggs, S., Habgood, M., Jameson, G., and Yan, Y. (2000), *Aggregate Structures Formed via a Bridging Flocculation Mechanism*, Chemical Engineering Journal 80, 13-22.

Binnie, C., Kimber, M., and Smethurst, G. (2002), *Basic Water Treatment*, Cambridge (UK): Royal Society of Chemistry.

Birdi, K. S. (2003), *Handbook of Surface and Colloid Chemistry*, London (UK): CRC Press.

Bohn, H. L., McNeal, B. L., and O'Connor, G. A. (1985), *Soil Chemistry*, New York (USA): Wiley.

Brady, P. V., Cygan, R. T., and Nagy, K. L. (1996), *Molecular Controls on Kaolinite Surface Charge*, J. Colloid Interface Sci. 183, 356-264.

Braggs, B. R. (1993), *The Controlled Modification and Characterisation of the Kaolinite Surface*, Ph.D. Thesis, University of South Australia.

Braggs B., Fornasiero D., Ralston J., Smart R. S. (1994), *The Effect of Surface Modification by an Organosilane on the Electrochemical Properties of Kaolinite*, Clays and Clay Minerals 42, 123-136.

Bratby, J. (1980), *Coagulation and Flocculation: With an Emphasis on Water and Wastewater Treatment*, Croydon (UK): Uplands Press, Ltd.

Brinkman, H. C. (1947), *A Calculation of the Viscous Force Exerted by a Flowing Fluid on a Dense Swarm of Particles*, Applied Scientific Research A1, 27.

Callaghan, I. C., and Ottewill, R. (1974), *Interparticle Forces in Montmorillonite Gels*, Faraday Discuss. Chem. Soc. 57, 110-118.

Camp, T. R., Root, D. A., and Bhoota, B. V. (1940), *Effect of Temperature on Rate of Floc Formation*, J. AWWA 32, 1913-1927.

Carman, P. C. (1938), *Fundamental Principles of Industrial Filtration (A Critical Review of Present Knowledge)*, Trans. Instn. Chem. Engrs. 16, 168-188.

Clark, M. M., and Flora, J. R. V. (1991), *Floc-Restructuring in Varied Turbulent Mixing*, J. Colloid Interface Sci. 147, 407.

Coles, A. A., and Yong, R. N. (2002), *Aspects of Kaolinite Characterisation and Retention of Pb and Cd*, Applied Clay Science 22, 39-45.

de Moor, A. E. L., and Gregory, J. (1982), *An Automated Method for Filterability Determination*, World Filtration Congress III, 253-261.

Dentel, S. K. (1991), *Coagulation Control in Water Treatment*, Crit. Rev. Environ. Control 21 (1), 41-47.

Dharmappa, H. B., Verink, J., Fujiwara, O., and Vigneswaran, S. (1993), *Optimal Design of a Flocculator*, Wat. Res. 27, 513-519.

Ditter, W., Eisenlauer, J., and Horn, D. (1982), In: *The Effect of Polymers on Dispersion Properties* (Tadros, Th. F., ed.), London (UK): Academic Press.

Duan, J. (1997), *Influence of Dissolved Silica on Flocculation of Clay Suspensions with Hydrolysing Metal Salts*, Ph.D. Thesis, University of London.

Duan, J., and Gregory, J. (2002), *Coagulation by Hydrolysing Metal Salts*, Adv. Colloid Interface Sci. 100-102, 475-502.

Elfarissi, F., and Pefferkorn, E. (2000), *Kaolinite/Humic Acid Interaction in the Presence of Aluminium Ion*, Colloids and Surfaces A: Physicochemical and Engineering Aspects 168, 1-12.

Faust, S. D., and Aly, O. M. (1983), *Chemistry of Water Treatment*, Woburn (USA): Butterworth Publishers.

Ferrick, M. R., Murtagh, J., and Thomas, J. K. (1989), *Macromolecules*, American Chemical Society 22, 4.

Ferris, A. P., and Jepson, W. B. (1975), *The Exchange Capacities of Kaolinite and the Preparation of Homoionic Clays*, J. of Colloid Interface Sci. 51, 245-259.

Fleer, G. J., Cohen-Stuart, M. A., Scheutjens, J. H. M. M., Cosgrove, F., and Vincent, B. (1993), *Polymers at Interfaces*, London (UK): Chapman & Hall.

Francois, R. J. (1987), *Strength of Aluminium Hydroxide Flocs*, Wat. Res. 21 (9), 1023-1030.

Freshwater, D. C. (1975), In: *The Scientific Basis of Flocculation*, (Ives, K. J., ed.), Alphen aan den Rijn (The Netherlands): Noordhoff International Publishers B.V.

Gale and Berkerville (1960), Water Pollution Control 67, 233-241.

Gale and Berkerville (1967), Chem. Ind., March, 355-366.

Glover, S. M., Yan, Y, Jameson, G. J., and Biggs, S. (2000), *Bridging Flocculation Studied by Light Scattering and Settling*, Chemical Engineering Journal 80, 3-12.

Gorczyca, B., and Ganczarczyk, J. (1999), *Structure and Porosity of Alum Coagulation Flocs*, Water Quality Research Journal of Canada, 34 (4), 653-666.

Grace, H. P. (1953), *Resistance and Compressibility of Filter Cakes (Part I and II)*, Chem. Eng. Prog. 49, 303-318.

Gregory, J. (1973), *Rates of Flocculation of Latex Particles by Cationic Polymers*, J. Colloid Interface Sci. 42 (2), 448-456.

Gregory, J. (1985), *Turbidity Fluctuations in Flowing Suspensions*, J. Colloid Interface Sci. 105, 357-371.

Gregory, J. (1986), In: *Progress in Filtration and Separation 4*, (Wakeman, R. J., ed.), The Netherlands: Elsevier.

Gregory, J. (1988), *Polymer Adsorption and Flocculation in Sheared Suspensions*, Colloids and Surfaces 31, 231-253.

Gregory, J. (1996), In: *Industrial Water Soluble Polymers*, (Flinch, C. A., ed.), Cambridge (UK): Royal Society of Chemistry.

Gregory, J. (1997), *The Density of Particle Aggregates*, Wat. Sci. Technol. 36 (4), 1-13.

Gregory, J. (1998), *Turbidity and Beyond*, Filtration and Separation, Jan/Feb, 63-67.

Gregory, J. (1999), *Particle Monitoring Techniques for Water Treatment Applications*, J. Environ. Sci. 11 (3), 328-333.

Gregory, J. (2000), *Colloidal Aspects of Solid-Liquid Separation*, Short Course Notes, World Filtration Congress 8, Brighton (UK).

Gregory, J., and Chung, H. (1995), *Continuous Monitoring of Floc Properties in Stirred Suspensions*, J. Water SRT - Aqua 44 (3), 125-131.

Gregory, J., and de Moor, A. E. L. (1984), *Filterability of Polymer-Flocculated Suspensions*, ACS Symposium Series No. 240.

Gregory, J., and Duan, J. (1998), *The Effect of Dissolved Silica on the Action of Hydrolysing Metal Coagulants*, Wat. Sci. Technol. 38 (6), 113-120.

Gregory, J., and Li, G. (1991), *Effects of Dosing and Mixing Conditions on Polymer Flocculation of Concentrated Suspensions*, Chem. Eng. Comm. 108, 3-21.

Gregory, J., and Nelson, D. W. (1984), In: *Solid-Liquid Separation*, (Gregory, J., ed.), Chichester (UK): Ellis Horwood.

Grim, R. E. (1968), In: *Clay Mineralogy*, (2nd edn.), New York (USA): McGraw-Hill, 596.

Hanson, A. T., and Cleasby, J. L. (1990), *The Effects of Temperature on Turbulent Flocculation: Fluid Dynamics and Chemistry*, J. AWWA 82, 56-73.

Healy, T. W., and La Mer, V. K. (1964), *Energetics of Flocculation and Redispersion by polymers*, J. Colloid Sci. 19, 323.

Higashitani, K., and Shibata, T. (1987), *Formation of Pellet Flocs from Kaoline Suspension and Their Properties*, J. Chem. Eng. Jpn. 20, 152-157.

Higgins, M. J., and Novak, J. T. (1997a), *The Effect of Cations on the Settling and Dewatering of Activated Sludges: Laboratory Results*, Wat. Environ. Res. 69 (2), 215-224.

Higgins, M. J., and Novak, J. T. (1997b), *Dewatering and Settling and Dewatering of Activated Sludges: The Case for Using Cation Analysis*, Wat. Environ. Res. 69 (2), 225-232.

Hogg, R. (1999), *The Role of Polymer Adsorption Kinetics in Flocculation*, Colloids and Surfaces A: Physicochemical and Engineering Aspects 146, 253-263.

Hogg, R. (2000), *Flocculation and Dewatering*, Int. J. Miner. Process. 58, 223-236.

Horn, A. F., and Merrill, E. W. (1984), *Midpoint Scission of Macromolecules in Dilute Solution in Turbulent Flow*, Nature 312, 140-141.

Huang, C. P., and Chen, C. P. (1996), *Use of the Fiber-Optical Monitor in Evaluating the State of Flocculation*, Wat. Res. 30, 2723-272.

Hutchison, P. R., and Healy, T. W. (1990), In: *Surface and Colloid Chemistry in Natural Waters and Water Treatment*, (Beckett, R., ed.), New York (USA): Plenum Press.

IDF. (1988), *Technical Manual for Drilling, Completion and Workover Fluids*, Uxbridge (UK): The Hillingdon Press.

Isaacs, A., Daintith, J., and Martin, E. (1991), *Concise Science Dictionary*, Bungay (UK): Oxford University Press.

Ivanauskas, A. (1984), *Floc Stability in Turbulent Flow*, Thesis, Forschungsinstitut für Aufbereitung, Freiberg.

Ivanauskas, A., Mühle, K., and Domasch, K. (1985), *Zur Charakterisierung von Flockeneigenschaften*, Freiberger Forschungshefte A 720, 47-62.

Ives, K. J. (1978), In: *The Scientific Basis of Flocculation*, (Ives, K. J., ed.), Alphen aan den Rijn (The Netherlands): Sijthoff & Noordhoff Publishers B.V.

James, R. O., and Healy, T. W. (1972), *Adsorption of Hydrolyzable Metal Ions at the Oxide-Water Interface*, J. Colloid Interface Sci. 40, 42-81.

Jepson, W. B. (1984), *Kaolins: Their Properties and Uses*, Philosophical Transactions of the Royal Society of London A 31, 411-432.

Jiang, Q. and Logan, B. E. (1991), *Fractal Dimensions of Aggregates Determined from Steady-State Size Distribution*, Environ. Sci. Technol. 25, 2031-2038.

Jorand F., Zartarian F., Thomas F., Block J. C., Bottero J. Y., Villemin G., Urbain V., and Manem J. (1995), *Chemical and Structural (2D) Linkage Between Bacteria within Activated Sludge Flocs*, Wat. Res. 29, 1639-1647.

Jullien, R., and Botet, R. (1987), *Aggregation and Fractal Aggregates*, World Scientific, Singapore, 50-51.

Kam, S. -K., and Gregory, J. (2001), *The Interaction of Humic Substances with Cationic Polyelectrolytes*, Wat. Res. 35 (15), 3557-3566.

Kan, C. C., and Huang, C. P. (1998), *Coagulation Monitoring in Surface Water Treatment Facilities*, Wat. Sci. Technol. 38 (3), 237-244.

Kan, C., Huang, C., and Pan, J. R. (2002), *Time Required for Rapid-Mixing in Coagulation*, Colloids and Surfaces A: Physicochemical and Engineering Aspects 203, 1-9.

Kasper, D. R. (1971), *Theoretical and Experimental Investigations of the Flocculation of Charged Particles in Aqueous Solutions by Polyelectrolytes of Opposite Charge*, Ph.D. Thesis, California Institute of Technology, Pasadena, California.

Klein, J., and Westerkamp, A. (1981), *Peculiarities of Polyacrylamide Analysis by Aqueous GPC*, J. Polym. Sci. 19, 707-718.

Knocke, W. R., Hamon, J. R., Dulin, B. E. (1987), *Effects of Coagulation on Sludge Thickening and Dewatering*, J. AWWA 86 (6), 89-98.

Kohler, H. -H. (1993), In: *Coagulation and Flocculation: Theory and Applications*, (Dobiáš, B., ed.), New York (USA): Marcel Dekker, Inc.

Koopal, L. K. (1993), In: *Coagulation and Flocculation: Theory and Applications*, (Dobiáš, B., ed.), New York (USA): Marcel Dekker, Inc.

Krubien, W. C., and Monk, G. D. (1943), *Permeability as a Function of the Size Parameters of Unconsolidated Sand*, Trans. AIME, 151, 359-369.

Kulicke, W. M. (1986), *Unusual Instability Effects Observed in Ionic and Non-ionic Water Soluble Polymers*, Macromol. Chem. 2, 137-153.

Kulicke, W. M., and Kniewske, R. (1981), *Long-Term Change in Conformation of Marcomolecules in Solution: 2. Poly(acrylamide-co-sodium acrylate)s*, Makromol. Chem. 182, 2277-2287.

La Mer V. K. (1966), *Filtration of Colloidal Dispersions Flocculated by Anionic and Cationic Polyelectrolytes*, Disc. Faraday Soc. 42, 248-254.

Lau, S. C. G. (2000), *Desalination of Tidal Thames River Using an Integrated Membrane Treatment Process*, M.Res. Thesis, University College London.

Lee, D. J. (1999), *Reply to Comments on Hydrodynamics Drag Forces Exerted on a Moving Floc and Its Implications to Free Settling Test*, Wat. Res. 33, 1116.

Lee, S. Y. (1991), The Flocculation of Charged Particles in Aqueous Solutions by Cationic Polyelectrolytes, Ph.D. Thesis, University College London.

Leentvaar, J., and Rebhun, M. (1983), *Strength of Ferric Hydroxide Flocs*, Water Res. 17 (8), 895-902.

Leu, R., and Ghosh, M. M. (1988), *Polyelectrolyte Characteristics and Flocculation*, J. AWWA 80 (4), 159-167.

Li, D. H., and Ganczarczyk, J. J. (1988), *Flow Through Activated Sludge Flocs*, Wat. Res. 22, 789-792.

Li, D. H., and Ganczarczyk, J. J. (1992), *Advective Transport in Activated Sludge Flocs*, Wat. Environ. Res. 64, 236-240.

Li, X-Y., and Logan, B. E. (2001), *Permeability of Fractal Aggregates*, Wat. Res. 35 (14), 3373-3380.

Logan, B. E., and Wilkinson, D. B. (1991), *Fractal Dimensions of Aggregates Determined from Steady-State Size Distributions*, Environ. Sci. Technol. 25 (12), 2031-2038.

Lu, C., Lin, C. -J., Liao, C. -H., Huang, R. -Y., and Ting, W. -P. (2003), *Dewatering of Activated Sludge by Fenton's Reagent*, Adv. Environ. Res. 7, 667-670.

Luckham, P. F., and Rossi, S. (1999), *The Colloidal and Rheological Properties of Bentonite Suspensions,* Adv. Colloid Interface Sci. 82 (1-3), 43-92.

Marshall, K. C. (1990), In: *Surface and Colloidal Chemistry in Natural Waters and Water Treatment*, (Beckett, R., ed.), New York (USA): Plenum Press.

Masschelein, W. (1992), *Unit Process in Drinking Water Treatment*, New York (USA): Marcel Dekker, Inc.

Meakin, P. (1988), *Fractal Aggregates*, Adv. Colloid Interface Sci. 28, 249-331.

Michaels, A. S., and Bolger, J. C. (1962), *Settling Rates and Sediment Volumes of Flocculated Kaolin Suspensions*, Ind. and Eng. Chem. 1 (1), 24-33.

Mikkelsen, L. H. (2001), *The Shear Sensitivity of Activated Sludge Relations to Filterability, Rheology and Surface Chemistry*, Colloids and Surfaces A: Physicochemical and Engineering Aspects 182, 1-14.

Mikkelsen, L. H., and Keilding, K. (2002), *Physico-Chemical Characteristics of Full Scale Sewage Sludges with Implications to Dewatering*, Wat. Res. 36, 2451-2462.

Morris, J. K., and Knocke, W. R. (1984), *Temperature Effects on the Use of Metal-Ion Coagulants for Water Treatment*, J. AWWA 76, 74-79.

Mortimer, D. A. (1991), *Synthetic Polyelectrolytes: A Review*, Polym. Int. 25, 29-41.

Mota, M., Teixeira, J. A., Bowen, W. R., and Yelshin, A. (2003*), Interference of Course and Fine Particles of Different Shape in Mixed Porous Beds and Filter Cakes*, Minerals Engineering 16, 135-144.

Mühle, K. (1993), In: *Coagulation and Flocculation: Theory and Applications*, (Dobiáš, B., ed.), New York (USA): Marcel Dekker, Inc.

Mühle, K., Domasch, K., and Neesse, T. (1989), Freiberger Forschungshefte A790, 115.

Narkis, N., and Rebhun, M. (1966), *Ageing Effects in Measurement of Polyacrylamide Solution Viscosities*, Polymer (London) 7, 507-512.

Norrish, K. (1954), *The Swelling of Montmorillonite*, Disc. Faraday Soc. 18, 120-134.

Owen, A. T., Fawell, P. D., Swift, J. D., and Farrow, J. B. (2002), *The Impact of Polyacrylamide Flocculant Solution Age on Flocculation Performance*, Int. J. Miner. Process. 67, 123-144.

Ozcan, O., Ruhland, M., and Stahl, W. (2000), *The Effect of Pressure, Particle Size and Particle Shape on the Shear Strength of Very Fine Mineral Filter Cakes*, Int. J. Miner. Process. 59, 185-193.

Packham, R. F. (1963), *The Coagulation Process - A Review of Some Recent Investigations*, Proc. Sco. Wat. Treat. Exam. 12, 15-19.

Parker, D. S., Kaufman, W. J., and Jenkins, D. (1972), *Floc Breakup in Turbulence Flocculation Processes*, J. Saint. Eng. Div., ASCE 98, 79-99.

Pefferkorn, E., and Widmaier, J. (1998), *Aggregation and Fragmentation of Lyophobic and Hydrated Colloids*, Colloids and Surfaces A: Physicochemical and Engineering Aspects 145, 25-35.

Rattanakawin, C. (1998), *Aggregate Size Distributions in Flocculation*, M.Sc. Thesis, The Pennsylvania State University, University Park, PA.

Rattanakawin, C., and Hogg, R. (2000), *Aggregate Size Distributions in Flocculation*, Colloids and Surfaces A: Physicochemical and Engineering Aspects 177 (2-3), 87-98.

Rogak, S. N., and Flagan, R. C. (1990), *Stokes Drag on Self-Similar Clusters of Spheres*, J. Colloid Interface Sci. 28, 1865-1874.

Rossini, M., Garcia Garrido, J., and Galluzzo, M. (1999), *Optimisation of the Coagulation-Flocculation Treatment: Influence of Rapid Mix Parameters*, Wat. Res. 33 (8), 1817-1826.

Sakurai, M., and Harano, Y. (1982), Int. Chem. Eng. 22, 116.

Sanin, F. D., and Vesilind, P. A. (1996), *Synthetic Sludge: A Physical/Chemical Model in Understanding Bioflocculation*, Wat. Environ. Res. 68 (5), 927-933.

Schofield, R. K., and Samson, H. R. (1953), Clay Miner. Bull. 2, 45.

Schramm, L. L. (2001), *Dictionary of Colloid and Interface Science*, New York (USA): Wiley.

Sharma, M. M., and Lei, Z. (1991), *A Model for Clay Filter Cake Properties*, Colloids and Surfaces 56, 357-381.

Shi, Y., Fan, M., Brown, R. C., Sung, S., and Van Leeuwen, J. (2004), *Comparison of Corrosivity of Polymeric Sulphate Ferric and Ferric Chloride as Coagulants in Water Treatment*, Chem. Eng. Process. 43, 955-964.

Smoluchowski, M. (1916), *Drei Vorträge Über Difussion, Brownische Molekular Bewegung und Koagulation von Kolloidteilchen*, Physik. Z. 17, 557.

Smoluchowski, M. (1917), *Versuch Einer Mathematischen Theorie der Koagulationskinetic Kolloider Losungen*, Z. Physik. Chem. 92, 129.

Sorensen, P. B., Christensen, J. R., and Bruus, J. H. (1995), *Effect of Small Scale Solids Migration in Filter Cakes during Filtration of Wastewater Solids Suspensions*, Wat. Environ. Res. 67, 25-32.

Spicer, P. T., Pratsinis, S. E., Raper, J., Amal, R., Bushell, G., and Meesters, G. (1998), *Effect of Shear Schedule on Particle Size, Density, and Structure During Flocculation in Stirred Tanks,* Powder Technology 97, 26-34.

Sposito, G. (1989), *The Chemistry of Soils*, New York (USA): Oxford University Press.

Srinivasan, P. T., Viraraghavan, T., and Subramanian, K. S. (1999), Aluminium *in Drinking Water: An Overview*, Water SA 25, 47-55.

Strenge, K. (1993), In: *Coagulation and Flocculation: Theory and Applications*, (Dobiáš, B., ed.), New York (USA): Marcel Dekker, Inc.

Stroh, G. (1993), In: *Coagulation and Flocculation: Theory and Applications*, (Dobiáš, B., ed.), New York (USA): Marcel Dekker, Inc.

Tambo, N., Hozumi, H. (1979), *Physical Characteristics of Flocs - II. Strength of Flocs*, Wat. Res. 13 (5), 421-427.

Taylor, M. L., Morris, G. E., Self, P. G., and Smart, R. C. (2002), *Kinetics of Adsorption of High Molecular Weight Anionic Polyacrylamide onto Kaolinite: The Flocculation Process*, J. Colloid Interface Sci. 250, 28-36.

Tebbutt, T. H. Y. (1990), *Basic Water and Wastewater Treatment*, London (UK): Butterworths.

Thomas, D. G. (1964), *Turbulent Disruption of Flocs in Small Particle Size Suspensions*, AIChE 10, 517.

Thomas, D. N., Judd, S. J., and Fawcett, N. (1999), *Flocculation Modelling: A Review*, Wat. Res. 33, 1579-1592.

Tomi, D. T. and Bagster, D. F. (1978), *The Behaviour of Aggregates in Stirred Vessels, Part 1 - Theoretical Considerations on the Effects of Agitation*, Trans. Instn. Chem. Engrs. 56, 1-8.

Tsou, G. W., Wu, R. M., Yen, P. S., and Lee, D. J. (2003), *Advection Flow Through Sludge Flocs*, Adv. Environ. Res. 7, 733-737.

Uehara, G., and Gillman, G. P. (1972), *The Mineralogy, Chemistry and Physics of Tropical Soils with Variable Charge Clays*, Westview Tropical Agricultural Series 4, Colorado (USA): Westview Press.

Uriarte, F. A. (1971), Ph.D. Thesis, Carnegie-Mellon University, (UM71-16479).

Van Benschoten, J., and Edzwald J. K. (1990), *Chemical Aspects of Coagulation Using Aluminum Salts: 1. Hydrolytic Reactions of Alum and Polyaluminum Chloride*, Wat. Res. 24 (12), 1519-1526.

Van de Ven, T. G. M., and Hunter, R. J. (1977), *The Energy Dissipation in Sheared Coagulated Sols*, Rheol. Acta. 16, 534-543.

Van Olphen, H. (1964), J. Colloid Interface Sci. 19, 313.

Vanni, M. (2000), *Creeping Flow Over Spherical Permeable Aggregates*, Chemical Engineering Science 55, 685-698.

Viessman, W., and Hammer, M. J. (1985), *Water Supply and Pollution Control*, New York (USA): Harper & Row, Publishers, Inc.

Way, C. T. (1983), *Sludge Dewatering: Manual of Practice 20*, Washington (USA): Water Pollution Control Federation.

Weiss, A., and Frank, R. (1961), *Über den Bau der Gerüste in Thixotropen Gelen*, Z Natur-forsch 16b, 141-142.

Wolynes, P. G., and McCammon, J. A. (1977), *Hydrodynamic Effect on the Coagulation of Porous Biopolymers*, Macromolecules 10, 86-87.

Wu, C. C., Wu, J. J., and Huang, R. Y. (2003a), *Effect of Floc Strength on Sludge Dewatering by Vacuum Filtration*, Colloids and Surfaces A: Physicochemical and Engineering Aspects 221 (1-3), 141-147.

Wu, C. C., Wu, J. J., Huang, R. Y. (2003b), *Floc Strength and Dewatering Efficiency of Alum Sludge*, Adv. Environ. Res. 7, 617-621.

Wu, R. M., Lee, D. J., Waite, T. D., and Guan, J. (2002), *Multilevel Structure of Sludge Flocs*, J. Colloid Interface Sci. 252, 383-392.

Wu, R. M., Tsou, G. W., and Lee, D. J. (2000), *Estimation of the Interior Permeability of Polymer-Flocculated Sludge Flocs*, Adv. Environ. Res. 4, 163-167.

Yen, Y. C. (1976), *Acrylamide and Polyacrylamide*, Stamford Research Institute Report 99, 203-204, 240, 250.

Yeung, A. K. C., and Pelton, R. (1996), *Micromechanics: A New Approach to Studying the Strength and Break-Up of Flocs*, J. Coll. Interface Sci. 184, 579-585.

Yong, R. N., Mohaned, A. M. O., and Warkentin, B. P. (1992), *Principles of Contaminant Transport in Soils*, New York (USA): Elsevier.

Yukselen, M. A., and Gregory, J. (2002), *Properties of Flocs Formed Using Different Coagulants*, Wat. Sci. Technol.: Water Supply 2 (5-6), 95-101.

Yukselen, M. A., and Gregory, J. (2004), *The Reversibility of Floc Breakage*, Int. J. Miner. Process. 73, 251-259.

Zbik, M., and Smart, R. St. C. (1999), In: *Clays for the Future*, (Kodama, H., Mermut, A. R. and Torrance, J. K., ed.), Proceedings of the 11th International Clay Conference, Ottawa (Canada), Publ. ICC97 Org. Cttee, 361-366.

Zbik, M., and Smart, R. St. C. (2002), *Dispersion of Kaolinite and Talc in Aqueous Solution: Nano-morphology and Nano-bubble Entrapment*, Mineral Engineering 15, 277-286.

Zhao, Y. Q. (2003), *Correlations between Floc Physical Properties and Optimum Polymer Dosage in Alum Sludge Conditioning and Dewatering*, Chem. Eng. J. 92, 227-235.

Zhou, Q., and Maurice, P. A. (1995), In: *Morphological Characterisation of KGa2 and KGal-b Kaolinites from Georgia*, (Goldschmidt, V. M., ed.), Conference Abstracts, Geochemical Society, Edinburgh, 102.